CALFED
BAY-DELTA
PROGRAM

Levees and Channels Technical Team
Seismic Vulnerability Sub-Team

Seismic Vulnerability of the Sacramento - San Joaquin Delta Levees

December 1998

FINAL DRAFT

Seismic Vulnerability of the Sacramento - San Joaquin Delta Levees

Levees and Channels Technical Team
Seismic Vulnerability Sub-Team
Members

Raphael A. Torres, Chair
Dr. Norman A. Abrahamson
Fred N. Brovold
Gilbert Cosio
Michael W. Driller
Dr. Leslie F. Harder, Jr.
Dr. N. Dean Marachi
Christopher H. Neudeck
Lynn Moquette O'Leary
Michael Ramsbotham
Dr. Raymond B. Seed

CALFED BAY-DELTA PROGRAM
SEISMIC VULNERABILITY
OF THE
SACRAMENTO/SAN JOAQUIN DELTA LEVEES

TABLE OF CONTENTS

TABLE OF CONTENTS

LIST OF FIGURES

LIST OF TABLES

CALFED BAY-DELTA PROGRAM
SEISMIC VULNERABILITY
OF THE
SACRAMENTO/SAN JOAQUIN DELTA LEVEES

FORWORD

The CALFED Bay-Delta program is an unprecedented collaboration among state and federal agencies and the state's leading urban, agricultural and environmental interests to address and resolve the environmental and water management problems associated with the Bay-Delta system. The mission of the CALFED Bay-Delta Program is to develop a long-term comprehensive plan that will restore ecological health and improve water management for beneficial uses of the Bay-Delta system. The objective of CALFED's Levee System Integrity Program is to reduce the risk of land use and associated economic activities, water supply, infrastructure, and the ecosystem from catastrophic damage associated with breaching of Delta levees.

Delta levees are the most visible man-made feature of the Bay-Delta system. They are an integral part of the Delta landscape and are key to preserving the Delta's physical characteristics and processes, including definition of the Delta waterways and islands. There is growing concern that California's Bay-Delta system levees are vulnerable to failure, especially during earthquakes. Levee failures in the Delta could flood farmland and wildlife habitat, and also interrupt water supply deliveries to urban and agricultural users and disrupt highway and rail use. Although there has never been a documented levee failure from a seismic event, the Delta has not experienced a significant seismic event since the levees have been at their current size. One goal of CALFED's Levee Program is to identify the risk of failure of Delta levees due to seismic events and develop recommendations to reduce levee vulnerability and improve levee seismic stability.

A Seismic Vulnerability Sub-Team of CALFED's Levees and Channels Technical Team was formed to assess the seismic risk. This sub-team, composed of seismic experts and geotechnical engineers with experience in the Delta, evaluated levee fragility and assessed the seismic vulnerability of the current levee system. This report presents the findings and conclusions of the Seismic Sub-Team. CALFED's Levee Program will conduct further studies to apply this information to overall risk assessment.

CALFED thanks DWR's Division of Engineering for sponsoring this exceptional study and also recognizes the superior efforts of the experts on the sub-team who contributed their unique technical knowledge, diverse views, and willingness to work long hours.

CALFED BAY-DELTA PROGRAM
SEISMIC VULNERABILITY
OF THE
SACRAMENTO/SAN JOAQUIN DELTA LEVEES

1 INTRODUCTION

1.1 BACKGROUND

The CALFED process has produced a draft programmatic environmental impact report that describes three alternatives for improving the Delta's environment, water quality, and water supply reliability. The seismic risk assessment described in this report provides an assessment of the Delta's current vulnerability to potential damage caused by an earthquake. This assessment also provides an estimate of the probability or likelihood that a damaging earthquake will occur. This information will be used to evaluate the CALFED alternatives with respect to the seismic impact to the Delta environment.

1.2 ORGANIZATION

This seismic risk assessment was performed by a sub-team of the Levees and Channels Technical Team of CALFED. The sub-team is comprised of geotechnical engineers and a seismologist. The members represent Federal and State government, local interests, and independent consultants. The members of the sub-team are:

Dr. Norman A. Abrahamson	Consulting Seismologist
Fred N. Brovold	GEI Consultants
Gilbert Cosio	Murray, Burns, and Kienlen, Consulting Engineers
Michael W. Driller	Department of Water Resources
Dr. Leslie F. Harder, Jr.	Department of Water Resources
Dr. N. Dean Marachi	The Mark Group, Consulting Engineers
Christopher H. Neudeck	Kjeldsen, Sinnock, Neudeck, Consulting Engineers
Lynn Moquette O'Leary	CALFED/U.S. Army Corps of Engineers
Michael Ramsbotham	CALFED/U.S. Army Corps of Engineers
Dr. Raymond B. Seed	Seismic Geotechnical Consultant
Raphael A. Torres - Chair	Department of Water Resources

1.3 BASIS FOR THE ASSESSMENTS

The seismic risk analyses and assessments presented in this report are based on the most current available information. Information on the seismic response of peat/organic soils is still being developed. Even though hundreds of borings describing the subsurface conditions of Delta levees were reviewed, these borings can only provide a limited characterization of the hundreds of miles of levees. Yet, it is not likely that a finite number of additional borings would significantly change the present characterization.

Additional investigations cannot be completed within the CALFED time frame. Consequently, a combination of sensitivity analyses and assumptions were used to fill this information void. The sub-team determined that even though there was little information available on some issues, a reasonable assessment of the Delta as a whole could still be achieved. This is described in more detail in the report.

Members of the Seismic Vulnerability Sub-Team:
Top Row, Left to Right: Michael W. Driller, Dr. Raymond B. Seed, Frederick N. Brovold, Dr. Leslie F. Harder, Jr., Dr. Norman A. Abrahamson, Michael Ramsbotham
Bottom Row, Left to Right: Christopher H. Neudeck, Gilbert Cosio, Dr. N. Dean Marachi, Lynn Moquette O'Leary, Raphael A. Torres

2 GEOLOGIC SETTING

2.1 GEOLOGY

The Sacramento-San Joaquin Delta, located at the confluence of the Sacramento and San Joaquin Rivers, is an unique feature of the California landscape (see Figure 2-1). The Delta is part of the Central Valley geomorphic province, a northwest-trending structural basin separating the primarily granitic rock of the Sierra Nevada from the primarily Franciscan Formation rock of the California Coastal Ranges (Converse et al., 1981). The Delta occurs in an area that contains 3 to 6 miles of sedimentary deposits, most of which accumulated in a marine environment from about 175 million years ago to 25 million years ago.

Since late Quaternary time, the Delta area has undergone several cycles of deposition, non-deposition, and erosion, resulting in the accumulation of a few hundred feet of poorly consolidated to unconsolidated overlying sediments. Delta peats and organic soils began to form about 11,000 years ago during a rise in sea levels (Shlemon and Begg, 1975). This rise in sea level created tule marshes that covered most of the Delta. Peat formed from repeated burial of the tules and other vegetation growing in the marshes.

During the cycles of erosion and deposition, rivers were entering from the north, northeast, and southeast. These included the Sacramento, Mokelumne, and San Joaquin Rivers. As the rivers merged, they formed a complex pattern of islands and interconnecting sloughs. River and slough channels were repeatedly incised and backfilled with sediments with each major fluctuation. These processes were complicated by concurrent subsidence and tectonic changes in land surface.

Debris produced by hydraulic mining during the gold rush of the mid-1800's disrupted the natural depositional history of the Delta. Hundreds of thousands of tons of silt were washed from the Sierra Nevada into the Delta. This sediment debris filled stream channels, caused flooding, and raised the natural levees along Delta streams and sloughs.

2.2 LEVEE BUILDING HISTORY

In the late 1800's, Delta inhabitants began fortifying existing natural levees and draining inundated islands in the Delta for agricultural use.

Most of the early levees in the Delta were constructed by Chinese laborers (Thompson, 1982) using hand shovels and wheelbarrows, and some were built using scrapers pulled by horses. Later, when the farmers realized that levees of sufficient height could not be efficiently built by hand, the barge-mounted, sidedraft-clamshell dredge was used. The levees were generally built of non-select, uncompacted materials without engineering design and without good construction methods.

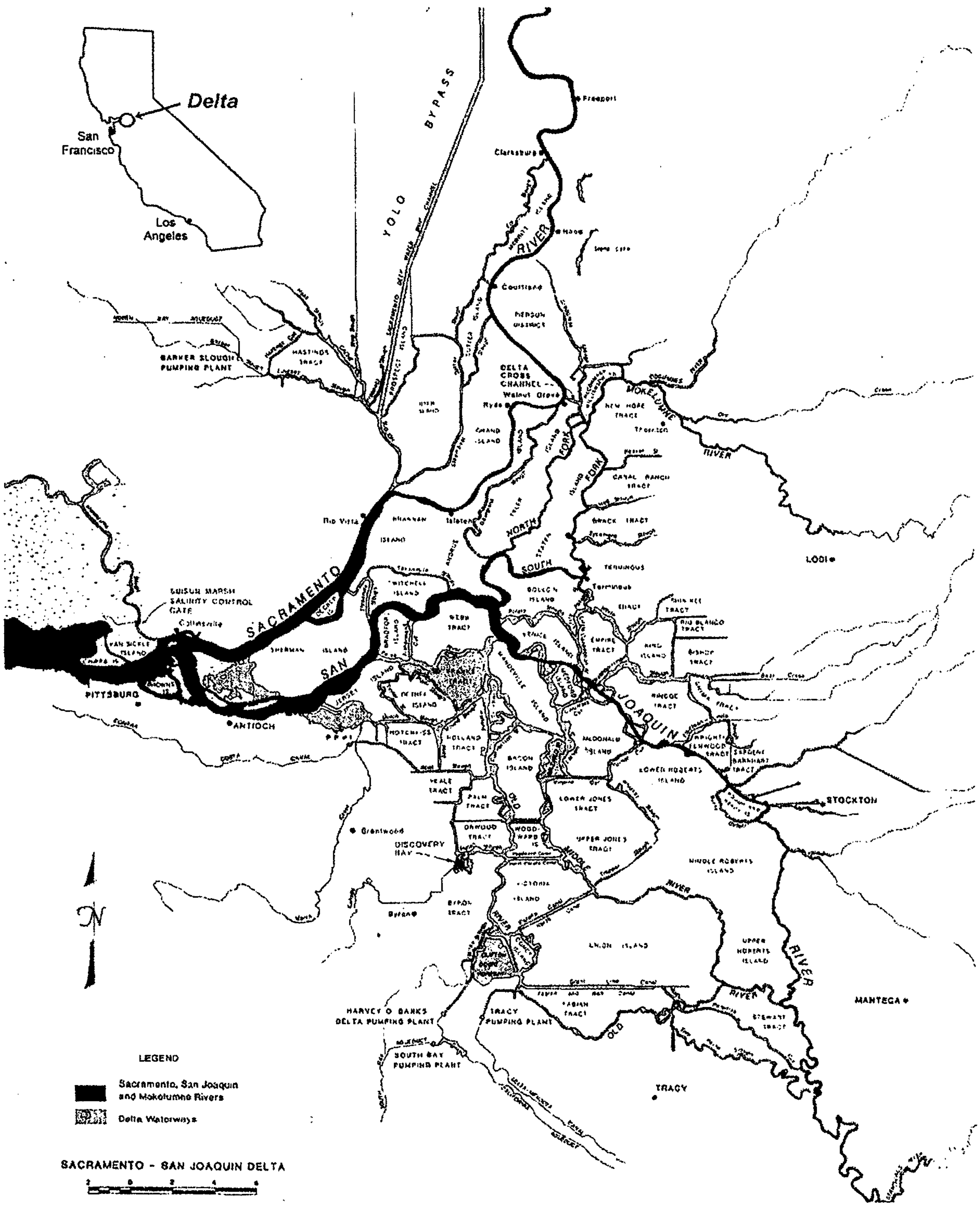

Figure 2-1: Sacramento - San Joaquin Delta

The original levees were usually less than five feet high, but continuous settlement of the levees and subsidence of the interior island soils since the initial levee construction has required the periodic addition of new fill to maintain protection against overtopping by waters of the Delta. The interiors of many islands are now commonly 10 to 15 feet below sea level. Presently, some levee crowns are 25 feet higher than the interior of their respective islands. Figure 2-2 illustrates the evolution of Delta levees over time.

In general, the upper portion of Delta levee embankments are comprised of mixtures of dredged organic and inorganic sandy, silty, or clayey soils that have been placed on either natural peat or natural sand and silt levees. The variability in foundation materials for Delta levees can be great, even between sites that are in close proximity to one another. Such heterogeneity is due to a history of continuous stream meandering and channel migration within the Delta.

2.3 LEVEE DAMAGE CAUSED BY PAST EARTHQUAKES

A review of available historical information indicates that there has been little damage to Delta levees caused by historical earthquakes (CDWR, 1992). No reports could be found to indicate that an island or tract had been flooded due to an earthquake-induced levee failure. Further, no report could be found to indicate that significant damage had ever been induced by earthquake shaking. The minor damage that has been reported has not significantly jeopardized the stability of the Delta levee system.

This lack of severe earthquake-induced levee damage corresponds to the fact that no significant earthquake motion has apparently ever been sustained in the Delta area since the construction of the levee system approximately a century ago. The 1906 San Francisco earthquake occurred 50 miles to the west, on the San Andreas Fault, and produced only minor levels of shaking in the Delta; as the levees were not very tall yet in 1906, these shaking levels posed little threat. Continued settlement and subsidence over the past 90 years has, however, significantly changed this situation. Consequently, the lack of historic damage to date should not lead, necessarily, to a conclusion that the levee system is not vulnerable to moderate-to-strong earthquake shaking. The current levee system simply has never been significantly tested.

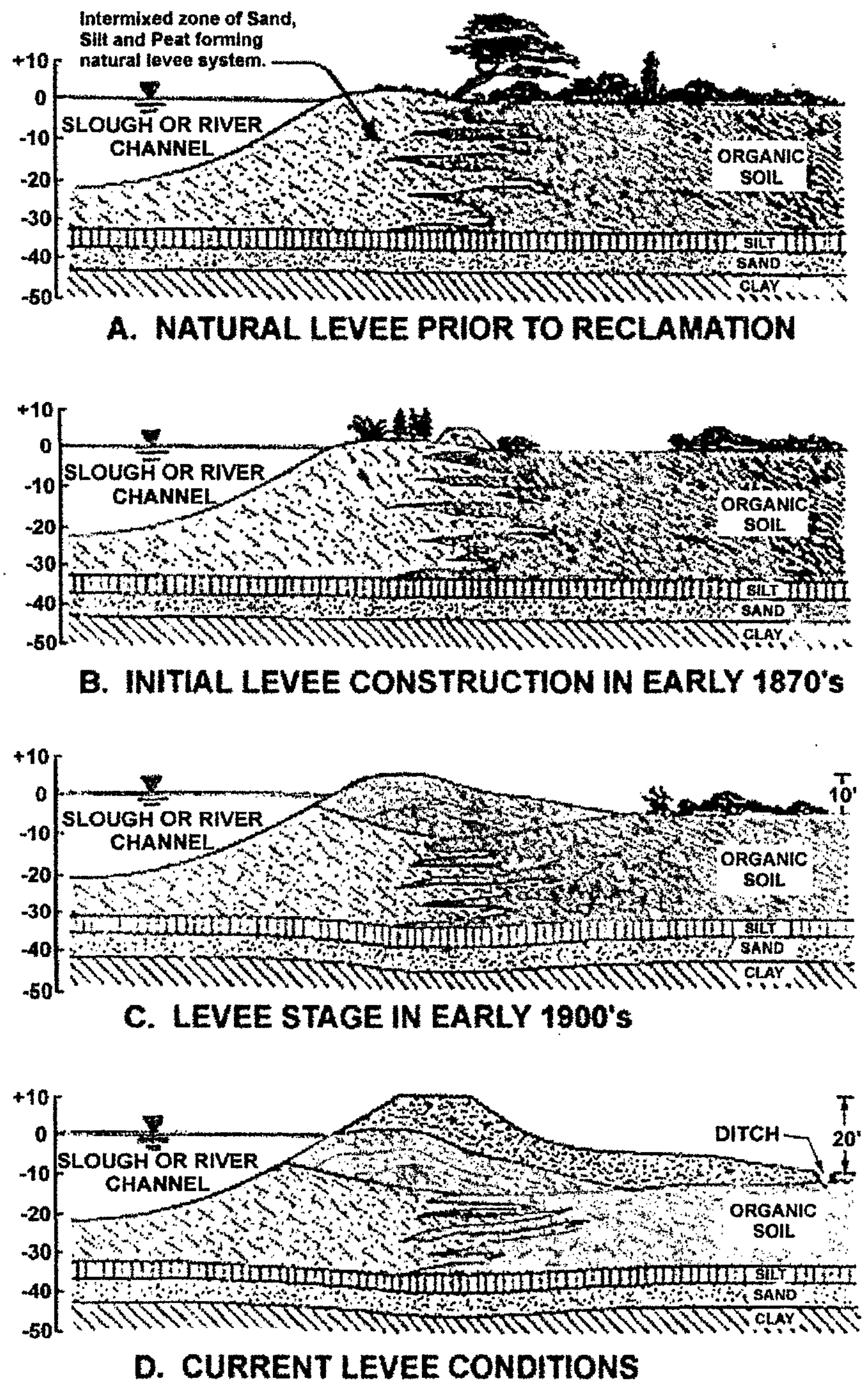

Figure 2-2: Evolution of Delta Levees Over Time

3.0 SEISMICITY OF THE DELTA REGION

3.1 REGIONAL FAULTING AND MODELS

The Delta Levees are located in a region of relatively low seismic activity as compared to the San Francisco Bay area. The major strike-slip faults in the Bay Area (San Andreas, Hayward, Calaveras faults) are located over 16 miles from the Delta region (see Figure 3-1). The less active Green Valley and Marsh Creek-Clayton faults are over 9 miles from the Delta region. There are also small but significant local faults in the Delta region, and there is a possibility that there are blind thrust faults along the western Delta (see Figures 3-1 and 3-2).

3.2 LOCAL FAULTING AND MODELS

In recent seismic studies of the Delta region, a series of blind thrust faults along the western edge of the central valley and extending through the Delta has typically been used in the seismic source characterization. However, there is large uncertainty in the location, activity, and even existence of these blind thrust faults in the Delta region. Although various names have been used for this theoretical system of blind thrust faults; in this study we have used the term Coast-Range Central Valley (CRCV) boundary thrust fault system. While there is clear evidence that the CRCV fault system exists and is potentially active to the south and north of the Delta, there is not clear evidence of potentially active blind thrust faults in the Delta region. The possibility that the CRCV fault system exists in the Delta region has a significant effect on the seismic risk to the Delta levees. Due to the large uncertainty in this important aspect of the source characterization, two alternative models of the local faulting have been used in this study: One that includes the CRCV feature in the Delta region, and an alternate one that includes smaller thrust faults west of the Delta region.

The first model is based on the seismic source characterization currently used by the California Division of Mines and Geology (1996) which are part of the state seismic hazard map. In this model, the CRCV is assumed to extend into the Delta region (see Figure 3-1). This model is called the "CRCV" model in this study.

The second model is based on a recent evaluation of the faulting in the Delta region by Lettis and Associates (1998). The Lettis study has concluded that the blind thrust faults do not exist in the Delta region. Instead, thrust faults located further west of the Delta region are postulated as accounting for the crustal shortening across the region (see Figure 3-2). This model is called the "Lettis" model in this study.

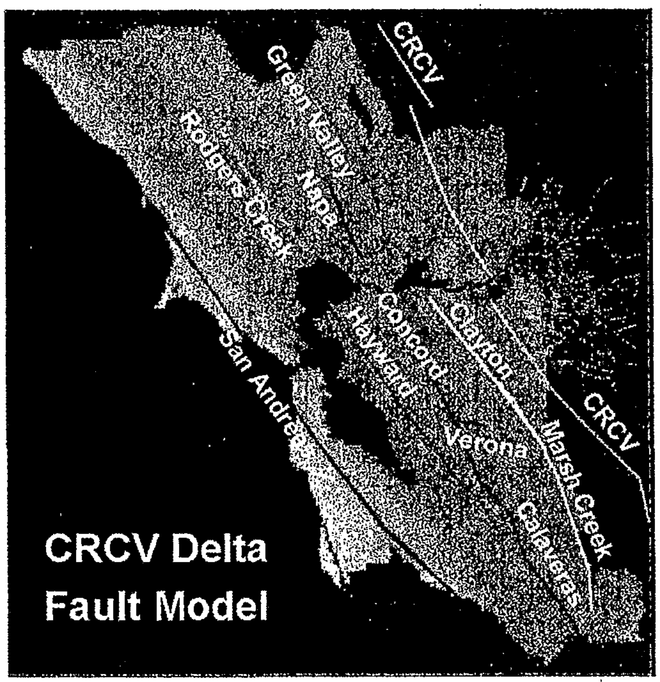

Figure 3-1: CRCV Delta Fault Model

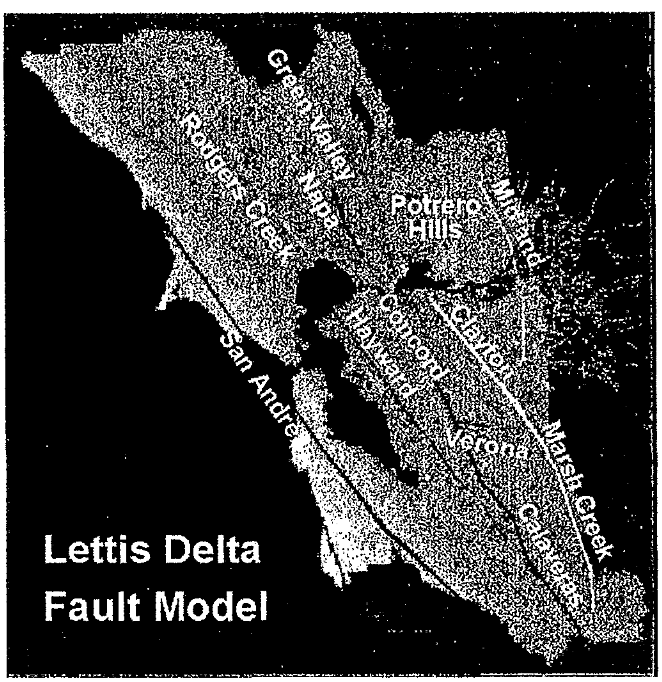

Figure 3-2: Lettis Delta Fault Model

3.3 SEISMIC HAZARD RESULTS

Although the two local faulting models are quite different, they produce similar levels of peak ground acceleration (PGA) at individual sites in the Delta region using a probabilistic analysis. For an outcrop of stiff soil or rock, the 100-year PGA ranges from 0.2g in the western Delta to 0.1g along the eastern Delta (see Figure 3-3). Figure 3-4 presents the estimated PGA at Sherman Island for a range of return periods. Once again, both the CRCV and Lettis models produce similar predictions of PGA. However, while the individual site PGA is similar for the two models, the magnitudes associated with them are different and this leads to very different predictions of performance of the Delta as a system which is discussed later.

For the western Delta, the dominant earthquake contributing to the 100-year PGA is a magnitude 5.8 to 6.2 earthquake at a distance of about 13 miles from local sources. For the eastern Delta, the magnitude 7.5 to 8.0 events on the San Andreas Fault and magnitude 7 events on the Hayward Fault also contribute significantly to the hazard, in addition to the local magnitude 5.5 to 6.0 earthquakes. The main magnitude contributing to the 100-year return period hazard for the eastern Delta is about magnitude 6.

Since the overall seismic hazard is dominated by moderate local events, it is unlikely that the entire Delta region will be subjected to large motions in any single earthquake. For example, a magnitude 6 event near the northern Delta may cause significant ground motions in the northern Delta, but not in the southern Delta, as peak accelerations produced by events of only moderate magnitude attenuate fairly rapidly with distance from the source (fault rupture).

Appendix A presents additional information regarding the seismic source models of the Delta region and the results of the probabilistic hazard analysis.

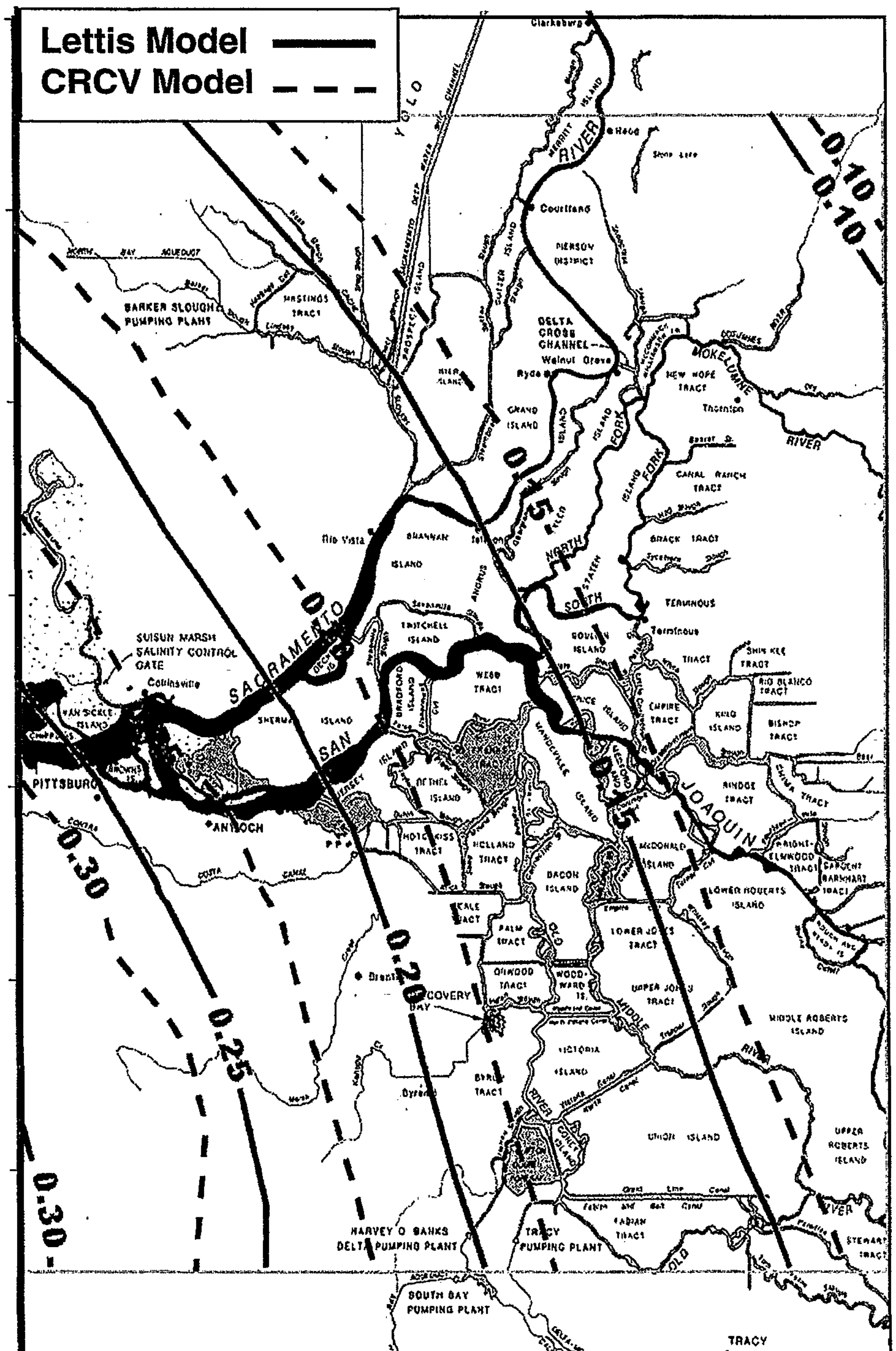

Figure 3-3: Acceleration Contours for 100-year Return Interval - both Models

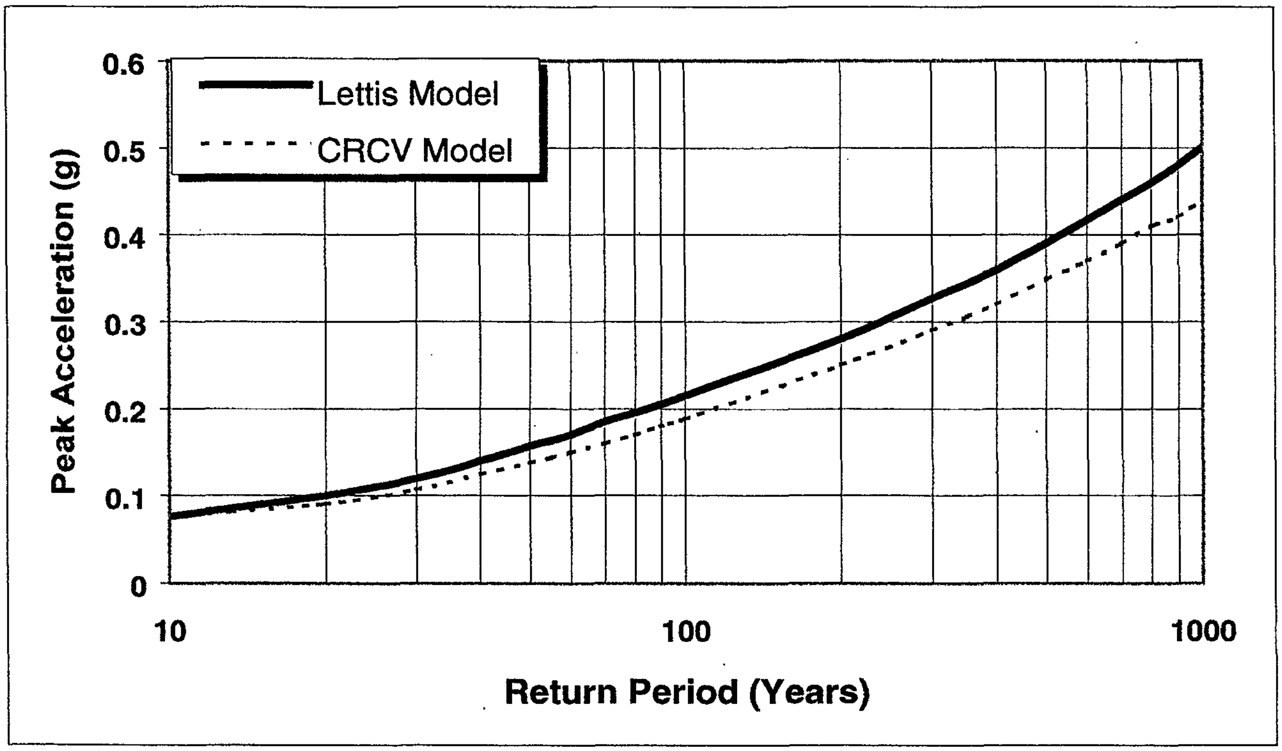

Figure 3-4: Peak Accleration vs Return Period for the CRCV and Lettis Models

4 ESTIMATES OF LEVEE FRAGILITY DUE TO EARTHQUAKE SHAKING

4.1 INTRODUCTION

Estimates of Delta levee fragility during different earthquake loadings were developed by members of the Seismic Vulnerability Sub-Team of the CalFed Levees and Channels Technical Team. Levee fragility is defined as a measure of the susceptibility of a levee to fail during a particular seismic loading. Members of the sub-team reviewed available geotechnical information associated with levees in the Delta and assessed the relative vulnerability of the levees and their foundations to earthquake shaking. Sub-team members also reviewed previous seismic stability studies of various areas in the Delta. The efforts of the sub-team were facilitated by geotechnical reports and data supplied by the California Department of Water Resources, U. S. Army Corps of Engineers; Kjeldsen Sinnock & Neudeck, and Murray Burns & Kienlen. The Bibliography (Section 8) presents a partial list of the reports and studies reviewed. In addition, members of the sub-team were privy to other unpublished data.

4.2 PROCESS

The process for assessing potential levee failures during earthquakes was to review the available information and to develop a range of estimates for the number of levee failures that might occur for various levels of earthquake acceleration. This levee fragility was expressed in a normalized form as the number of expected levee failures per 100 miles of levee. Different ranges of fragility were estimated for different regions in the Delta, and for different levels of earthquake shaking. This information is used in a later section, together with the probabilistic seismicity estimates, to develop estimates of the number of failures likely within an exposure period.

Failure was defined as sufficient distress to the levee in the form of slumping and/or cracking that would lead to a complete breach and uncontrolled flooding of the island. Failure was considered to occur either during the earthquake, or within a very short period of time following the earthquake. Levees could be extensively damaged during or subsequent to earthquake shaking, but unless a full breach of the levee resulted, failure was not considered to have occurred.

Precise quantitative estimates of levee failures cannot be made because geotechnical information for over 600 miles of levees remains limited, particularly for the levees themselves. The sub-team members relied upon the available information and their individual knowledge and experience to develop individual assessments of the frequencies of levee failure for different levels of earthquake shaking. These individual assessments were then discussed by the sub-team and refined into a single consensus range of values.

4.3 EARTHQUAKE MOTIONS CONSIDERED

The likely range of bedrock/stiff soil motions that might be experienced on an outcrop of such materials within the Delta within the next 30 to 300 years is between 0.05 and 0.30g (see Section 3). Such motions are expected to be generally associated with a Magnitude 6 event. However, the Delta has thick and deep deposits of soft organic and mineral soils overlying the top of bedrock and/or stiff soils. Layers of soft soils overlying stiffer deposits are generally expected to amplify earthquake motions developed in the deeper, stiffer deposits. Based on the studies by CDWR (1992) and Boulanger, et al. (1997), the most likely acceleration amplification factors between deep and stiff base layers to the levee crowns range between 1 and 2. For the purposes of the current assessments, an average amplification factor of approximately 1.6 was used. This crown amplification accounted for both soft soil amplification as well as topographic amplification. Accordingly, the earthquake parameters considered in these fragility assessments can be summarized as follows:

Earthquake Magnitude: 6.
Peak Bedrock/Stiff Soil Outcrop Accelerations: 0.05 to 0.30g.
Base Layer Outcrop to Levee Crown Amplification Factor: 1.6.

Magnitude scaling factors to correct the "equivalent" acceleration levels for earthquakes having magnitudes other than Magnitude 6 were incorporated in the probabilistic seismicity analyses (see Appendix B). These scaling factors account for the fact that larger magnitude events typically cause longer durations of shaking (more cycles of shaking), and these duration differences affect the severity of the loading.

4.4 DAMAGE POTENTIAL ZONES

Two principal modes of potential earthquake-induced levee failure were considered while developing the different damage potential zones: 1) Flow slides and lateral spreading associated with strength loss (liquefaction) of levee embankment or foundation soils, and 2) Inertially-induced seismic deformations of levees experiencing no liquefaction. Potential failure mechanisms included overtopping, seepage erosion due to cracking, and exacerbation of existing seepage problems due to deformations and cracking. Seasonal variations in river and slough water elevations, and their interactions with tides, were also considered. This evaluation resulted in dividing the Delta area into four Damage Potential Zones as described in Table 4-1 and shown in Figure 4-1.

Qualitative assessments of high, medium, and low failure potential during earthquake shaking were made for different regions within the Delta. The principal geotechnical parameters affecting this assessment included the following:

- The presence of loose, cohesionless sandy and silty layers in the levee embankment generally lead to a high or medium-high failure potential rating. Such soils are liquefiable when saturated. Since levees are manmade and not formed by intermittent natural processes, loose soils are expected to have greater lateral continuity within a levee than in a natural deposit. The presence of such soil beneath the phreatic line within the manmade levee embankment, as detected by penetration testing, indicates a relatively high potential for a liquefaction-induced levee failure. Levees with substantial amounts of liquefied material are likely to exhibit flow slides and lateral spreading as very loose, cohesionless soils have low post-liquefaction shear strengths.

- The presence of loose, cohesionless sandy and silty layers in the levee foundation was also considered detrimental because of the potential for liquefaction. However, it was not considered as serious as having such materials within the levee. This is because such layers within the natural foundation are more likely to be discontinuous. Foundation liquefaction beneath a levee is also generally less critical than liquefaction within the levee embankment as the post-liquefaction shear resistance necessary to prevent flow and lateral spreading is lower due to geometry and net driving force considerations. In addition, somewhat higher penetration resistance is commonly reported for such foundation layers and this suggests somewhat higher liquefaction resistance and post-liquefaction shear strength.

- High levees on thick, soft foundations were considered more fragile because of their potential to have marginal static stability. Levee sections with only marginal static stability were considered to be likely to slide and experience significant displacements during earthquake shaking even without liquefaction.

- Levees with narrow cross sections, limited freeboard, or histories of previous distress were also considered to have a higher probability of failure.

TABLE 4-1: DAMAGE POTENTIAL ZONES WITHIN THE DELTA

Damage Potential Zone	Levee Length in Zone (miles)	Description
I	20	**High susceptibility** to earthquake-induced levee failure. This zone encompasses only Sherman Island and was considered to have high potential for failure due to the presence of substantial liquefiable soils within the non-project levees especially those along the San Joaquin River. These levee reaches have an unusually high amount of cohesionless sandy and silty soils within the levee section, are relatively narrow, are founded on thick deposits of soft soil, and have a history of distress.
II	301	**Medium to medium-high susceptibility** to earthquake-induced levee failure. This zone is within the central Delta and generally includes levees with high sections founded on thick deposits of soft soil. Most of the levees which have had histories of distress or that have failed during flood events are located within this zone. Vulnerability varies significantly within this region, even along adjacent levee reaches, principally as a function of the presence or absence of liquefiable soils at the base of the levee embankment sections.
III	116	**Low to medium susceptibility** to earthquake-induced levee failure. This zone is located on the southern and western periphery of the Delta and generally involves levees of smaller heights founded on thinner layers of soft soil.
IV	223	**Low to medium susceptibility** to earthquake-induced levee failure. This zone is located on the northern and eastern periphery of the Delta and generally involves levees of smaller heights founded on thinner layers of soft soil.
TOTAL LENGTH	660 miles	

4.5 ESTIMATES OF LIQUEFACTION-INDUCED LEVEE FAILURES

Liquefaction fragility estimates (failures per 100 miles of levee) were developed by the sub-team for different earthquake loadings based on the sub-team's experience with the performance of similar earth structures. The three principal steps in developing these estimates were as follows:

1. Levee geometries and geotechnical data from over 34 "sites" within the Delta were reviewed and evaluated. Each "site" was a levee reach (or length), and these varied from as little as a few hundred feet to reaches many hundreds of feet in length. The information reviewed included results from boring logs, Standard Penetration Tests (SPT), Cone Penetration Tests (CPT), soil classification testing, and shear strength testing.

2. The liquefaction potential of sandy and silty soils within both the levee and foundation soil strata was evaluated using the penetration test data and the well-established correlation developed by Seed, et al. (1984), with suitable corrections for magnitude and duration effects. Post-liquefaction shear strengths were evaluated based on the correlation developed by Seed and Harder (1990), and the performance of similar earth structures during recent earthquakes.

   Post-liquefaction shear strength estimates were used to evaluate the associated displacement and deformation potential of levees following the triggering of liquefaction. The displacement or deformation evaluation was used to obtain an estimate of the potential for levee sections at each site to fail following an earthquake.

3. The resulting estimated potentials for levees to fail due to liquefaction distress were then used to statistically characterize the likelihood of liquefaction-induced levee failures, for various levels of shaking, within each of the four Damage Potential Zones shown in Figure 4-1. The evaluations outlined in these three steps were performed in both qualitative assessments as well as with quantitative approaches, and the evaluations developed by various sub-team members were resolved to develop consensus ranges of fragility estimates. These estimates also incorporate differences in risk associated with daily (tidal) and seasonal variations in water levels in the rivers and sloughs.

The resulting liquefaction-related fragility estimates for each of the four Delta Damage Potential Zones are presented in Table 4-2. For peak accelerations less than 0.1g, the estimated fragility values are relatively low. This is in good agreement with the documented performance of Delta levees subjected to historical earthquakes. Peak base accelerations from historical earthquakes have been estimated to have been less than about 0.08g since reclamation of the Delta began in 1868 (see CDWR, 1992). However, as base accelerations (seismic loading) increase, the estimated levee fragility also increases for all four damage potential zones.

One of the important findings from the liquefaction fragility estimates is that the hazard associated with this mode of failure is much greater for Zone I (Sherman Island) than for the other three zones. This is because extensive layers of liquefiable sandy soils are known to exist within the levees protecting Sherman Island. No other levee is known to have such a large extent of liquefiable soils present in the levee. Similarly, Sherman Island is the western-most island, and so is closest to the principal seismic source zones and thus the island most likely to experience strong shaking levels.

Another important finding is that globally, across all four Damage Potential Zones, the fragility associated with potential soil liquefaction is much higher than that associated with potential non-liquefaction failure modes. This has important ramifications with regard to potential options for reducing seismic fragility along levee sections.

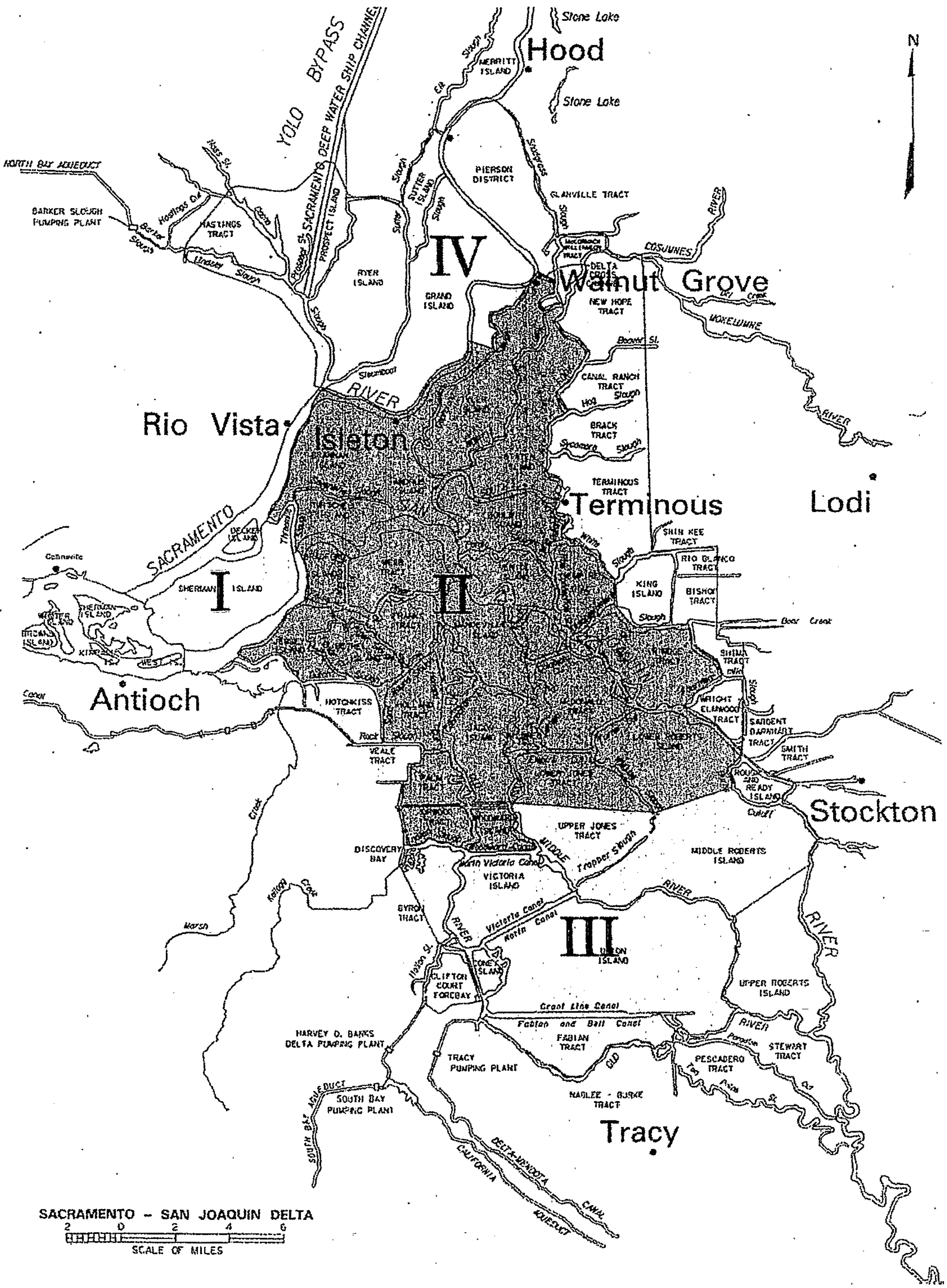

Figure 4.1: Damage Potential Zones within the Delta

D —0 3 2 4 0 6

4.6 ESTIMATES OF LEVEE FAILURES FOR NON-LIQUEFACTION EARTHQUAKE-INDUCED DISPLACEMENTS

The sub-team also believes that some marginally-stable levees will deform significantly during an earthquake due to cyclic inertial loading. Such deformations could lead to levee failure even if the levee and foundation soils did not experience liquefaction. The sub-team estimated levee fragility for the non-liquefaction deformation mode of failure using the following approach:

- The sub-team first estimated the number of marginally stable levee sites in each Damage Potential Zone. The members of the sub-team, and their aggregated personal knowledge of individual islands and levee reaches, was particularly important here. Three levels of marginal stability were considered and the number of marginal sites for each level was estimated for each zone.

- The levee deformation that would be induced by earthquake shaking was estimated for each level of marginal stability using one-dimensional dynamic response analyses coupled with Newmark-type double-integration deformation calculations. The response analyses were used to develop estimates of deformation potential specifically appropriate to the usual foundation soil conditions prevalent throughout the Delta. Levee deformation estimates were generated for a range of base accelerations.

- The estimated levee deformations were then converted into probabilities of failure using a relationship developed by the sub-team. This relationship considered daily and seasonal variations in outboard (river) water levels, varying freeboard, cracking, and seepage erosion and piping potential. The failure probabilities were then summed for each level of marginal stability within a zone, and then expressed as a levee fragility in terms of expected failures per 100 miles of levee within each zone for a range of base accelerations. These results are presented in the last two columns of Table 4-2.

4.7 ESTIMATES OF LEVEE FRAGILITY DURING SEISMIC EVENTS

Table 4-2 presents levee fragility values estimated for both liquefaction and non-liquefaction deformation modes of failure. In comparison with the liquefaction mode of failure, the deformation levee fragility values are much lower, only approximately 10 percent of the liquefaction values. In addition, while there is a significant difference in the liquefaction fragilities estimated for Zones I and II, there is not as large a difference in the non-liquefaction deformation fragilities. This is principally because the number of marginally stable sites per levee mile are believed to be within the same order of magnitude within both Zones I and II in the central Delta.

TABLE 4-2: ESTIMATED FAILURE RATE (FRAGILITY) FOR BOTH LIQUEFIED AND NON-LIQUEFIED REACHES - FAILURES PER 100 MILES

Magnitude 6.0 Rock/Stiff Soil Peak Acc. (g)	Damage Potential Zone	Levee Length (miles)	Estimated Fragility - Number of Levee Failures per 100 miles	
			Liquefied Reaches	Non-Liq. Reaches
	I	20	0.005 - 0.50	0.030 - 0.075
	II	301	0,001 - 0.083	0.015 - 0.036
0.05	III	116	0.001 - 0.033	0.003 - 0.010
	IV	223	0.001 - 0.033	0.003 - 0.010
	I	20	0.20 - 2.5	0.050 - 0.12
	II	301	0.080 - 0.33	0.023 - 0.052
0.10	III	116	0.050 - 0.15	0.004 - 0.017
	IV	223	0.050 - 0.15	0.004 - 1.016
	I	20	2.5 - 10.	0.16 - 0.35
	II	301	0.66 - 1.7	0.070 - 0.15
0.15	III	116	0.29 - 1.2	0.010 - 0.057
	IV	223	0.29 - 1.2	0.011 - 0.049
	I	20	5. - 20.	0.36 - 0.77
	II	301	1.7 - 5.0	0.16 - 0.33
0.20	III	116	0.88 - 2.3	0.022 - 0.13
	IV	223	0.88 - 2.3	0.025 - 0.11
	I	20	15. - 30.	1.5 - 3.2
	II	301	5.0 - 10.	0.66 - 1.4
0.30	III	116	2.4 - 5.9	0.092 - 0.53
	IV	223	2.4 - 5.9	0.11 - 0.46

4.8 MAGNITUDE CORRECTION FACTORS

The estimates for levee failures and fragility presented in the previous table are for earthquake shaking associated with a magnitude 6.0 event. For the same level of shaking, larger magnitude earthquakes will produce longer durations of shaking (more cycles), and so will induce more damage and more levee failures than smaller magnitude events because larger magnitude earthquakes have longer durations and larger numbers of strong cycles of shaking. To adjust the fragilities for earthquake magnitudes other than Magnitude 6.0, the following scaling factors were used:

A. Liquefaction Mode of Failure:

A magnitude correction factor for the liquefaction mode of failure was developed using the Idriss (1997) magnitude scaling factors for triggering of liquefaction. These corrections are slightly larger than those previously used by Seed, et al. (1984), and are slightly lower than those recommended by the NCEER Liquefaction Working Group (Youd, et al, 1998).

B. Non-Liquefaction Deformation Mode of Failure:

A magnitude correction factor for the non-liquefaction deformation mode of failure was developed using the Earthquake Severity Index described by Bureau et al. (1988). This correction is much larger than the one for liquefaction, but is comparable with the cyclic inertial deformation results obtained by Makdisi and Seed (1977).

Appendix B presents additional information regarding the estimates of the levee fragilities and the associated evaluations and calculations used to develop them.

5 PROBABILISTIC EVALUATION OF LEVEE FAILURES

5.1 METHODOLOGY

The seismic hazard analysis (or Probabilistic Seismicity Evaluation, as described in Section 3) was combined with the levee fragility evaluation to develop a probabilistic evaluation of the number of levee failures that would be expected to occur in a single earthquake, as a function of return period or annual likelihood of occurrence of different levels of earthquake intensity.

The levee failure probability analysis is an extension of standard probabilistic seismic hazard analysis. The difference is that instead of calculating the probability of the ground motion exceeding a specified value at a location, the probability of a specified number of levee failures being exceeded in a single earthquake was computed. In this way, the performance of the entire levee system was considered simultaneously. This avoids the problems of using individual site hazard curves, which may represent different earthquakes at different parts of the Delta.

These analyses consider the performance of the Delta levees for specific earthquake scenarios. For each earthquake scenario, the probability of one or more levee failures occurring within the Delta was computed. This process is repeated for two or more failures, three or more failures, and so on. Following the probabilistic seismic hazard analysis, rather than considering just one or two scenarios, it was then feasible to consider all possible earthquake scenarios and to keep track of their probabilities of occurring.

The probability of a given number of levee failures for an earthquake scenario is multiplied by the probability of the scenario earthquake actually occurring. This rate of failure is then summed over all of the scenarios to give the total rate of various numbers of levees failing in a single earthquake. A Poisson assumption for the earthquake occurrence is used to convert the rate of failures into a probability of failures. The result is a hazard curve for the "expected" number of levee failures in a single earthquake. The details of the mathematical formulation used in the calculation of the probability of levee failures is described in Appendix C.

The resulting median hazard curves for levee failures are shown in Figure 5-1. Two curves are presented; one for the CRCV seismicity model and one for the Lettis model (see Section 3). The large difference in the number of failures for the Lettis and CRCV models reflects the impact of the assumption of the existence (or non-existence) of a large CRCV blind thrust fault under the west end of the Delta. At low numbers of breaks, the two source models lead to similar levee failure hazard because this part of the curve is controlled by large distant earthquakes on the Hayward and San Andreas fault as well as small local earthquakes which are included in both models. At larger numbers of breaks, the differences between the two fault models become more pronounced.

Considering the uncertainties in the two fault models, and the uncertainties inherent in the various elements of the overall seismic fragility and hazard evaluation; and based on their collective judgement, the sub-team developed the final, overall estimate of seismic levee fragility shown in Figure 5-2. This represents the final consensus opinion, and includes allowances for current sources of uncertainty with regard to both seismicity (loading) and seismic levee fragility (resistance).

The same Levee Fragility estimates are alternately shown with respect to return periods of 50, 100, and 200 years (see Figure 5-3). These graphs show the probability of exceeding a particular number of levee breaks in a single event during a given exposure time period.

5.2 ILLUSTRATIVE SCENARIO EVENTS

In order to further illustrate the results shown in Figure 5-1, this methodology was used to develop scenario predictions for the following three illustrative scenario events:

1. Magnitude 7.1 earthquake on the Hayward Fault
2. Magnitude 6.25 earthquake on the Concord Fault
3. Magnitude 6.0 earthquake on the CRCV Fault, immediately northwest of Sherman Island

Figures 5-4 to 5-6 show the estimated number of levee breaks per zone, and the peak acceleration contours for stiff soil or rock, for each of these three scenario events.

As shown in Figure 5-4, a Magnitude 7.1 event on the relatively distant Hayward Fault produces relatively low to moderate levels of acceleration, but of fair duration, and results in a low predicted number of levee failures (on the order of 0 to 4 failures throughout the Delta).

As shown in Figure 5-5, a Magnitude 6.25 Concord Fault event produces similar levels of peak acceleration at the western end of the Delta (on the order of 0.1g), but these rapidly decrease to the east. This, coupled with a relatively short duration, results in a significantly lower level of predicted levee failures than for the Hayward fault event shown in Figure 5-4.

Figure 5-6 illustrates the third scenario event, in this case a Magnitude 6.0 on the CRCV Fault at the northwestern edge of the Delta. The proximity of the fault rupture produces much higher levels of acceleration, and results in much higher predicted numbers of levee failures, especially in Zones I and II. The numbers of predicted failures for this scenario event are fairly high (on the order of 13 to 32 through the entire Delta), but the annual likelihood of occurrence of this even is much lower than for the events illustrated in Figures 5-4 and 5-5.

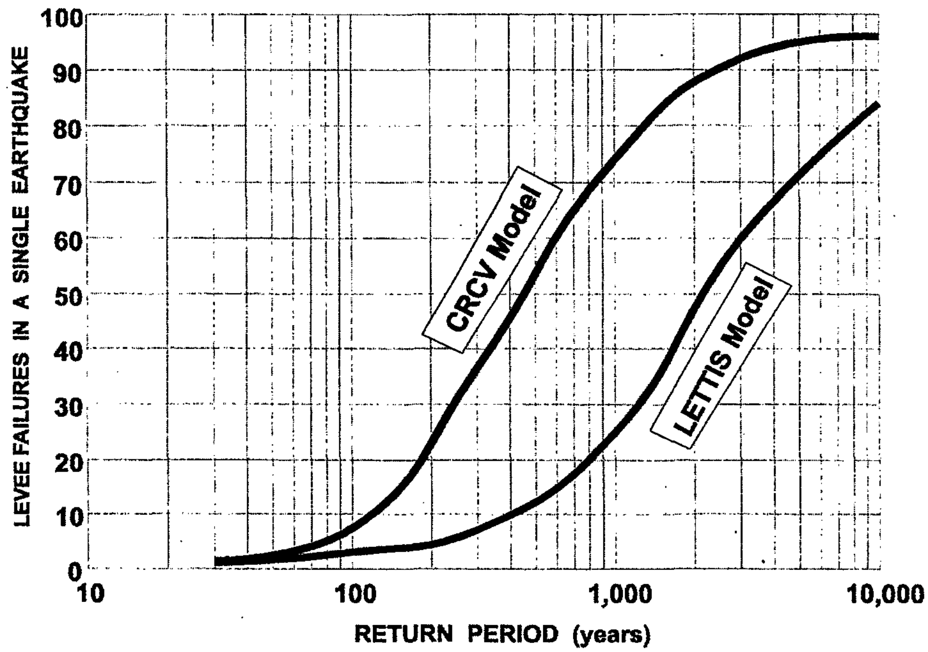

Figure 5.1: Number of Levee Failures in a Single Earthquake–both Fault Models Shown

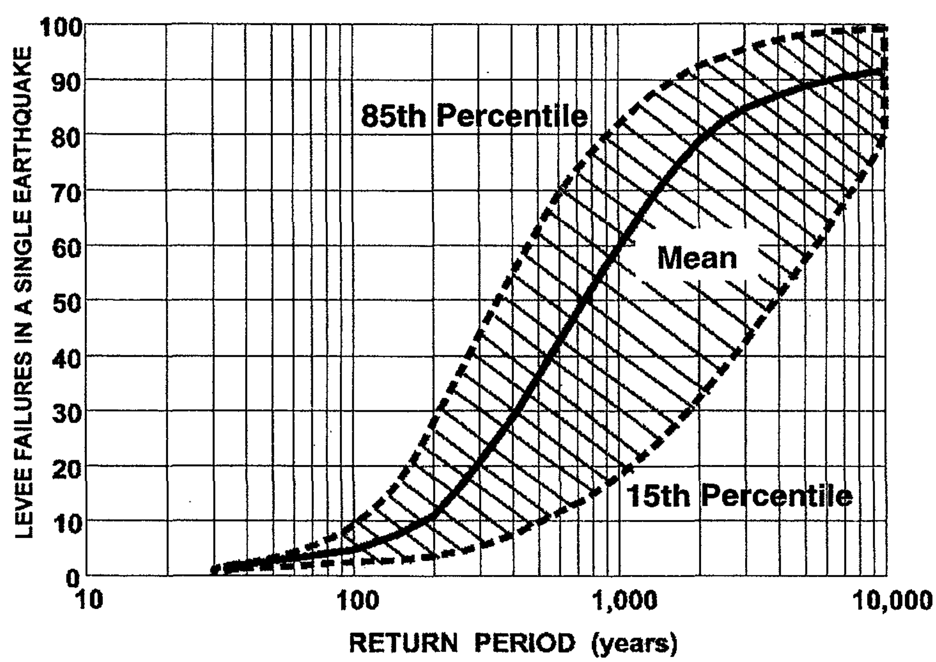

Figure 5-2: Number of Levee Failures in a Single Earthquake-Fault Models Combined

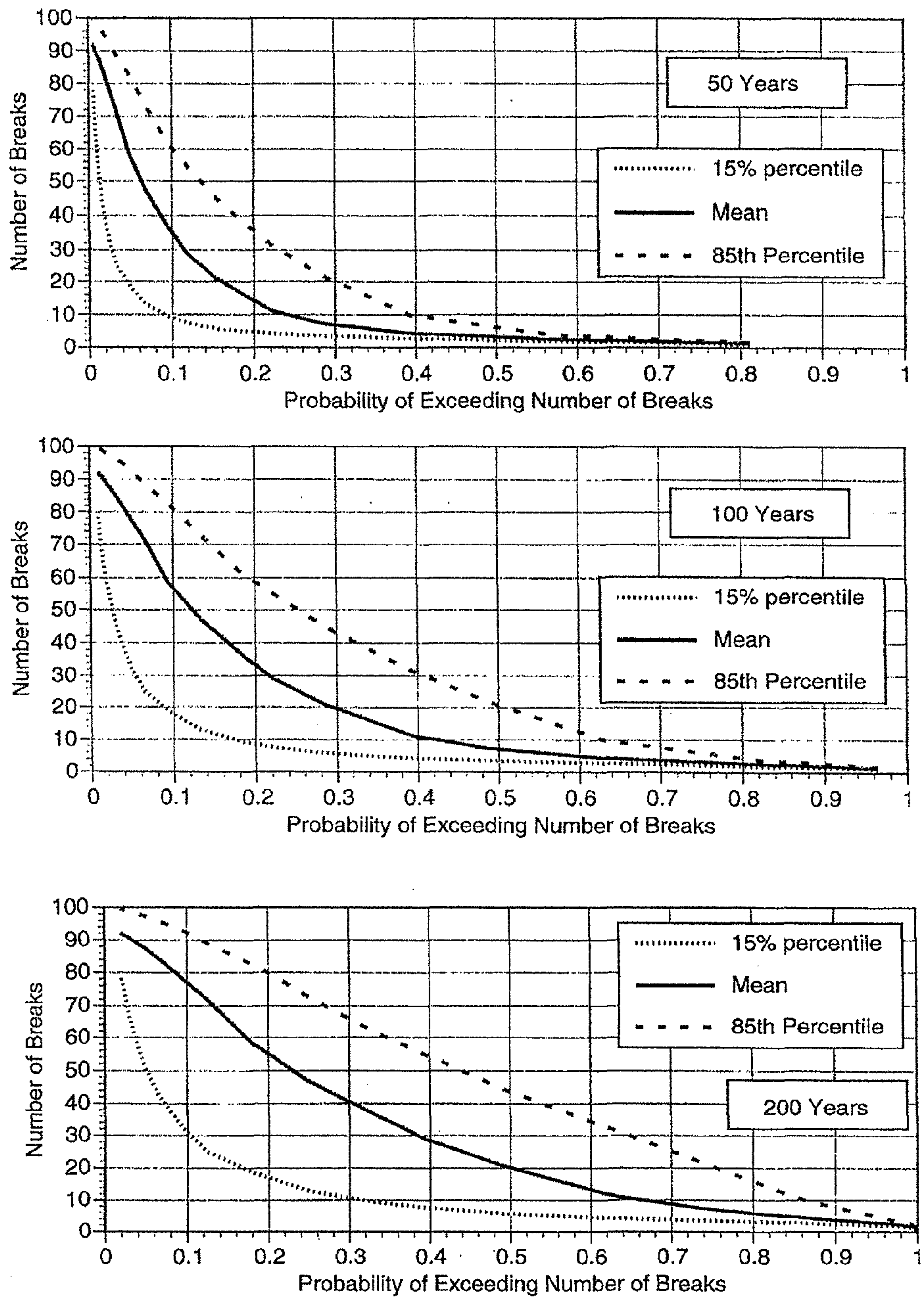

Figure 5-3: Probability of Exceedance vs Number of Levee Breaks for 50, 100 and 200 Year Return Periods

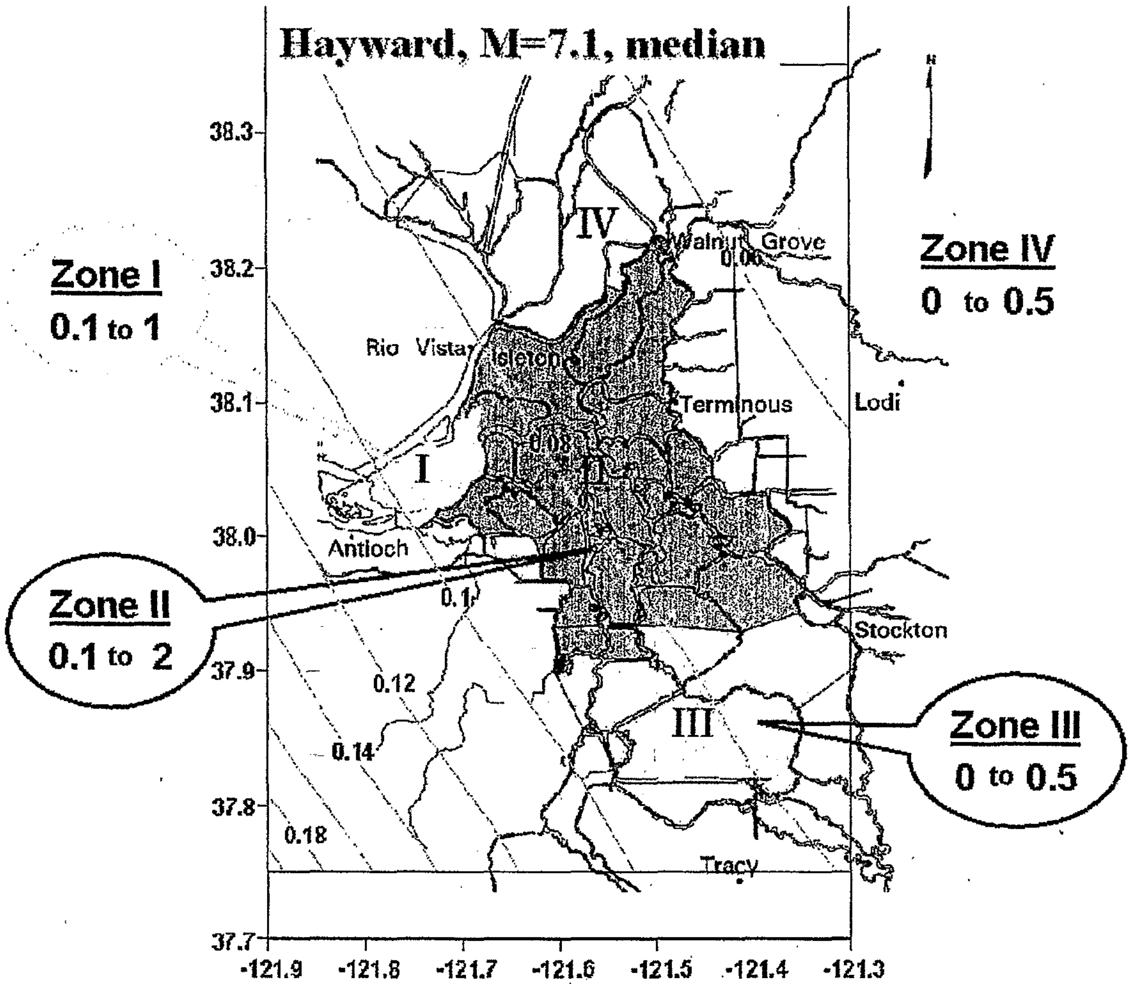

Figure 5-4: Acceleration Contours and Expected Number of Levee Failures for a Magnitude 7.1 Earthquake on the Hayward Fault

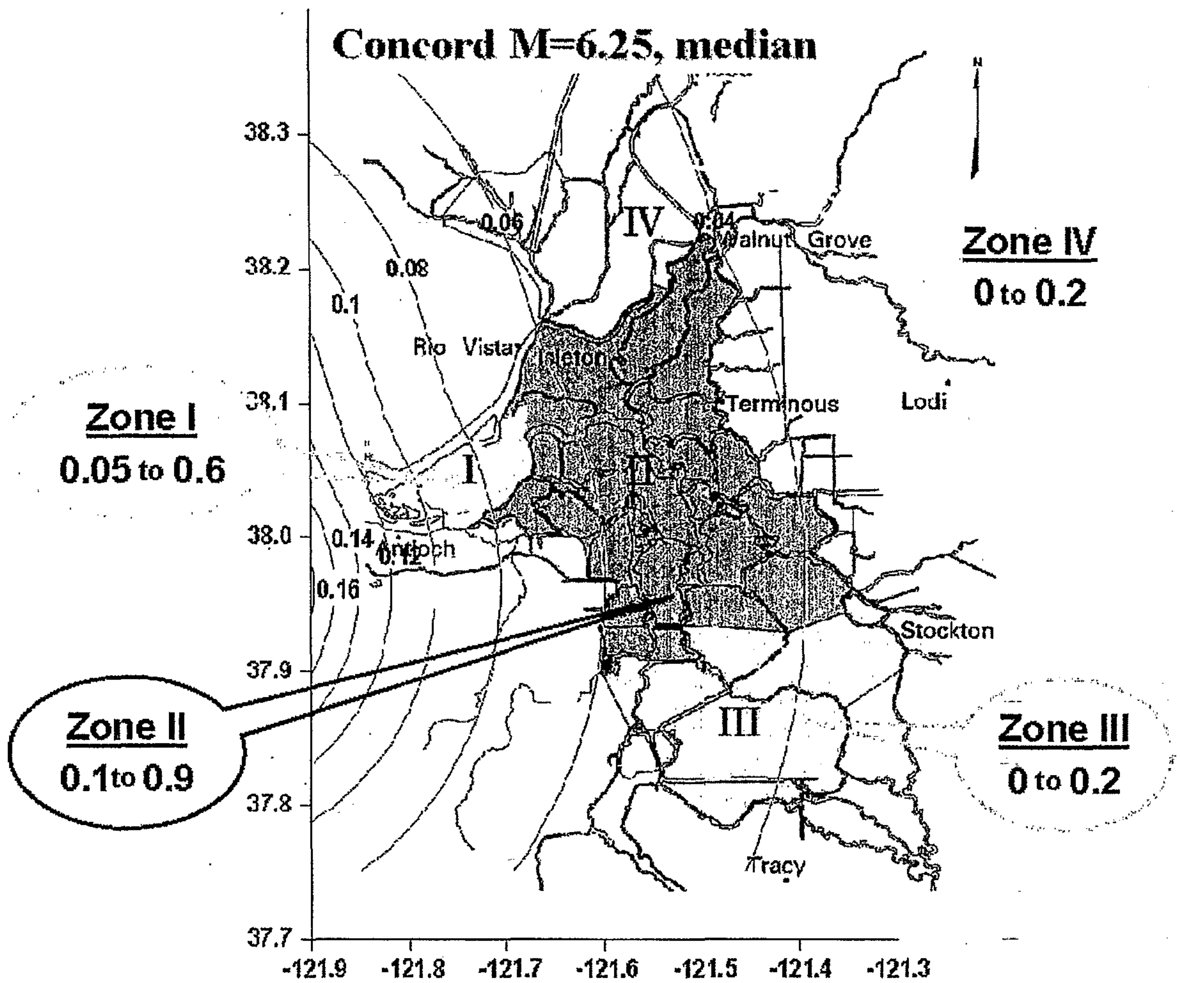

Figure 5-5: Acceleration Contours and Expected Number of Levee Failures for a Magnitude 6.25 Earthquake on the Concord Fault

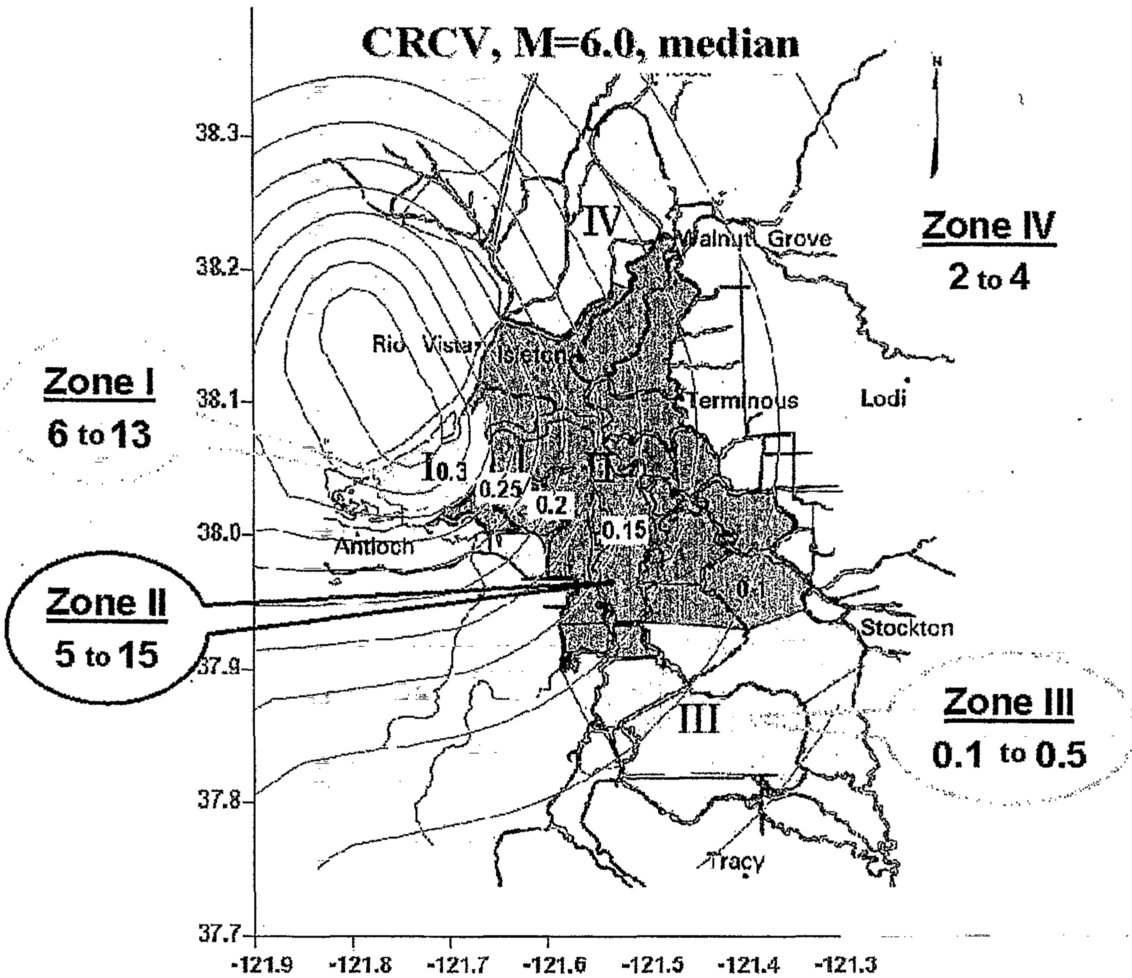

Figure 5-6: Acceleration Contours and Expected Number of Levee Failures for a Magnitude 6.0 Earthquake on the CRCV Fault

6 MITIGATION OF SEISMIC LEVEE VULNERABILITY

A determination as to the acceptability of the current level of seismic vulnerability for Delta levees is beyond the scope of the sub-team. It is, however, appropriate at this juncture for the sub-team to comment on the general feasibility of various actions that might be considered for reducing this hazard exposure and/or their impact on the environment, water quality, water conveyance, farming, etc.

In general, there are at least four types of approaches which might be considered in order to reduce either seismic levee vulnerability and/or at least some of its potential impacts. These include:

1. Improvement of seismic levee stability in order to directly reduce seismic vulnerability.

2. Improvement of post-earthquake response capability to speed levee repairs.

3. Development of seismically-protected routes for water conveyance, either through the Delta or around the Delta.

4. Development of increased storage capacity south of the Delta to reduce the impact of a disruption in water conveyance and water export capacity.

The simplest and most straight-forward approach to consider is the direct improvement of seismic levee stability. Unfortunately, it is extremely complex and expensive. Simple levee upgrades currently being considered to improve static (non-seismic) stability (e.g. PL84-99 upgrades) are largely ineffective at reducing seismic fragility. These types of "static" upgrades will do very little to reduce the risk of levee failures associated with soil liquefaction, and are unlikely to reduce the exposure levels shown in Figures 5-2 and 5-3 by more than about 10% (almost no change in seismic exposure).

A significant reduction in seismic vulnerability would require improvement of the loose levee embankment and foundation soils, by densification, or major geometric improvements in levee cross-sections. This work requires careful engineering and monitoring to avoid levee or foundation failures during construction. The cost of such seismic improvements, per linear foot of levee, is usually much higher than the cost of non-seismic improvements. Properly engineered and implemented, seismically-targeted levee improvements could reduce seismic vulnerability, at least for selected islands or levee sections, but it would be very difficult (at any cost) to fully eliminate potential seismic vulnerability.

A second potential measure for reducing seismic levee vulnerability, and its impact, would be to improve emergency response capability. At the present time, the ability to

D-032418

respond to more than a limited number levee failures following a seismic event is probably very limited. Response capability is limited by lack of suitable or available barges and equipment, by limited availability of construction materials (e.g. rockfill borrow material, plastic sheeting and filter fabric), limited access, and by a lack of pre-planned and coordinated response plans. A significant improvement in response capability would probably be a very economical interim step in reducing overall seismic exposure. Purchase and maintenance of barges and cranes, stockpiling of coarse rock at several sites, increased deployment of stocks of plastic sheeting and filter fabric on most islands, planning and coordination of response by various groups and agencies, etc., would greatly increase the number of failures that could either be prevented or addressed and repaired within a given time-frame (e.g. within six months, or within a given water season, etc.).

The development of seismically-protected water conveyance routes, either through the Delta or around the Delta, has been considered for various reasons by other groups in the CALFED process. Either approach is technically feasible, in principle, but at considerable cost. Evaluating the environmental and/or political ramifications of such an alternative is beyond the scope of the sub-team.

Similarly, it is beyond our scope to comment on the cost or feasibility of expanding storage capacity south of the Delta.

7 SUMMARY OF FINDINGS

The studies presented in the previous sections were completed to provide an evaluation of the current seismic vulnerability of levees in the Sacramento-San Joaquin Delta. The major findings of this study are summarized as follows:

- Figures 3-1 and 3-2 show the principal faults considered in the development of a probabilistic assessment of seismicity. Two models were considered in this analysis: One which included a potentially significant blind thrust fault system along the western edge of the Delta, and one which did not. Although both fault models predict about the same general levels of peak accelerations for a given return period, the earthquake magnitudes associated with the motions are different, with somewhat higher magnitudes resulting from the fault model with the blind thrust fault (see Figures 3-3 and 3-4).

- This study characterized the levee fragility of the Delta by subdividing the Delta into four Damage Potential Zones (see Figure 4-1). Seismic vulnerability is highest in Zone I, Sherman Island, due to poor levee embankment and foundation soils, and higher exposure to seismic shaking at the western edge of the Delta. Zone II, the central area of the Delta, has the next highest overall level of seismic levee fragility. Zones III and IV, with levees of lower heights founded on general firmer soils, have generally lower levels of levee fragility.

- Levee fragility, or the risk of levee failures within each of the four damage potential zones, was estimated for a range of potential earthquake shaking. The two potential modes of levee failure used in this assessment were:

  (1) Soil liquefaction (loss of strength of saturated sandy and silty soils).

  (2) Inertially-driven deformations of "weak," marginally-stable levee sections.

  Levee fragility values for both of these potential modes of failure are presented in Table 4-2.

- Finally, seismic vulnerability was evaluated by combining the probabilistic assessment for various earthquake motions (loading) with the estimated seismic fragility (resistance) of different levee reaches. The fault model without the blind thrust fault gave lower predicted numbers of levee failures (e.g. 3 vs. 7 levee failures in a single earthquake for a return period of 100-years). As it is not presently possible to conclusively select between the two faulting models studied, this study ended up averaging the results from the two fault models, with the final levee vulnerability results shown in Figures 5-2 and 5-3.

- A brief discussion of some of the options for reducing the current seismic vulnerability of Delta levees was also presented in Section 6. Briefly, it was concluded that attempting to significantly reduce seismic levee fragility would be both difficult and expensive, and that simply making minor modifications (e.g.: along the lines of PL84-99 criteria) would not significantly reduce seismic vulnerability. Developing improved emergency response plans and measures (including stockpiling of critical materials and equipment) was thought to have considerable merit, especially in the short-term.

- The next phase of this committees' studies should include further examination of various proposed long-term mitigation alternatives.

8 BIBLIOGRAPHY

Abrahamson, N. A. and W. Silva (1997). Empirical Response Spectral Attenuation Relations for Shallow Crustal Earthquakes, *Seis. Re. Letters*, Vol. 68, No.1, 94-127.

Ake., J., J. Wilson, D. Ostenaa, and R. LaForge (1991), "Preliminary Seismic Risk Analysis for the Delta Water Management Study, North Delta;" Seismotectonic Report 91-3, U.S. Bureau of Reclamation, Denver, CO, 40 p.

Almgren, A. A. (1978), "Timing of Tertiary Submarine Canyons and Marine Cycles of Deposition in the Southern Sacramento Valley, California;" in Stanley, D. J., and Kelling, Gilbert, eds., Sedimentation in Submarine Canyons, Fans, and Trenches, Stoudsburg, PA, Dowden, Hutchison, and Ross, p. 276-291.

American Society for Testing Materials, Volume 4.08, Soils and Rock; Dimension Stone; Geosynthetics.

Association of California Water Agencies (1991), "California's Water Future, An Overview and Call to Action."

Astaneh, A., V. V. Bertero, B. A. Bolt, S. A. Mahin, J. P. Moehle, and R. B. Seed (1989), "Preliminary Report on the Seismological and Engineering Aspects of the October 17, 1989 Santa Cruz (Loma Prieta) Earthquake;" Earthquake Engineering Research Center, University of California at Berkeley, Report No. UCB/EERC-89/14, 51 p.

Bakun, W. H., R. S. Clark, R. S. Cockerham, W. L. Ellsworth, A. G. Lindh, W. H. Prescott, A. F. Shakal, P. Spudich (1984), "The 1984 Morgan Hill, California, Earthquake," Science, Vol. 225.

Ballesteros, R., verbal communication.

Bell, T., verbal communication.

Bender, B. and D. M. Perkins (1987), "SEISRISK III, a Computer Program for Seismic Hazard Estimation;" U. S. Geological Survey, Bulletin 1772, 48 p.

Boore, et al. (1997)

Bolt, Bruce (1982), "Earthquake Ground Motions, San Joaquin Delta Region."

Boulanger, et al. (1997)

Brandt, C., verbal communication.

Bureau, et al (1988), Magnitude Scaling for inertial def's.

California Department of Water Resources, Allsup and Duddley (1976), "Organic Isopach Map."

California Department of Water Resources, the Resources Agency, State of California (1957), "Drill Log - Salinity Control Barrier Investigation - Elmwood and Sargent Barnhart Tract."

California Department of Water Resources, State of California (1967), "Pilot Levee Maintenance Study, Sacramento-San Joaquin Delta." Bulletin 167, 24 p.

California Department of Water Resources (1981), "Seismicity Hazards in the Sacramento-San Joaquin Delta;" State of California, Central District, Sacramento, CA, 26 p.

California Department of Water Resources (1982), "Delta Levees Investigation, State of California;" Department of Water Resources Bulletin 192-82.

California Department of Water Resources, Central District (1982), "Discovering and Rediscovering the Fragility of Levees and Land in the Sacramento-San Joaquin Delta, 1870-1879 and Today."

California Department of Water Resources (1983), "Alternatives for Delta Water Transfer."

California Department of Water Resources (1986), "Delta Subsidence Investigation," Progress Report.

California Department of Water Resources (1987), "Sacramento-San Joaquin Delta Atlas."

California Department of Water Resources (1989), "Delta Levee Special Project Investigation, Sacramento-San Joaquin Delta, California."

California Department of Water Resources (1990), "Actions and Priorities, Delta Flood Protection Act, Eight Western Delta Islands."

California Department of Water Resources (1992),

California Division of Mines and Geology (1975), Note No. 43.

California Division of Mines and Geology (1975), Fault Map of California, Compiled by Charles W. Jennings.

California Division of Mines and Geology (1981), Preparation of Isoseismal Maps and Summaries of Reported Effects for Pre-1900 California Earthquakes, Open File Report 81-11 SAC, EDMG, 182 p.

California Division of Mines and Geology (1996)

Caltrans (1982), "Geology Map Along Potato Slough Bridge," Route 12, Bridge No. 29-101, Post Mile 4.7, Sheet 1 of 2.

Caltrans (1987), "Geology Map Along Potato Slough Bridge," Route 12, Bridge No. 29-101, Post Mile 4.7, Sheet 4 of 6.

Campbell (1997)

Chirapuntu, S. and J. M. Duncan (1975), "The Role of Fill Strength in the Stability of Embankments on Soft Clay University of California, Berkeley."

Chirapuntu, S. and J. M. Duncan (1977), "Cracking and Progressive Failure of Embankments on Soft Clay Foundations," Geotechnical Engineering Report No. TE 75-3, University of California, Berkeley.

Clark, M. M., K. K. Harms, J. J. Lienkaemper, D. S. Harwood, K. R. Lajoie, R. V. Sharp, J. D. Sims, J. C. Tinsley III, Late Quaternary Faults of California; U. S. Geological Survey Open-File Report 84-106.

Cornell (1968)

Converse, Ward, Davis, and Dixon (1981), Partial Technical Background Data for the Mokelumne Aqueduct Security Plan; unpublished report for East Bay Municipal Utility District, Oakland, CA.

Converse, Ward, Davis, and Dixon (1982), Partial Technical Background Data for the Mokelumne Aqueduct Security Plan.

Cornell, C. A. and E. H. Vanmarcke (1969), "The Major Influences of Seismic Risk," Proc. of the 4th World Conference on Earthquake Engineering, Santiago, Vol. 1, p. 69-83.

Dames and Moore (1985), "McDonald Island Levee Stability Study, McDonald Island, California;" unpublished report for Pacific Gas and Electric Company, Vol. 2, data report.

Dames and Moore (1987), "Pipeline 131 Levee Stability Study, Sherman Island, California;" prepared for Pacific Gas and Electric Company.

Dames and Moore (1988), "Reevaluation - Pipeline 131 Levee Stability Study, Sherman Island, California;" prepared for Pacific Gas and Electric Company.

Dames and Moore (1991), "General Seismic and Geotechnical Risk Assessment, Sacramento-San Joaquin Delta, California."

De Alba, P., H. B. Seed, E. Retamal, and R. B. See (1987), "Residual Strength of Sand from Sam Failures in the Chilean Earthquake of March 3, 1985, "Earthquake Engineering Research Centra, Report NO. UCB/EERC-87/11, University of California, Berkeley.

Dickenson, S. E. and R. B. Seed (1991), "Correlations of Shear Wave Velocity and Engineering Properties for Soft Soil Deposits in the San Francisco Bay Region." Draft Report EERC 91-XX, Earthquake Engineering Research Center, Report No. UCB/EERC-87/11, University of California, Berkeley.

Donovan, N. C. and A. E. Bornstein (1975), "A Review of Seismic Risk Applications;" Second International Conference on Applications of Statistics and Probability in Soil and Structural Engineering, Aachen, Vol. 1, p. 265-280.

Driller, M. W. (1990), "Analysis of Safe Slopes for Levees in the Sacramento-San Joaquin Delta." Project submitted in partial satisfaction of the requirements for the degree of Master of Science, California State University, Sacramento.

Duncan, J. M. and W. N. Houston (1981), "Estimating Failure Probabilities for California Levees," Geotechnical Journal, American Society of Civil Engineers.

Dutra, E. (1976), "History of Sidedraft Clamshell Dredging in California.

Earth Science Associates (1982), "Seismotectonic Study of Contra Loma Dam and Vicinity;" unpublished contract report to U.S. Bureau of Reclamation, Denver, Colorado, 112 p.

East Bay Municipal Utility District (1982), Addendum to Converse Word Davis Dixon Consultants' December 1981 Report "Partial Technical Background Data for the Mokelumne Aqueduct Security Plan (MASP);" East Bay Municipal Utility District, Project Engineering Division, Design Section, Oakland, California.

EERI (1990), Reconnaissance Report, Loma Prieta Earthquake of October 17, 1989.

Engineering News Record, October 14, 1991, Funding Quake Repairs Still Draws Controversy, p. 9.

Evening Bee, April 18, 1906.

Finch, M.O. (1983), "Earthquake Damage in the Sacramento-San Joaquin Delta," California Geology, February, p. 39-44.

Finch, M. O. (1987), "Liquefaction Potential of the Sacramento-San Joaquin Delta, California;" Thesis for Master of Science in Geology, University of California, Davis, 181 p.

Finch, M. O. (1988), "Estimated Performance of the Twitchell Island Levee System, Sacramento-San Joaquin Delta, Under Maximum Credible Earthquake Conditions;" Bull. Asso. Geol., Vol. XXV, No. 2, p. 207-217.

Foott (1991), "Investigation of Threatened Levees on Sherman Island." Roger Foott Associates, Inc. Job No. 085-002.

Fredlund, D. (1985), "PC Slope Stability Analysis User's Manual S-30," Geoslope Programming, Ltd.

Frame, R. G. (1944), "Rio Vista Gas Field;" California Division of Oil and Gas, Summary of Operations-California Oil Field, Vol. 30, No. 1, p. 5-14.

Gamble, J. C. (1991), verbal communication with Raphael A. Torres.

Geomatrix (1992). Seismic ground motion study for San Joaquin River - Antioch Bridge, Report to Caltrans, Contract No. 59N772.

Goter, S. K. (1988), "Seismicity of California," National Earthquake Information Center, U.S. Geological Survey.

Gutenberg, B. and C. F. Richter (1954), "Seismicity of the Earth;" Princeton University Press, 2nd ed., P. 16-25.

Gutenberg, B. and C. F. Richter (1956), "Seismicity of the Earth;" Princeton University Press, 2nd ed., p. 16-25.

Hanks, T. C. and H. Kanamori (1979), "A Moment Magnitude Scale;" Journal of Geophysical Research, Vol. 82, P. 2981-2987.

Hansen, Gladys and Emmet Condon (1989), "Denial of Disaster, The Untold Story of the San Francisco Earthquake and Fire of 1906," Cameron and Company, San Francisco.

Harding Lawson Associates (1990), "Seismic Design Criteria for Wilkerson Dam, Bouldin Island, California."

Harding Lawson Associates (1990), "Bouldin Island Field Testing Results of Downhole Survey and Resonant Column Test for Peat and Silt."

Herd, D. G. (1979), "The San Joaquin Fault Zone - Evidence for Later Quaternary Faulting Along the West Side of the Northern San Joaquin Valley, California;" [abstract] Geological Society of America, Abstract with Programs, Vol. 11, p. 83.

Houston, W. N. and J. M. Duncan (1978), "Probability of Failure of Levees in the Sacramento-San Joaquin Delta, California." Final Report. Sacramento, California.

Idriss, I. M. (1985), "Evaluating Seismic Risk in Engineering Practice;" in proceeding of the 11th International Conference on Soil Mechanics and Foundation Engineering, San Francisco.

Idriss, I. M. (1989), Sample Input File for Computer Program "HAZARD": "SRD. HAZ, Sample No. LA", on HAZARD Diskette.

Idriss, I. M. (1990), "Response of Soft Soil Sites During Earthquakes;" paper presented at a memorial symposium to honor Harry Bolton Seed at Berkeley, California.

Idriss, I. M. (1991), "HAZARD", Seismic-Hazard Evaluation Program (written in QuickBasic), Diskette.

Idriss, I. M. (1991), "Seismic Source Characterization" (draft); originally an appendix to report by Woodward-Clyde Consultants to Rockwell International re: Seismic Hazard Evaluation at the Shuttle Site at Vandenberg Air Force Base.

Idriss, I. M. (1997)

Idriss, I. M. (1997), San Francisco notes.

Idriss, I. M. (1998), verbal communication with Raphael A. Torres.

Jennings, C. W. (1975), Fault Map of California, Scale 1:750,000, California Division of Mines and Geology.

Jennings, C. W. (1994). Fault activity map of California and adjacent areas with locations and ages of recent volcanic eruptions, Calif. Div. Mines Geol., Map No. 6.

Joyner, W. B. and D. M. Boore (1981), Peak Horizontal Acceleration and Velocity from Strong-Motion Records, Including Records from the 1979 Imperial Valley, California, Earthquake; Bulletin Seis. Soc. Amer., Vol. 71, p. 2011-2039.

Joyner, W. B. and D. M. Boore (1984), Peak Horizontal Acceleration and Velocity from Strong-Motion Records, Including Records from the 1979 Imperial Valley, California Earthquake, in Bulletin of the Seismological Society of America, Vol. 71, No. 6, p. 2011-2038.

Joyner, W. B. and D. M. Boore (1988), "Measurement, Characterization, and Prediction of Strong Ground Motion;" Spec. Pub. 20, Amer. Soc of Civil Engineers, New York, NY, p. 3-102.

Kanamori, H. (1977) "The Energy Release in Great Earthquakes;" Journal of Geophysical Research, Vol. 82, p. 2981-2987.

Keefer, David K. (1978), "Liquefaction and Damage to Dikes Caused by the Off-Miyagi-Prefecture Earthquake of June 12, 1978. the Miyagi-ken-oki Earthquake of June 12, 1978." Earthquake Engineering Research Inst., Reconnaissance Report.

Khamenehpour, B. (1983), "Seismic Stability Problems in Earth Dam Design." Dissertation submitted in partial satisfaction of the requirements for the degree of Doctor of Philosophy, University of California, Berkeley.

Kjeldsen, K. verbal communication with Raphael A. Torres.

Lawson, A. C., Chairman (1908), "The California Earthquake of April 16, 1906;" Report of the State Earthquake Investigation Commission, Carnegie Institute of Washington Publication 87, Vol. 2.

Lettis and Associates (1998)

Lodi Sentinel, May 5, 1906.

Makdisi, F. I. and H. B. Seed (1977), "A Simplified Procedure of Estimating Earthquake-Induced Deformations in Dams and Embankments," Earthquake Engineering Research Center Report UCB/EERC-77/19, University of California, Berkeley.

Marchetti, E., verbal communication with Raphael A. Torres.

Maxey, L., verbal communication with Raphael A. Torres.

McEvilly, T. V. and K. B. Casaday (1967), "The Earthquake Sequence of September 1965 near Antioch, California." Bulletin of the Seismological Society of America. Vol. 57, No. 1, p. 113-124.

McClure, C. R. (1956), "Investigation of the Sacramento-San Joaquin Delta, Ground Water Geology;" Report No. 1, Water Project Authority of the State of California.

Miller, Dr. B. J. (1990), "A New View of the Sacramento-San Joaquin Delta."

Mitchell, D., verbal communication with Raphael A. Torres.

Newmarch, G. (1985), "Seismicity;" (unpublished report) California Department of Water Resources, Technical Information Record 1462-CD-08, Central District, Delta Impact Analysis Program, 103 p.

New Your Tribune, April 19, 1906.

Northrup, J., verbal communication with Raphael A. Torres.

Ostenaa, D., R. LaForge, and J. Wilson (1989), "Preliminary Seismic Risk Analysis for the Delta Water Management Study, South Delta;" (unpublished report) Seismotectonic Report 89-1, U. S. Bureau of Reclamation, Denver, Colorado, 29 p.

Ponce, R., verbal communication with Raphael A. Torres.

Pucci, I., verbal communication with Raphael A. Torres.

Reedy, L., verbal communication with Raphael A. Torres.

River News-Herald and Isleton Journal, January 30, 1980. Salinas Daily Index, April 20, 1906.

Sadigh, et al. (1997)

Schnabel, P. B. and H. B. Seed (1973), "Accelerations in Rock for Earthquakes in the Western U. S.;" Bull. Seis. Soc. Amer., Vol. 63, p. 501.

Schnabel, P. B., J. Lysmer, and H. B. Seed (1972), "SHAKE, a Computer Program for Earthquake Response Analysis of Horizontally Layered Sites;" Earthquake Engineering Research Center, Report No. EERC-72-12, Berkeley, California 88 p.

Schwartz, D. P., K. J. Coppersmith, and F. H. Swan, III (1984), "Method for Estimating Maximum Earthquake Magnitudes;" Proceedings for the 8th World Conference on Earthquake Engineering, Vol. I, p. 279-285.

Seed, H. B., and I. M. Idriss (1970), "Analyses of Ground Motions at Union Bay, Seattle During Earthquakes and Distant Nuclear blasts;" Bulletin of the Seismological Society of America, Vol. 60, No. 1, p. 125-136.

Seed, H. B., and I. M. Idriss (1970), "Soil Moduli and Damping Factors for Dynamic Response Analyses;" Report No. EERC 70-10, Earthquake Engineering Research Center, University of California, Berkeley, California.

Seed, H. B., C. Ugas, and J. Lysmer (1974), "Site Dependent Spectra for Earthquake-Resistant Design," Earthquake Engineering Research Center, EERC 74-12, University of California, Berkeley.

Seed, H. B., F. I. Makdisi, and P. DeAlba (1977), "The Performance of Earth Dams During Earthquakes," Report No. UCB/EERC 77/20, Earthquake Engineering Research Center, University of California, Berkeley.

Seed, H. B., and I. M. Idriss (1982), "Ground Motions and Soil Liquefaction During Earthquakes;" Monograph No. 5, Monograph Series, Earthquake Engineering Research Institute, Berkeley, California, 134 p.

Seed, H. B., I. M. Idriss and I. Arango (1983), "Evaluation of Liquefaction Potential Using Field Performance Data;" ASCE Journal of Geotechnical Engineering, Vol. 109, No. 3, p. 458-482.

Seed, H. B., et al. (1984), "Moduli and Damping Factors for Dynamic Analyses of Cohesionless Soils," Report No. EERC 84-14, Earthquake Engineering Research Center, University of California, Berkeley.

Seed, H. B., K. Tokimatsu, L. F. Harder, R. M. Chung (1984), "The Influence of SPT Procedures in Soil Liquefaction Resistance Evaluations," Earthquake Engineering Research Center, Report No. UCB/EERC-84/15, University of California, Berkeley.

Seed, H. B., R. B. Seed, S. S. Lai, and B. Khamenehpour (1985), "Seismic Design of Concrete Faced Backfill Dams," Procs., Symposium on Concrete Face Rockfill Dams -- Design, construction, and Performance, ASCE, Detroit, Michigan.

Seed, R. B., and L. F. Harder (1990), "SPT Based Analysis of Cyclic Pore Pressure Generation and Undrained Residual Strength;" Proceedings, H. Bolton Seed Memorial Symposium.

Seed, R. B., et al. (1990), "Preliminary Report on the Principal Geotechnical Aspects of the October 17, 1989 Loma Prieta Earthquake;" Report No. EERC 90-05, Earthquake Engineering Research Center, University of California, Berkeley.

Shimasaki, K., verbal communication with Raphael A. Torres.

Shlemon, R. J., E. L. Begg, and A. B. Carlton (1973), "Holocene Evolution of the Sacramento-San Joaquin Delta, California;" International Union for Quaternary Research Sponsored by the Royal Society of New Zealand.

Shlemon, R. J. and E. L. Begg (1975), "Holocene Evolution of the Sacramento-San Joaquin Delta, California;" International Union for Quaternary Research Sponsored by the Royal Society of New Zealand.

Slemmons, D. B. (1982), "Determination of Design Earthquake Magnitudes for Microzonation," in Proceedings of the Third International Earthquake Microzonation Conference, Vol. 1, p. 119-130.

Smart, J. D. and L. L. Von Thun (1983), "Seismic Design and Analysis of Embankment Dams - Recent Bureau of Reclamation Experience," published in Seismic Design of Embankments and Caverns, ASCE Publisher, Terry Howard, Editor.

Stover, C. W., G. R. Reagor, F. W. Baldwin, and L. R. Brewer (1990), "Preliminary Isoseismal Map for the Santa Cruz (Loma Prieta), California Earthquake of October 18, 1898," UTC: U. S. Geological Survey, Open-File Report 90-18.

Sun, J. I. et al. (1988), "Dynamic Moduli and Damping Ratios for Cohesive Soils," Report No. EERC 88-15. Earthquake Engineering Research Center, University of California, Berkeley.

Sykora, D. W. (1987), "Creation of a Data Base of Seismic Shear Wave: Velocities for Correlation Analysis;" U. S. Army Corps of Engineers, Miscellaneous Paper GL-87-26, Vicksburg, Mississippi, 97 p.

Thompson, J. (1982), "The People of the Sacramento Delta," Golden Notes, Sacramento Historical Society.

Toppazada, T. R., D. L. Parke and C. T. Higgins (1978), "Seismicity of California 1900-1931," CDMG Spec. Rept. 135, 39 p.

Toppazada, T. R., C. R. Real, and D. L. Parke (1981), "Preparation of Isoseismal Maps and Summaries of Reported Effects for pre-1900 California Earthquakes;" California Division of Mines and Geology open-file report 81-11 SAC, Sacramento, California, 182 p.

Trifunac, J. D. and A. G. Brady (1975), "On the Correlation of Seismic Intensity Scales With the Peaks of Recorded Strong Ground Motion," Bulletin of the Seismological Society of America, Vol. 65, No. 1.

U. S. Army Corps of Engineers (1982), "Sacramento-San Joaquin Delta, California," Sacramento District. Documentation Report.

U. S. Army Corps of Engineers (COE) (1987), Office Report, "Sacramento-San Joaquin Delta Levees, Liquefaction Potential," Geotechnical Branch, U. S. Army Engineer District, Sacramento, 116 p.

U. S. Army Corps of Engineers (1987), "Sacramento-San Joaquin Delta Levees Liquefaction Potential," Office Report.

U. S. Geological Survey (USGS) (1988), "Probabilities of Large Earthquakes in California on the San Andreas Fault;" by the Working Group on California Earthquake Probabilities, USGS open-file report 88-398, Menlo Park, California, 62 p.

U. S. Geological Survey (USGS) (1990), "Probabilities of Large Earthquakes in the San Francisco Bay Region, California;" by the Working Group on California Earthquake Probabilities, USGS Circular 1053, 51 p.

U. S. Geological Survey (USGS) (1996),

Unruh, J. R. and E. M. Moores (1991), "Quaternary Blind Thrusting in the Southwestern Sacramento Valley, California," Manuscript (second revision), submitted to Tectonics (in press).

Von Thun, J. L. and C. W. Harris (1981), "Estimation of Displacements of Rockfill Dam Due to Seismic Shaking;" in: Prakesh, S., ed., Proceedings of the International Conference on Recent Advances in Geotechnical Earthquake Engineering and Soil Dynamics, Vol. 1, St. Louis, Missouri, P. 417-423.

Von Thun, J. L., L. H. Roehm, G. A. Scott, and J. A. Wilson (1988), "Earthquake Ground Motions for Design and Analysis of Dams;" in: Von Thun, J. L., ed., Proceedings of the Speciality Conference Earthquake Engineering and Soil Dynamics II - Recent Advances in Ground Motion Evaluation, A.S.C.E. Geotechnical Special Publication No. 20, P. 463-481.

Vucetic and Dorby (1991), "Effect of Soil Plasticity on Cyclic Response." ASCE Journal of Geotechnical Engineering, Vol 117, No. 1, p. 89-107.

Wallace, R. E. (1990), "The San Andreas Fault System, California," U. S. Geological Survey Professional Paper P1515.

Wells, D. and K. Coppersmith (1994). Updated empirical relationships among magnitude, rupture length, rupture area, and surface displacement, *Bull Seism. Soc. Am.*, Vol 84, 974-1002.

Wesnousky, S. G. (1986), "Earthquakes, Quaternary Faults, and Seismic Hazard in California;" Journal of Geophysical Research, Vol. 91, No. B12, P 12, 587-12, 631.

Wills, C. J. and E. W. Hart (1992), "Alquist-Priolo Investigations of the Concord Fault: A Progress Report," presented at the Second Conference on Earthquake Hazards in the Eastern San Francisco Bay Area, California State University, Hayward.

Wong, I. G, R. W. Ely, and A. C. Kollman (1988). Contemporary seismicity and block tectonics of the northern California and central Coast ranges-Sierran Block Boundary Zone, California, Journal of Geophysical Research, 93, 7813-7833.

Wong, I. G. (Woodward-Clyde Consultants, Walnut Creek, California) (1991), verbal communication with Raphael A. Torres.

Wong, I. G. (Woodward-Clyde Consultants, Walnut Creek, California) (1991), written communication.

Youd, T. L. and S. N. Hoose (1978), "Historic Ground Failures in Northern California Triggered by Earthquakes." Geological Survey Professional Paper 993. Washington, D.C., U. S. Department of the Interior, Geological Survey.

Youd, et al. (1988), NCEER Workshop Report.

APPENDIX A:

SEISMICITY OF THE DELTA REGION

APPENDIX A: SEISMICITY OF THE DELTA REGION

A1. INTRODUCTION

The Delta is located in a region of relatively low seismic activity. However, if a large earthquake (M≈6.5-7) occurs on a local fault in the Delta region, then there will be large ground motions (with peak horizontal accelerations exceeding 0.2g) at the western edge of the Delta. Although a large local event cannot be ruled out, it has a low probability of occurring. Probabilistic seismic hazard analysis is a method that explicitly considers how often earthquakes of various sizes are likely to occur, and what is the likely ground motion that will result if an earthquake occurs. In this manner, it allows for an evaluation of the seismic risk of the levees.

The probabilistic approach used in this study follows the standard approach first developed by Cornell (1968), with some modifications to more fully address all sources of variability.

There are three main components of variability that are considered in a seismic hazard analysis: what are the likely magnitudes of the earthquakes, where are the earthquakes likely to be located, and what is the likely ground motion given that an earthquake of a specified magnitude has occurred at a specified location.

The source characterization describes the expected rate of earthquakes as well as the distribution of magnitudes and locations. The attenuation relationships describe how strong the resulting ground shaking will be for an event of a given magnitude and location. These components of the hazard analysis are briefly described below. The resulting horizontal peak acceleration hazard is then discussed.

A2. DESCRIPTION OF SEISMIC SOURCES

The faults considered in the hazard analysis are shown in Figure A-1 and A-2, for the two alternative models of the Delta region thrust faults considered in this study. The mean slip-rate, fault width, and maximum magnitude of the faults are listed in Table A-1. The main strike-slip faults in the Bay area (San Andreas, Hayward, Calaveras) contribute to the hazard in the Delta for short return periods, but the smaller (and more local) faults contribute more significantly to the overall hazard at longer return intervals.

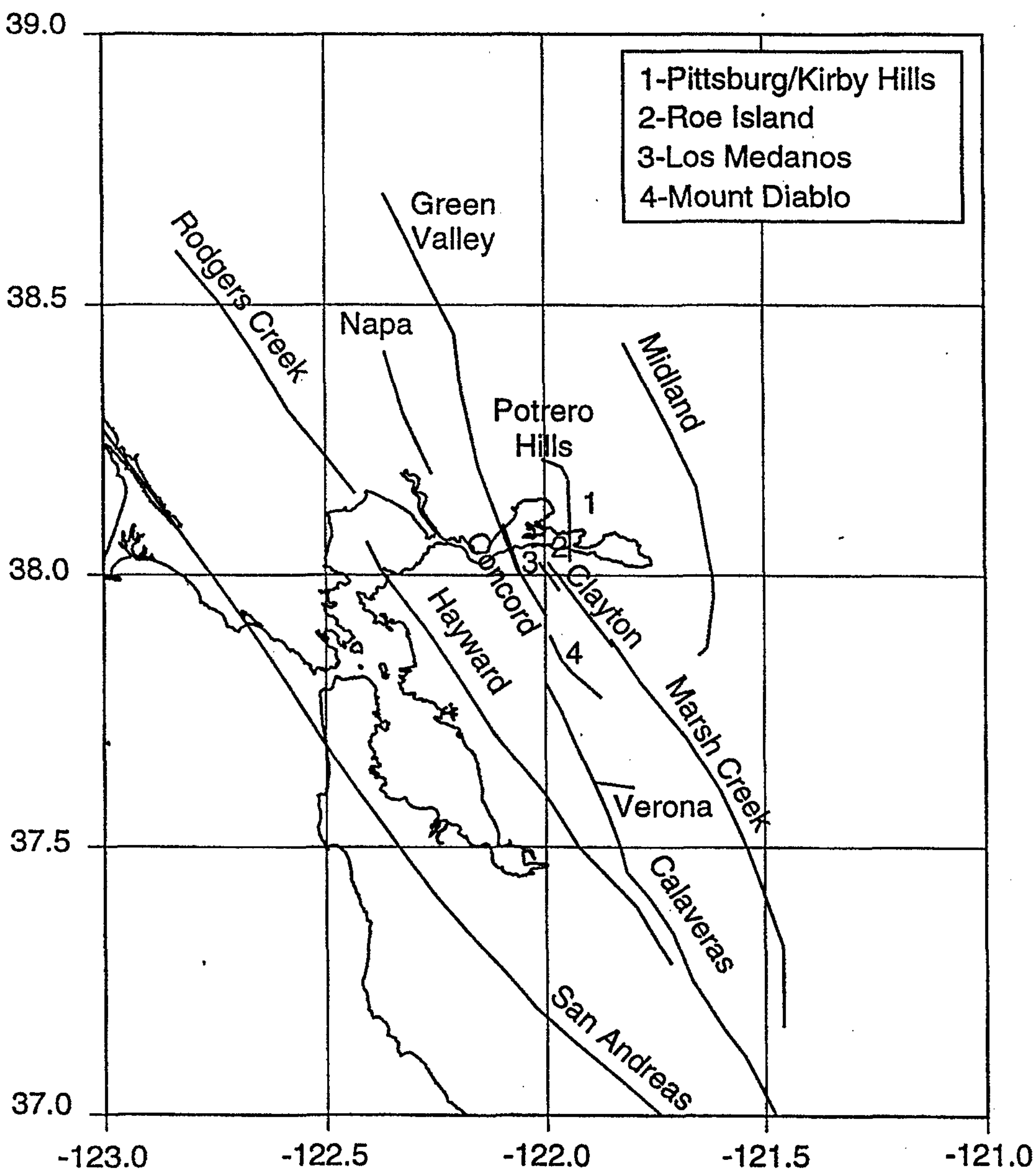

Figure A-1: Map showing the significant faults in the Delta region used in the seismic hazard computations based on the Lettis Delta fault model.

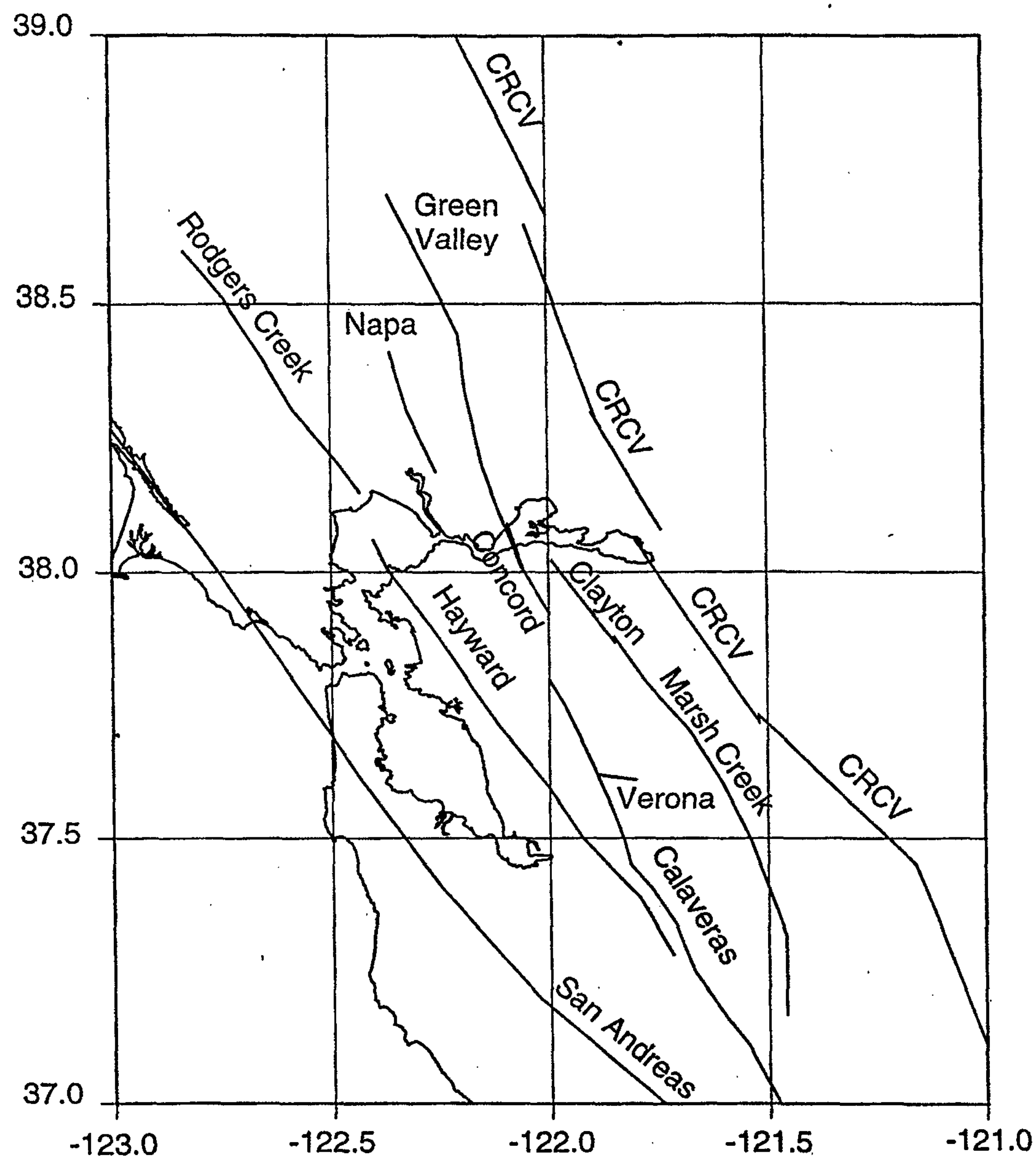

Figure A-2: Map showing the significant faults in the Delta region used in the seismic hazard computations based on the CRCV Delta fault model.

Table A-1. Seismic Source Parameters

Fault	Slip Rate (Weight)	Fault Width (Weights)	Max Magnitude (Weights)
Concord	3.0, 4.0, 6.0 (0.25, 0.5, 0.25)	12.0 (1.0)	6.4, 6.6, 6.8 (0.2, 0.6, 0.2)
Calaveras (North)	2.0, 6.0, 8.0 (0.25, 0.5, 0.25)	12.0 (1.0)	6.7 (1.0)
Calaveras (South)	13.0, 15.0, 17.0 (0.25, 0.5, 0.25)	12.0 (1.0)	6.8 (1.0)
Hayward	7.0, 9.0, 11.0 (0.25, 0.5, 0.25)	12.0 (1.0)	7.1 (1.0)
Marsh Creek/Greenville	0.5, 2.0, 3.0 (0.25, 0.5, 0.25)	12.0 (1.0)	6.7 (1.0)
Clayton	0.2, 0.5, 1.0 (0.25, 0.5, 0.25)	12.0 (1.0)	6.7 (1.0)
Green Valley	1.5, 4.0, 5.0 (0.2, 0.6, 0.2)	12.0 (1.0)	6.6 (1.0)
Napa	0.1, 0.3, 0.5 (0.3, 0.5, 0.2)	12.0 (1.0)	6.5 (1.0)
Rogers Creek	6.0, 8.0, 11.0 (0.25, 0.5, 0.25)	12.0 (1.0)	7.0 (1.0)
San Andreas	19.0, 24.0, 29.0 (0.2, 0.6, 0.2)	15.0 (1.0)	7.8, 8.0 (0.8, 0.2)
Verona	0.1 (1.0)	10.0 (1.0)	6.1 (1.0)
Antioch	0.3 (1.0)	15.0 (1.0)	6.5 (1.0)
Mt. Diablo Thrust[1]	1.3, 1.7, 5.0 (0.3, 0.6, 0.1)	11.0 (1.0)	6.25, 6.75 (0.30, 0.70)
Los Medanos Thrust[1]	0.3, 0.7 (0.8, 0.2)	13.0 (1.0)	6.00, 6.25 (0.8, 0.2)
Roe Island Thrust[1]	0.1, 0.3, 0.7 (0.1, 0.7, 0.2)	14.0 (1.0)	5.75, 6.00 (0.5, 0.5)
Potrero Hills Thrust[1]	0.1, 0.3, 0.6 (0.3, 0.6, 0.1)	14.25 (1.0)	6.00, 6.25 (0.8, 0.2)
Pittsburg/Kirby Hills Thrust[1]	0.2, 0.3, 0.7 (0.5, 0.4, 0.1)	15.0 (1.0)	6.00, 6.50 (0.4, 0.6)
Midland Thrust[1]	0.1, 0.2 (0.6, 0.4)	13.0 (1.0)	6.00, 6.25 (0.7, 0.3)
CRCV[2]	0.5, 1.5, 2.5 (0.25, 0.5, 0.25)	10.0 (1.0)	6.8 1.0

1 Lettis source model for the Delta region.
2 CRCV source model for the Delta region.

In addition to the known faults, a background source zone is also included to capture the earthquakes expected to occur on other fault sources. The background zone is based on the smoothed historical regional background seismicity ($M \geq 4.0$) developed by USGS (1996) and used by the CDMG in the state hazard maps (Reference). This background seismicity is smoothed over a distance of 50 km, resulting in very smooth background seismicity. The rate of magnitude 5 or greater earthquakes per 100 years per 100 square km is shown in Figure A-3. To avoid double counting seismicity, the background zone is used for magnitudes 5-6 and the individual known faults are used for magnitudes greater than 6.0.

The two alternative models for the thrust faults are discussed in more detail below.

DELTA REGION THRUST FAULTS

Geodetic data indicates that there is crustal shortening of about 3 mm/yr in the direction normal to the San Andreas fault between the Pacific Plate and the North American Plate. The primarily strike-slip earthquakes in the Bay Area region accommodate some of this shortening, but some additional thrust faults are needed to explain the remainder of the shortening between the Pacific and North American plates in this region. These thrust faults generally do not reach the surface and are considered "blind thrust" faults.

In most recent studies, most of the additional shortening has been assumed to be accommodated along the western edge of the central valley along a feature called the Coast Range/Central Valley Thrust (CRCV) fault zone (also called the Coast Range Sierran Block Boundary Zone).

There have been several earthquakes over magnitude 6 that have occurred along the CRCV fault zone to the north and to the south of the Delta region, but there are no known CRCV events of $M \geq 6$ in the vicinity of the Delta. The 1983 Coalinga earthquake ($M=6.4$) and the 1985 Kettleman Hills earthquake ($M=6.1$) occurred on the CRCV. The 1892 Winters-Vaccaville earthquake ($M=6.4$) may also have occurred on the CRCV, but its location is not well constrained (Toppozada, Real, and Parke, 1981). The CRCV is clearly an active fault in some regions, but it may not exist in the Delta region, or it may not be active in the Delta region.

In this evaluation, we consider two alternative models of the thrust faults in the Delta region: the CRCV model and the Lettis and Associates model. These two alternative models are discussed below.

D-032439

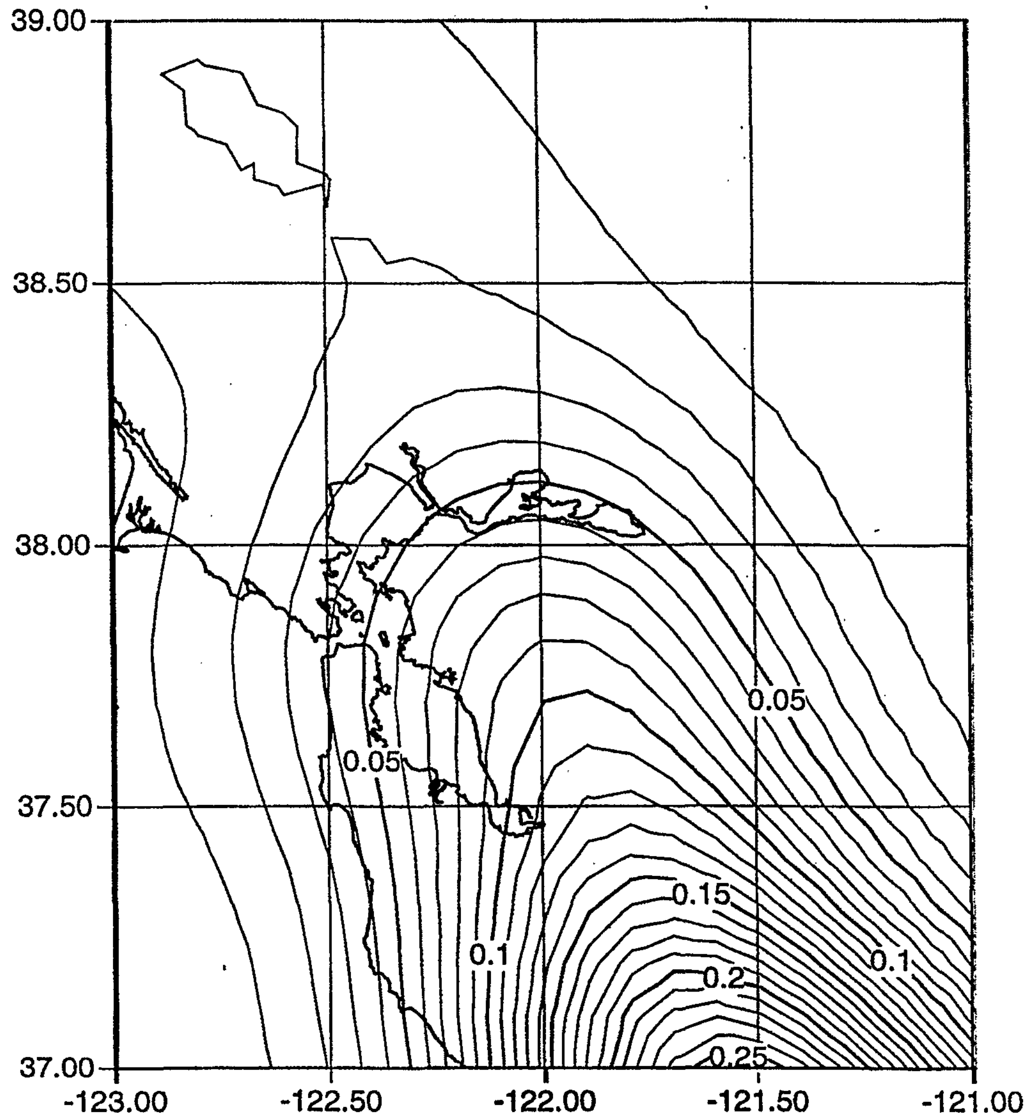

Figure A-3. Map showing the contour of smoothed background seismicity for magnitude 5.0 and greater per 100 years per 100 square kilometers. Based on the USGS gridded seismicity maps (1996).

CRCV THRUST FAULT MODEL

The CRCV extends about 600 km along the western edge of the Central Valley in central and Northern California (Wong et al., 1988), but the faulting is discontinuous. Most of the segment lengths are 5 to 20 km with a maximum segment length of about 50 km. In the CRCV model, this set of thrust faults extends through the Delta region and runs near Sherman Island (Figure A-2).

The CRCV model has been used in the state hazard maps developed by the California Division of Mines and Geology (CDMG). The slip-rate of the CRCV in the Delta region is uncertain. We have used a range of slip-rates from 0.5 to 3.0 mm/yr. The CDMG (1996) used a slip-rate of 1.5 mm/yr and that is the mean value that is used in this study.

The exact location of the CRCV fault in the Delta region in uncertain. In this study, the top of the fault is located at a depth of 8 km with a dip of __ degrees. For a down-dip fault width of 15 km and a segment length of 40 km, the Wells and Coppersmith (1994) magnitude vs. fault area relation gives a mean maximum magnitude of $M_w \approx 6.8$.

LETTIS AND ASSOCIATES MODEL

A recent study by Unruh (Lettis and Associates written comm., 1998) suggests that the CRCV is not present in the Delta region. According to this model, the CRCV begins to decrease in activity north of the San Luis Reservoir and south of Lake Berryessa. In the Delta region, the CRCV ceases to exist, or ceases to be active. As an alternative to the CRCV, the Lettis and Associates model postulates a different set of thrust faults slightly further to the west (Figure A-1) to accommodate the crustal shortening.

These faults, the Pittsburg/Kirby Hills, Roe Island, Los Medanos, and Mount Diablo faults are all short faults with lengths of less than 20 km located 10-20 km west of the western edge of the Delta. The mean slip-rates of these faults range from 0.3 to 2 mm/yr. The maximum magnitudes of the small thrust faults range from $M_w \approx 6.0$ to 6.6.

This model also includes the Midland fault located beneath the Delta, but with a small mean slip-rate of 0.15 mm/yr. Although the Midland fault has a length of about 60 km, the maximum magnitude of the Midland fault in this model is only $M_w \approx 6.2$.

A3. ATTENUATION RELATIONS

There are many attenuation relations that can be used for the deep soil site conditions (below the peat) in the Delta. In this study, we have selected four of the most recent attenuation models: Abrahamson and Silva (1997), Boore, et al. (1997), Campbell (1997), and Sadigh, et al. (1997) as being appropriate. These models are given equal weight in the hazard analysis.

A4. PROBABILISTIC HAZARD RESULTS

The probabilistic hazard is shown separately for the Lettis and the CRCV models of the Delta thrust faults. The results for the Lettis model are shown first, and the results for the CRCV model are shown second. Sherman Island and Terminous Island are used as example locations representative of the western and edges of the Delta, respectively. All acceleration levels shown are peak horizontal accelerations at surface outcrops of deep, stiff soils (soils underlying the softer and organic superficial Delta deposits.)

Figures A-4 and A-5 show the peak acceleration hazard for Sherman Island and Terminous Island, respectively, based on the Lettis thrust fault model. At a return period of 100 years (annual probability of 0.01), the hazard at Sherman Island is dominated by the local thrust faults, with significant contribution from the background zone and "other" faults. For Terminous Island, the background zone and thrust faults contribute about equally to the overall 100 year return-interval level of hazard.

The magnitudes and distances of the earthquakes dominating the hazard can be estimated by deaggregating the hazard. The distributions of contribution to the hazard are shown in Figures A-6 and A-7. For Sherman Island, the hazard is primarily from moderate magnitude events ($M \approx 5.5$-6.5) at distances of 10 to 30 km. For Terminous Island, the more distant sources also contribute significantly to the hazard, and there is a wide range of magnitudes and distances ($M \approx 5$-6 at distances of 10-30 km to $M \approx 7$-7.5 at 100 km) contributing to the hazard. Figures A-8 and A-9 show the mean magnitude and mean distance of the earthquakes contributing to the hazard as a function of the return period.

A similar set of plots for the CRCV model is shown in Figure A-10 and A-11. The main difference is that for the CRCV model, the local CRCV thrust faults are the principal controlling source for both Sherman Island and Terminous Island.

The hazard for the Lettis and CRCV models is compared in Figure A-12. This figure shows that the hazard from these two models is very similar for both the Sherman Island and Terminous Island sites when expressed in terms of expected peak horizontal acceleration. The models differ, however, in terms of the principal magnitudes that contribute to these acceleration hazard levels. These differences in contributing magnitudes, in turn, imply differences in the duration of shaking, and this has a potentially significant impact on both the liquefaction and cyclic inertial deformation hazard evaluations for Delta levees.

The two models are given equal weight in the final hazard analysis. Contours of the peak acceleration in the Delta region for return period of 43 years, 100 years, 200 years, and 475 years (building code level) are shown in Figures A-13 through A-16. The hazard systematically decreases from the southwest to the northeast.

For the top of stiff soils, the 100 year return-interval horizontal peak acceleration ranges from 0.2 g in the western Delta to 0.1 g in the northeastern Delta. Since the hazard is dominated by moderate magnitude local events, it is unlikely that the entire Delta will be subject to the 100-year ground motion in a single 100-year earthquake.

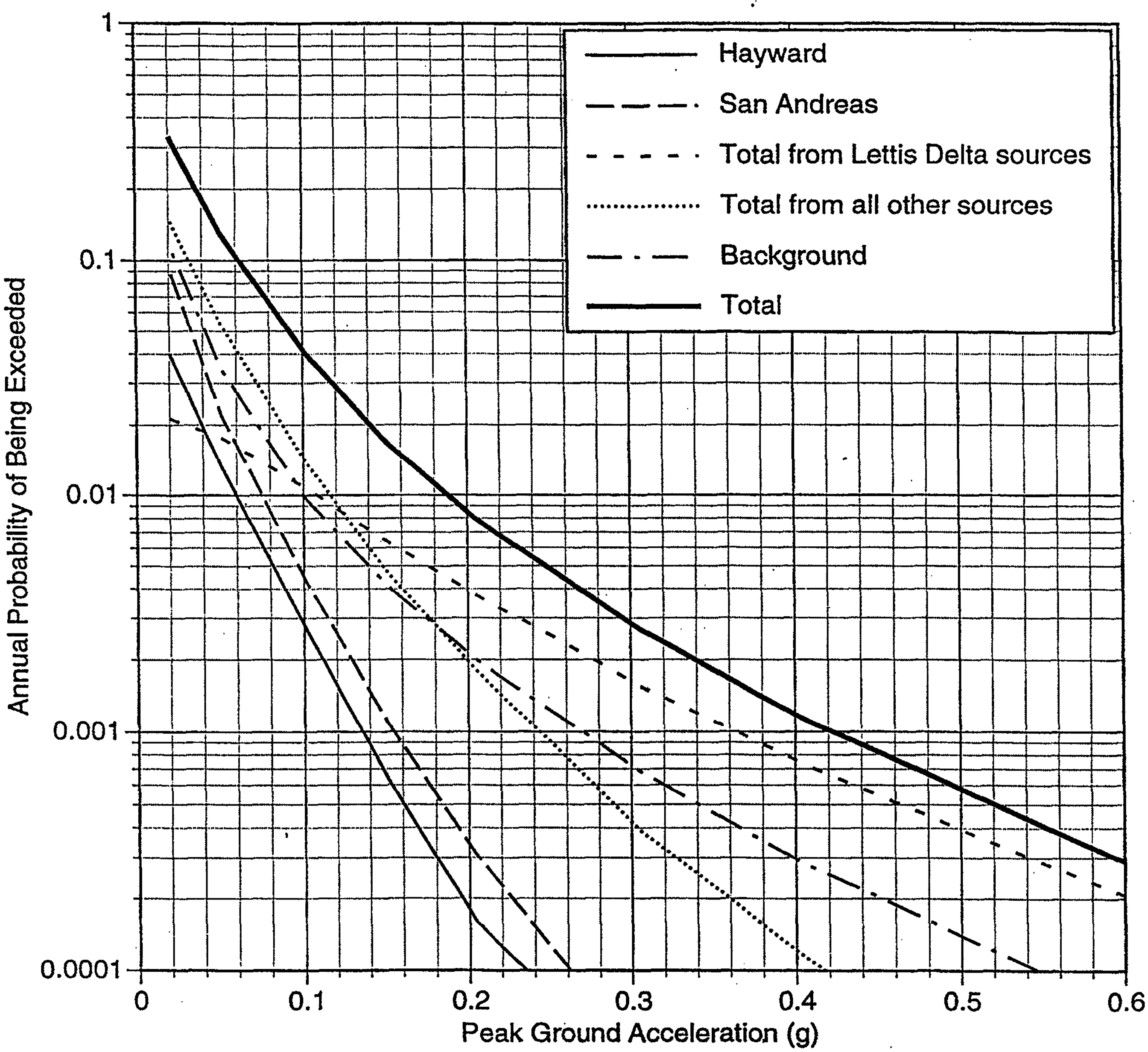

Figure A-4. Seismic hazard curves for the Sherman Island site. The hazard curves are based on the Lettis seismic model for the Delta region. The contribution to the total hazard is shown for the significant faults.

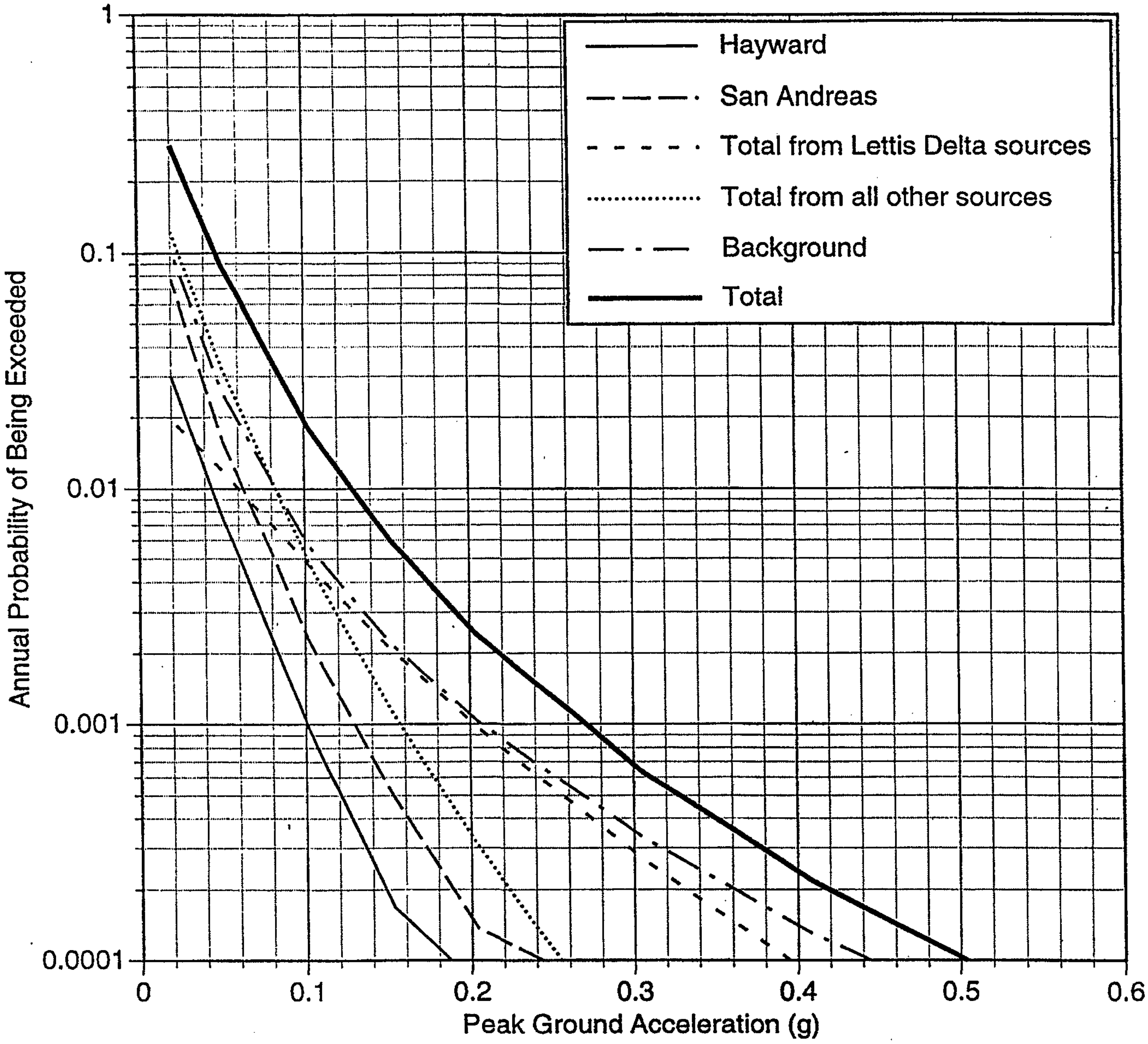

Figure A-5. Seismic hazard curves for the Terminous site. The hazard curves are based on the Lettis seismic source model for the Delta region. The contribution to the total hazard is shown for the significant faults.

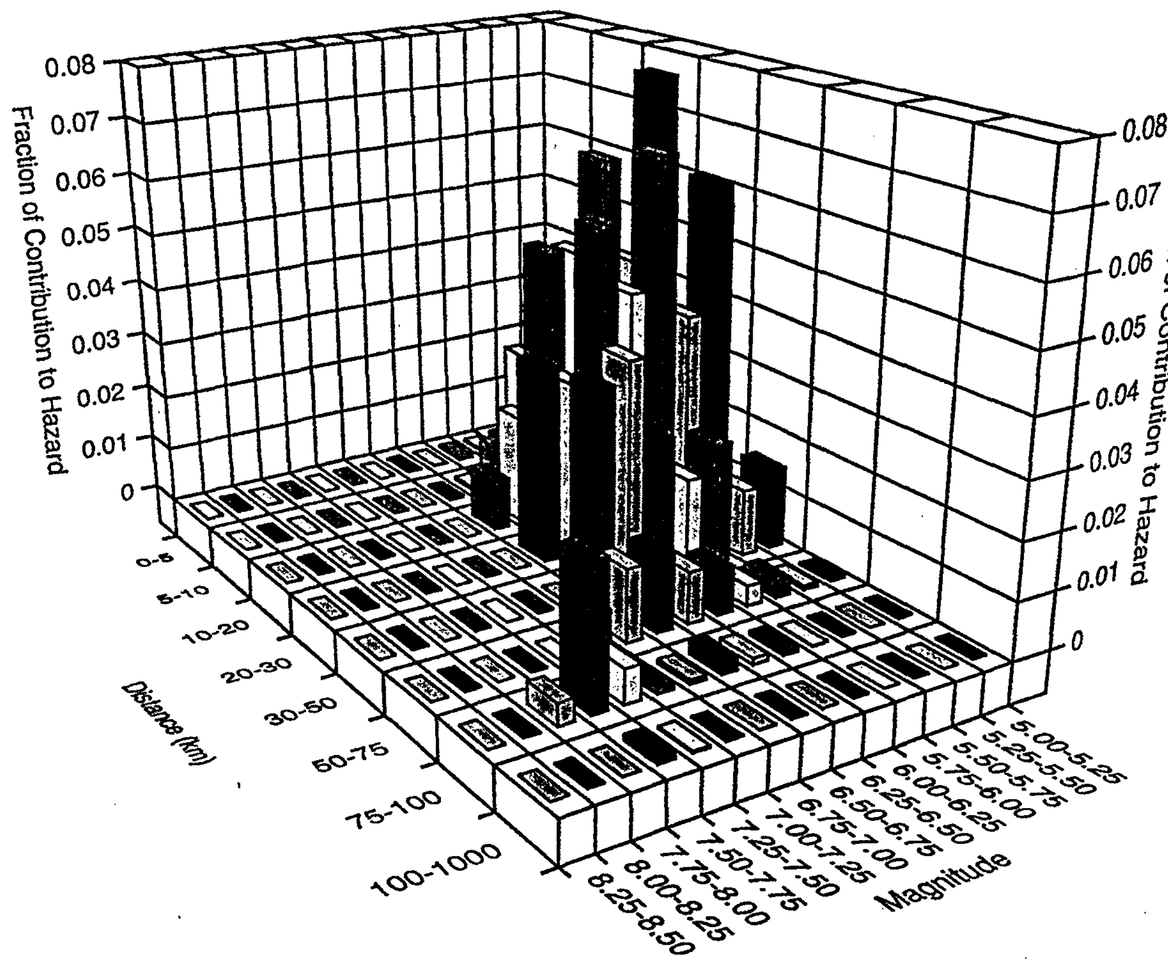

Figure A-6. Deaggregation of the seismic hazard (100 year return period) for the Sherman Island site based on the Lettis seismic source model for the Delta region.

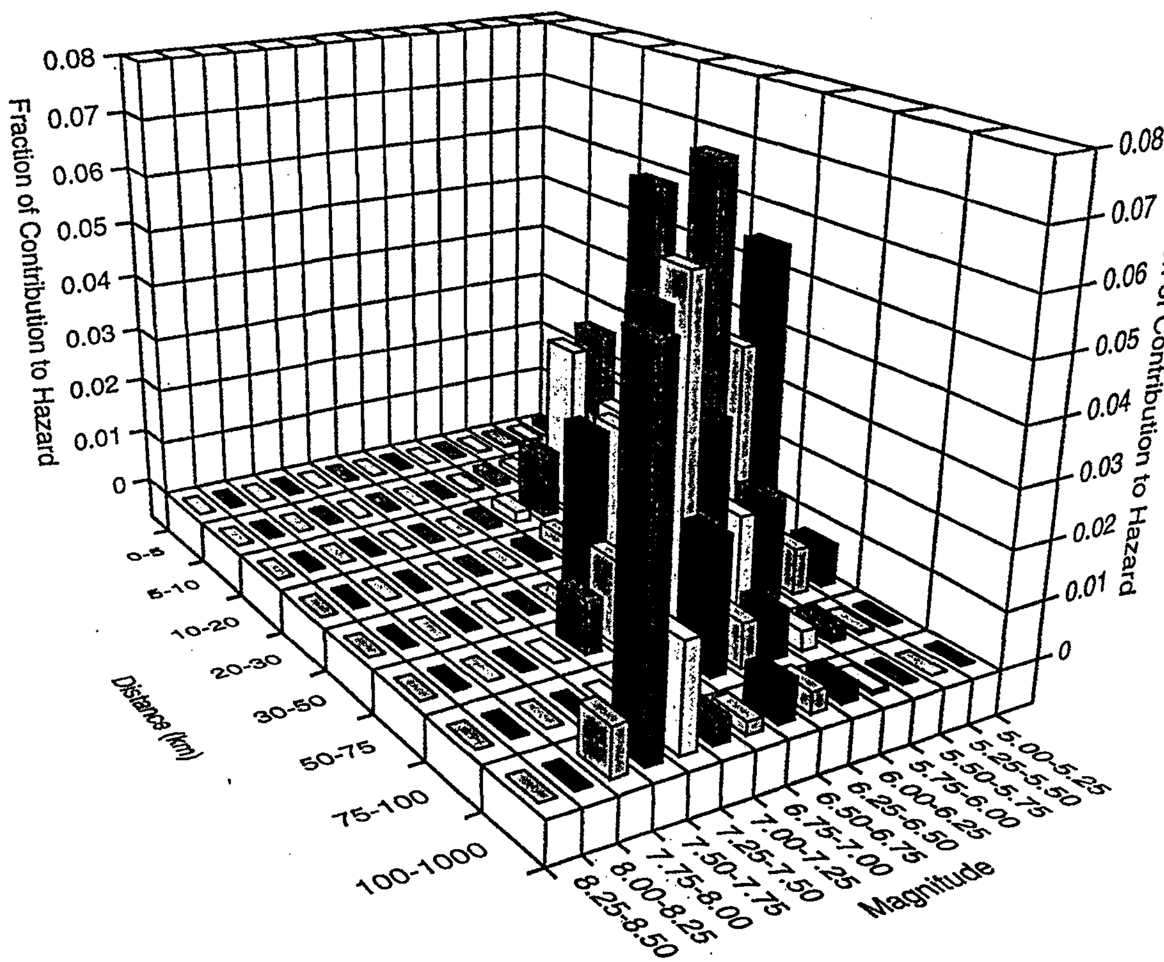

Figure A-7. Deaggregation of the seismic hazard (100 year return period) for the Terminous site based on the Lettis seismic source model for the Delta region.

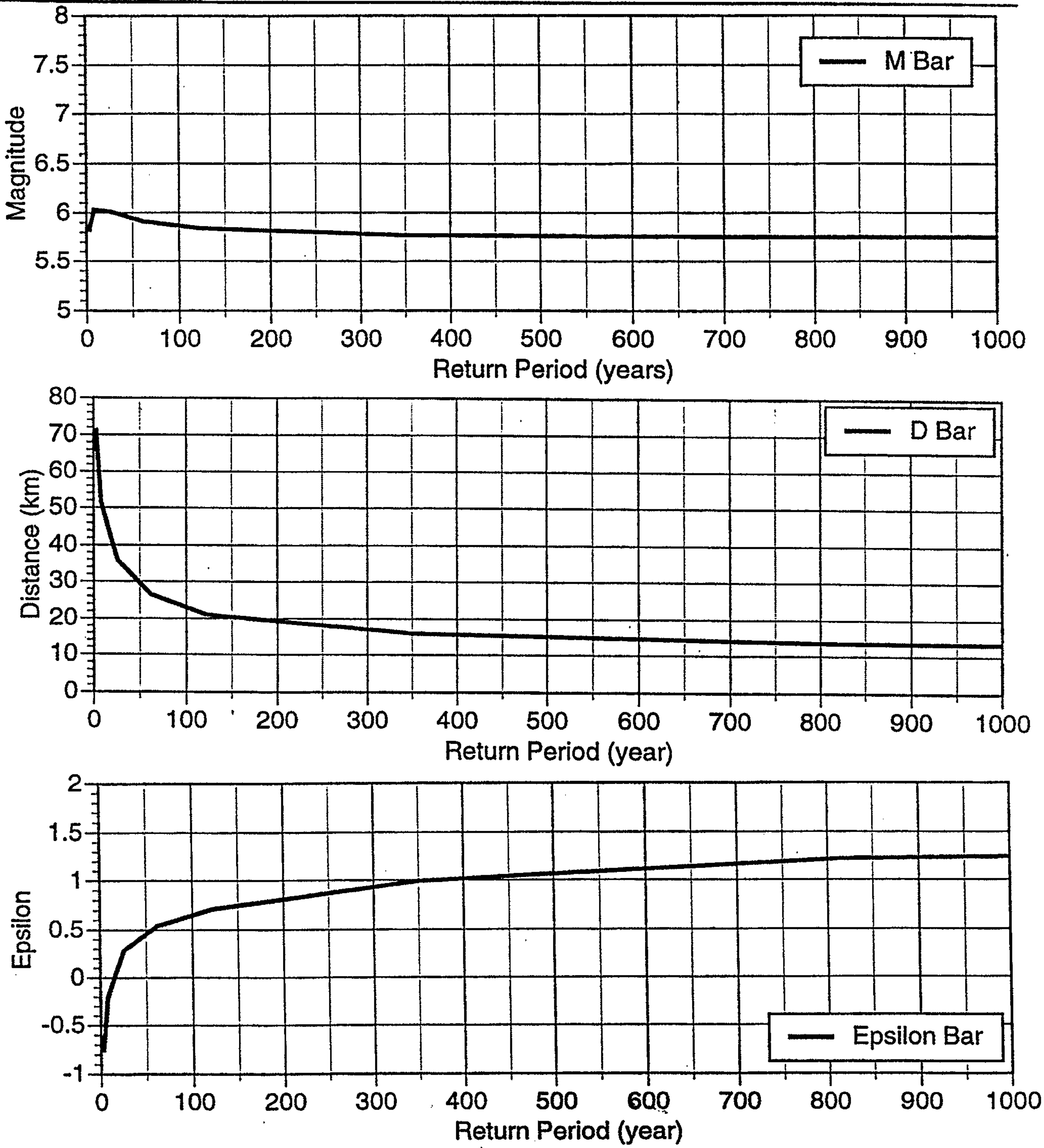

Figure A-8. Magnitude, distance and epsilon bar for the Sherman Island site based on the Lettis seismic source model for the Delta region.

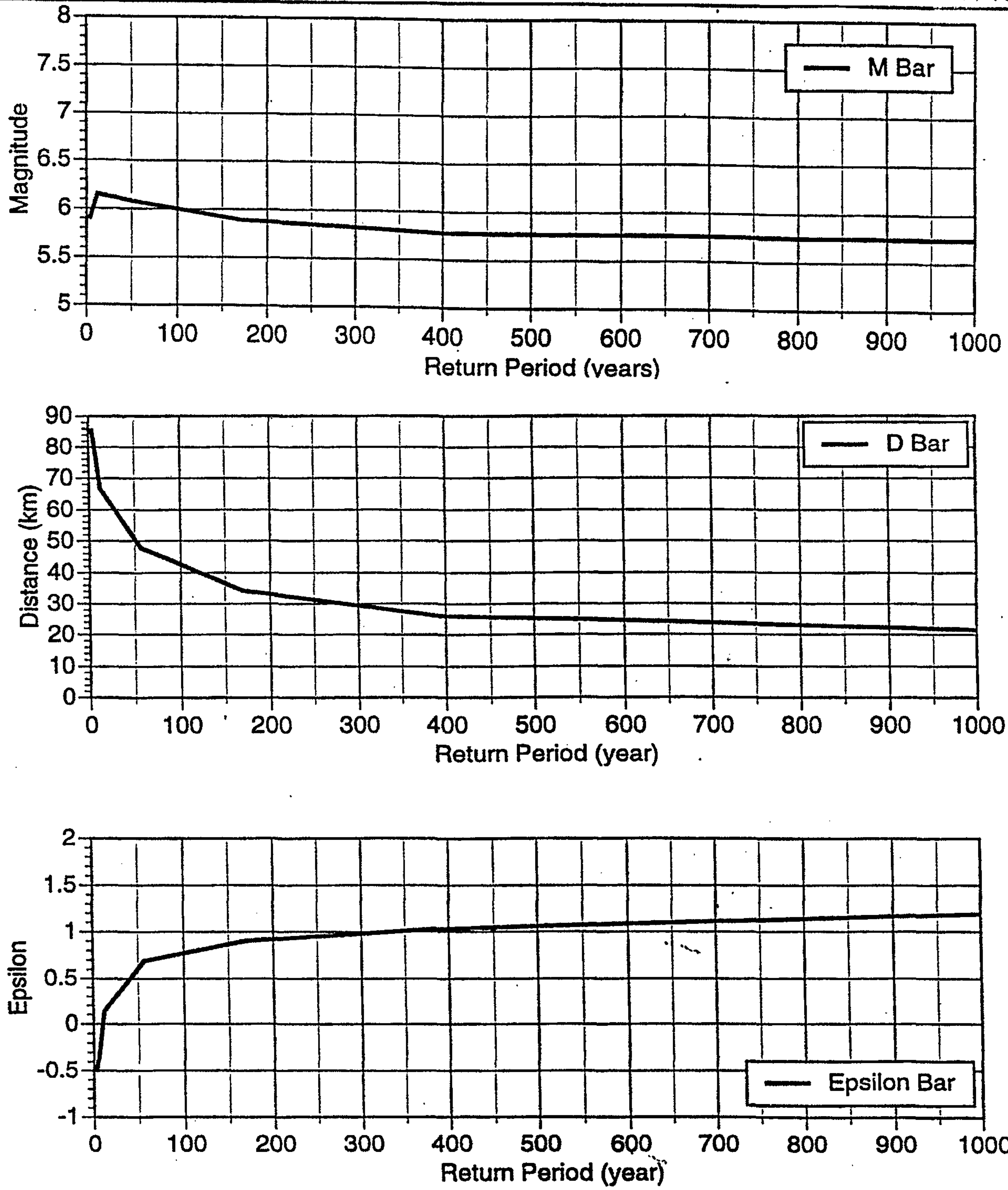

Figure A-9. Magnitude, distance and epsilon bar for the Terminous site based on the Lettis seismic source model for the Delta region.

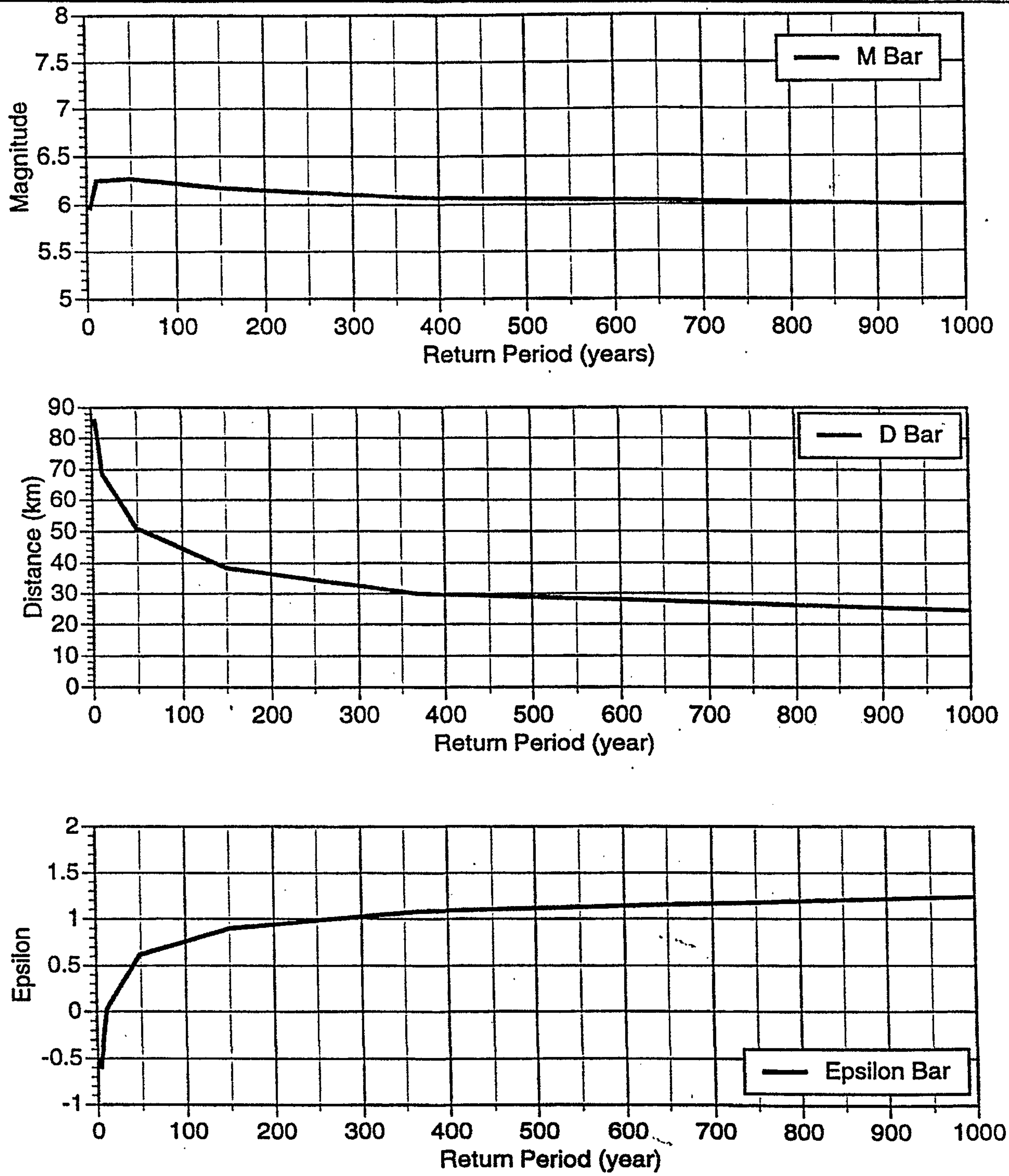

Figure A-10. Magnitude, distance and epsilon bar for the Sherman Island site based on the CRCV seismic source model for the Delta region.

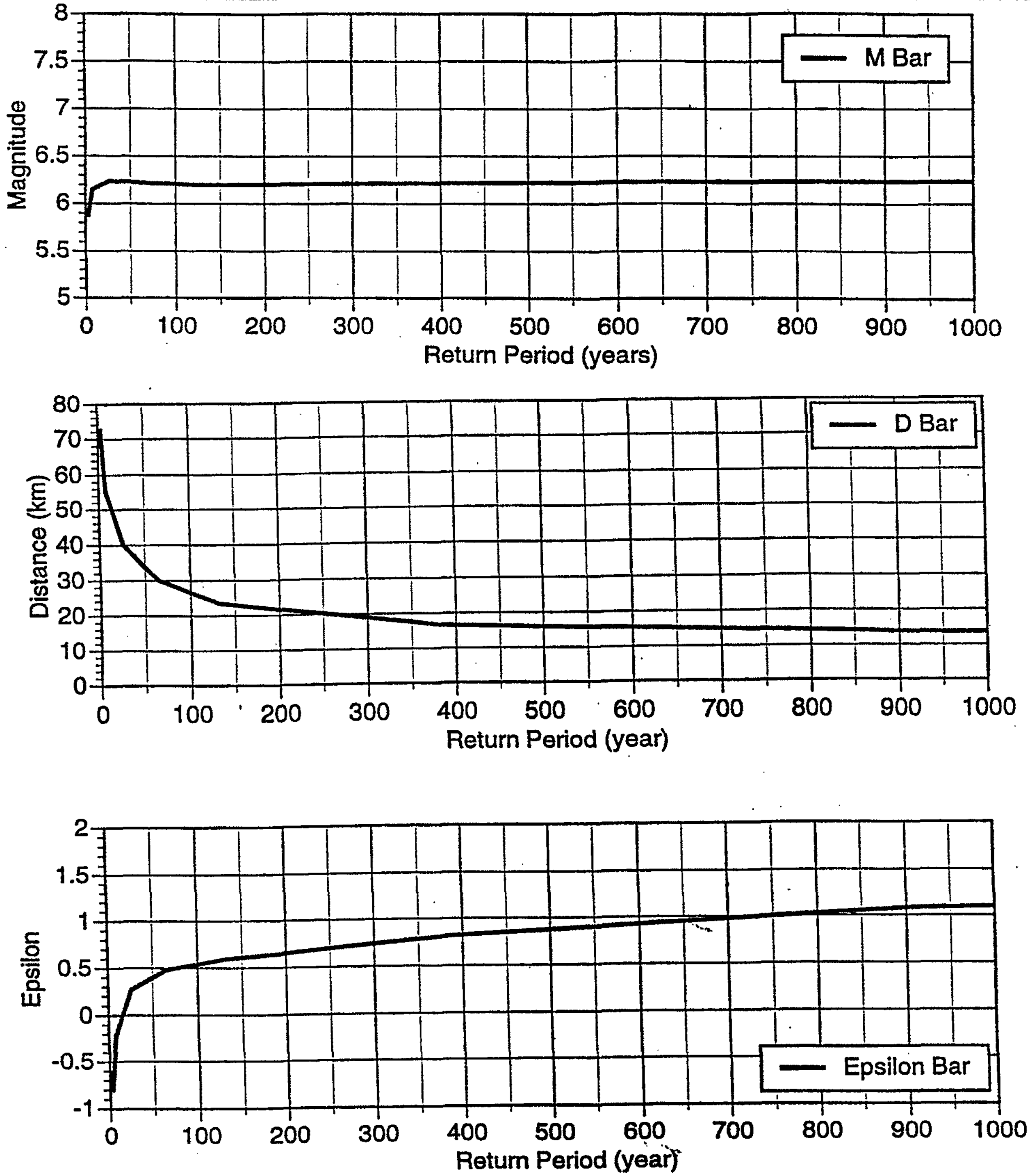

Figure A-11. Magnitude, distance and epsilon bar for the Sherman Island site based on the CRCV seismic source model for the Delta region.

D-032451

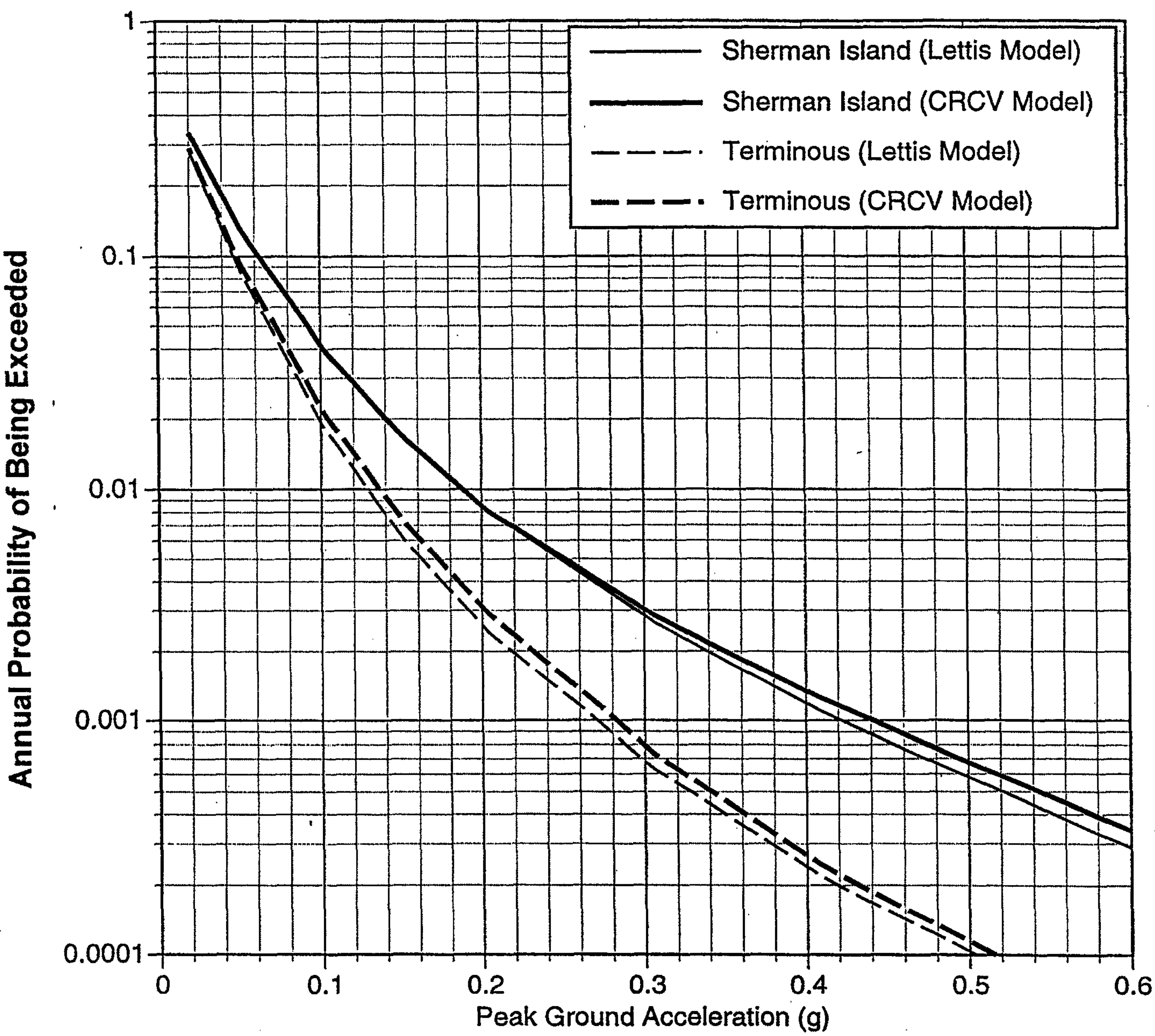

Figure A-12. Comparison of the seismic hazard for the Sherman Island and Terminous sited based on both the Lettis and CRCV seismic source model for the Delta region.

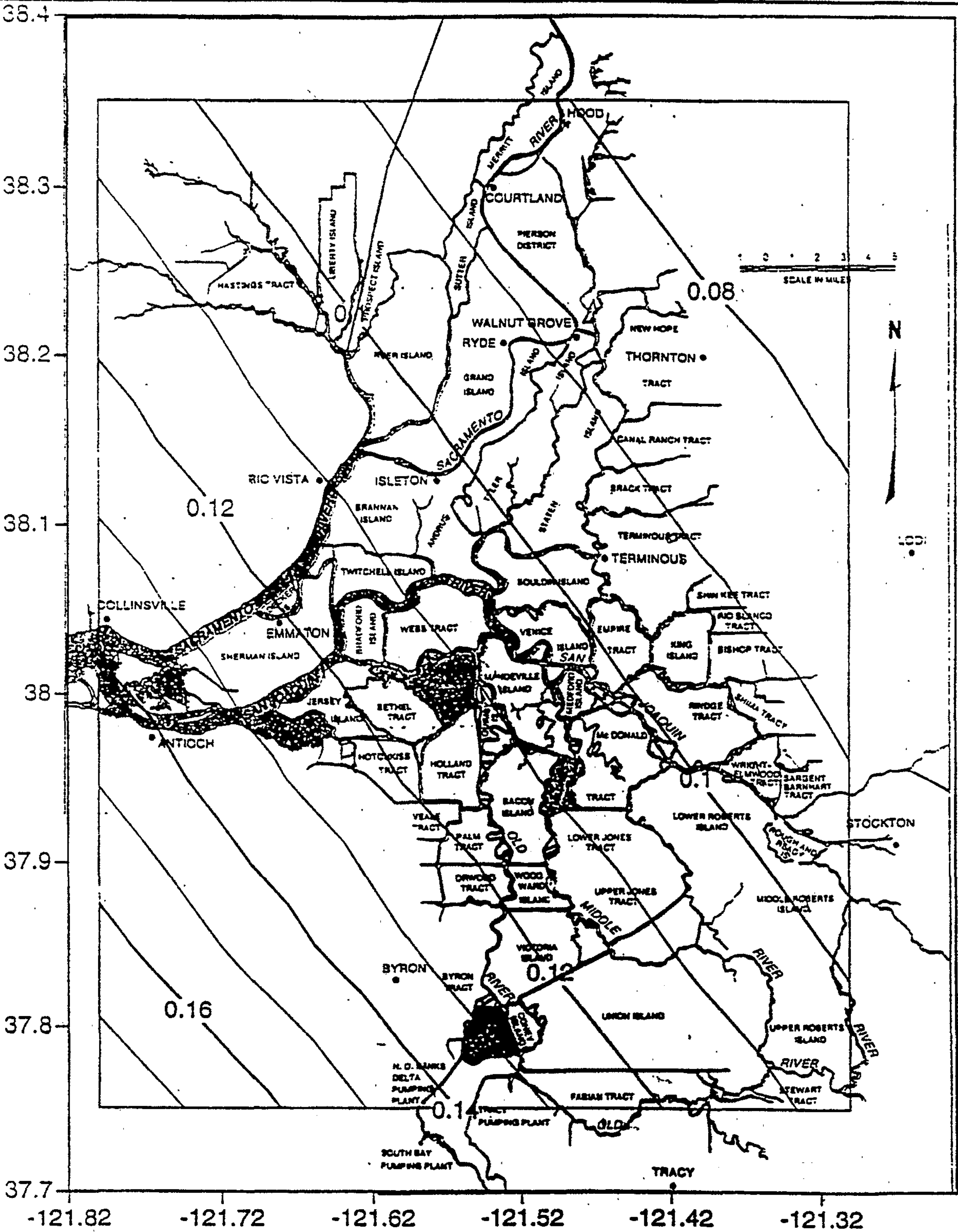

Figure A-13. Contour map of seismic hazard (PGA) for soil site conditions for a return period of 43 years.

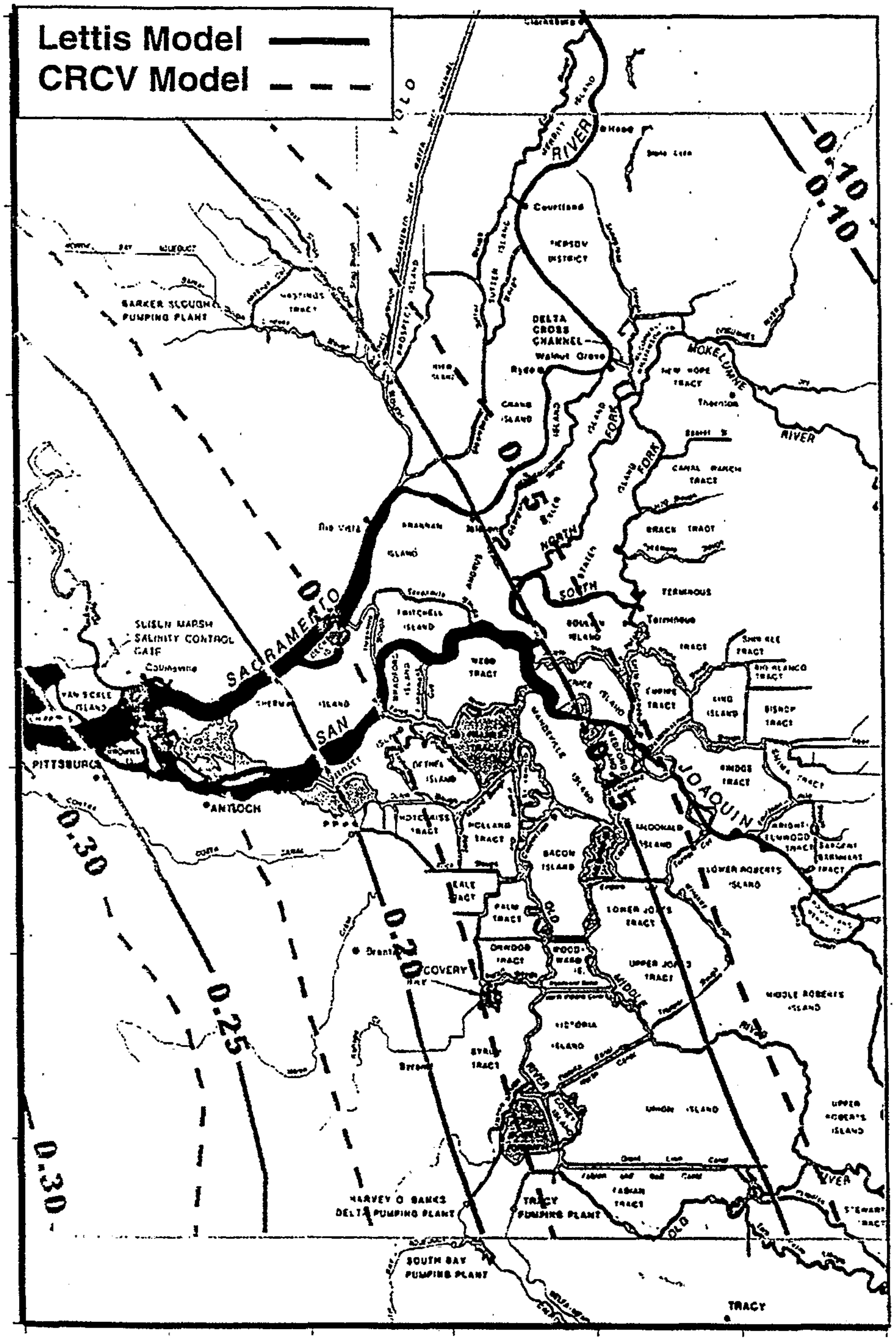

Figure A-14. Contour map of seismic hazard (PGA) for soil site conditions for a return period of 100 years.

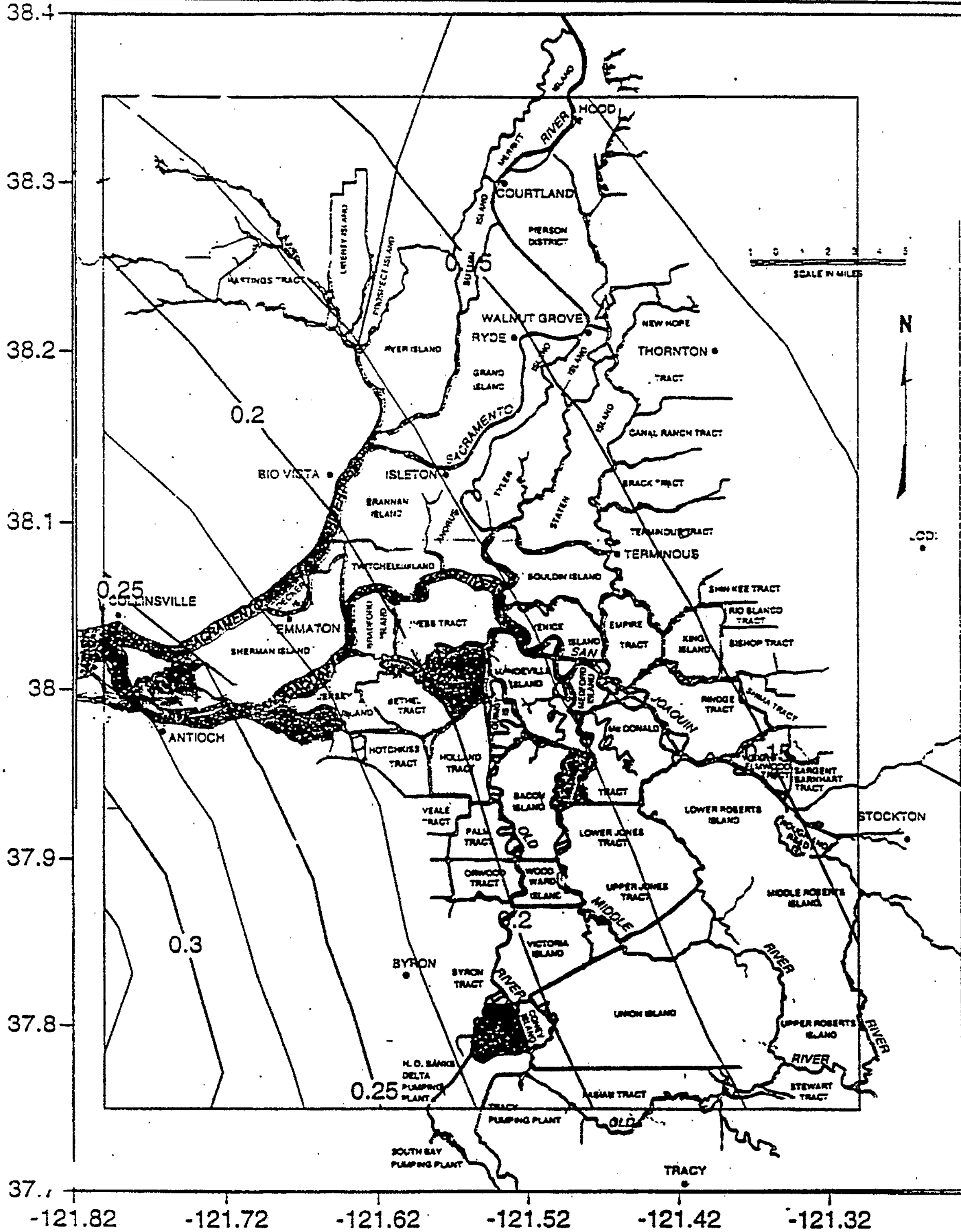

Figure A-15. Contour map of seismic hazard (PGA) for soil site conditions for a return period of 200 years

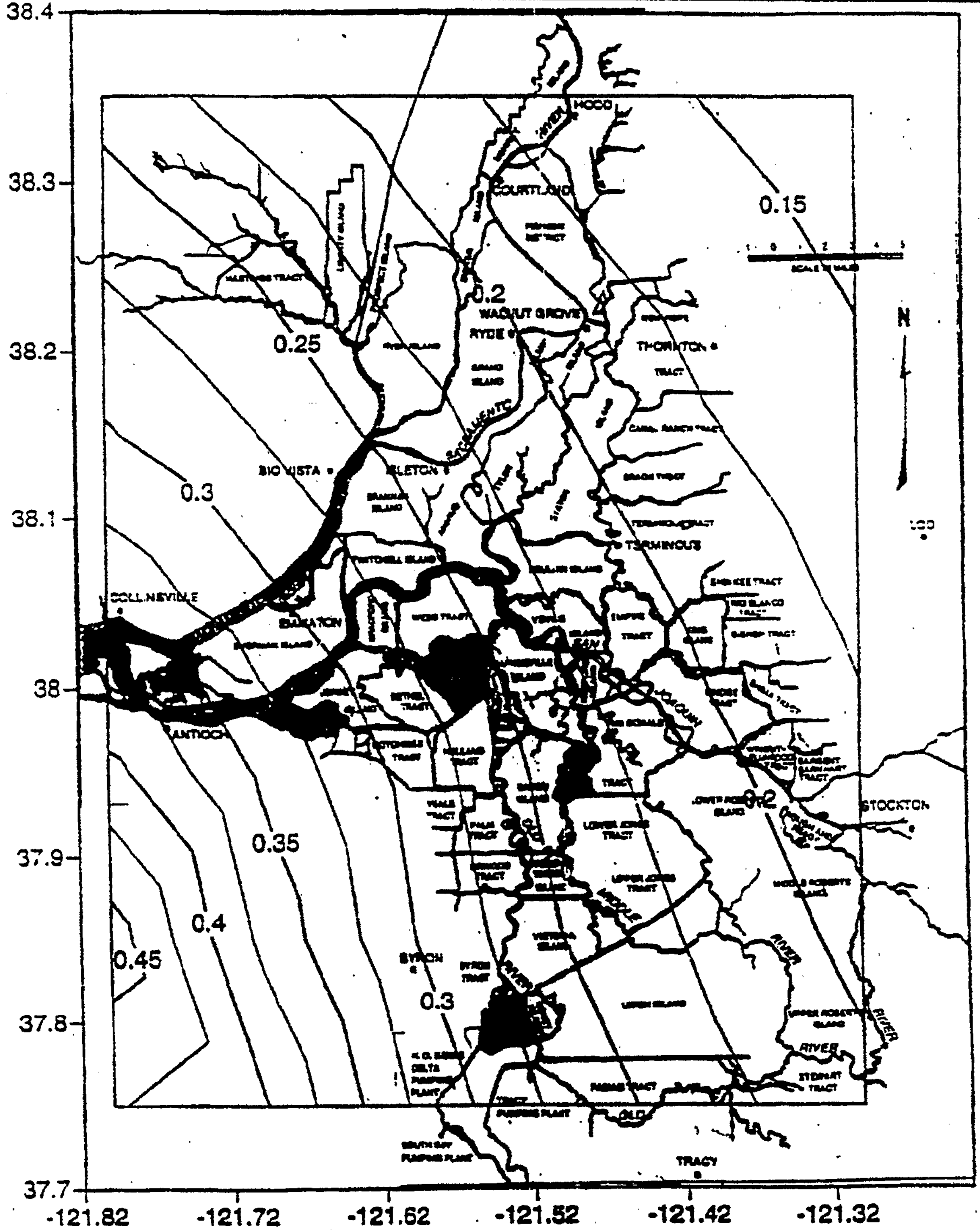

Figure A-16. Contour map of seismic hazard (PGA) for soil site conditions for a return period of 475 years.

APPENDIX B:

EVALUATION OF LEVEE FRAGILITY

- **Liquefaction Mode of Failure**
- **Non-Liquefaction Deformation of Mode Failure**

APPENDIX B: EVALUATION OF LEVEE FRAGILITY

GENERAL

This appendix presents more detailed information regarding the development of levee fragility estimates for potential levee failures due to future seismic events. The fragility estimates were previously described in general terms in Chapter 4. Many of the estimates were based on consensus judgements made by the sub-team members. Sub-team members applied their knowledge of the performance of similar earth structures to the conditions which currently exist in the Delta, and to the potential seismic loadings which might develop in the future. In addition, a number of geotechnical earthquake engineering analyses were also performed to provide information for these judgements, and to extend the estimates for a range of loadings.

The seismic risk analyses and assessments presented in this report are based on the most current available information. Information on the seismic response of peat/organic soils is still being developed. Also, even though hundreds of borings describing the subsurface conditions of Delta levees were reviewed, these borings can only provide a limited characterization of the hundreds of miles of levees in the Delta. It does not appear likely that additional borings will significantly change the present characterization in the near future.

DAMAGE POTENTIAL ZONES

As previously described in Chapter 4, the central portion of the Delta was divided into four Damage Potential Zones in order to allow for different levels of levee fragility in different areas of the Delta (see Figure 4-1). The criteria used for establishing the zoning was discussed previously in Chapter 4. The four zones encompass essentially all of the Delta land which lies below sea level and includes approximately 660 levee miles. Another 440 miles of levee exist at higher elevations within the legal limits of the Delta, but were not included because these levees retain significant depths of water only during flood season. Table B-1 summarizes the Delta islands and tracts included in the four zones along with the lengths of levees to be found in each zone.

ESTIMATES OF LIQUEFACTION-INDUCED LEVEE FAILURES

The sub-team gathered data from borings and CPT soundings to establish "typical" conditions at a number of representative levee reaches throughout the Delta. Data from prior seismic fragility studies, DWR data, and data supplied by individual sub-team members were all reviewed. Liquefaction potential (i.e. resistance to "triggering" or

TABLE B-1: DELTA ISLANDS AND LEVEE LENGTHS CONSIDERED IN EVALUATING POTENTIAL EARTHQUAKE-INDUCED LEVEE FAILURE

Damage Potential Zone	Delta Island/ Reclamation District	Project Levee[1] (miles)	Non-Project[1] Levee (miles)	Total Levee Length[1] (miles)
I	Sherman	9.7	9.8	19.5 [19.5]
	Bacon		14.3	14.3
	Bethel		11.5	11.5
	Bouldin		18.0	18.0
	Bradford		7.4	7.4
	Brannan	9.3	10.1	19.4
	Empire		10.5	10.5
	Holland		10.9	10.9
	Jersey		15.6	15.6
	Lower Jones		8.8	8.8
	Lower Roberts		16.0	16.0
II	Mandeville		14.3	14.3
	McDonald		13.7	13.7
	Medford		5.9	5.9
	Orwood		10.9	10.9
	Palm		7.5	7.5
	Quimby		7.0	7.0
	Rindge		15.7	15.7
	Staten		25.4	25.4
	Twitchell	2.5	9.3	11.8
	Tyler	12.2	10.7	22.9
	Venice		12.3	12.3
	Webb		12.8	12.8
	Woodward		8.8	8.8 [301.4]
	Byron		9.7	9.7
	Coney		5.4	5.4
	Fabian		18.8	18.8
	Hotchkiss		6.3	6.3
III	Middle Roberts	6.1	3.7	9.8
	Rough and Ready		5.5	5.5
	Union	1.0	29.2	30.2
	Upper Jones		9.3	9.3
	Veale		5.7	5.7
	Victoria		15.1	15.1 [115.8]
	Andrus	10.0		10.0
	Bishop		5.8	5.8
	Brack		10.8	10.8
	Canal Ranch		7.5	7.5
	Dead Horse		2.6	2.6
	Grand	29.0		29.0
	Hastings	4.0	1.0	5.0
	King		9.0	9.0
	Liberty Island	9.0	9.0	18.0
	McCormack-Williamson		8.8	8.8
IV	New Hope		18.6	18.6
	Pierson	10.0		10.0
	Prospect	7.0	5.0	12.0
	Rio Blanco		4.0	4.0
	Ryer	20.6		20.6
	Sacramento Co.	2.0	5.0	7.0
	Shima		6.6	6.6
	Sutter	12.5		12.5
	Terminous		16.1	16.1
	Walnut Grove	1.0	1.2	2.2
	Wright Elmwood		6.8	6.8 [222.9]

[1] Levee lengths listed in Sacramento-San Joaquin Delta Atlas, DWR (1993) [659.6]Miles

initiation of liquefaction) for sandy and silty soils of low plasticity was evaluated using the SPT-based methodology described by Seed and Harder (1990), as updated by the NCEER Liquefaction Workshop expert panel (Youd, et al., 1998). Of particular concern to the sub-team was the presence of cohesionless sandy and/or silty soils within the manmade levee embankment. When present, such soils often had SPT $(N_1)_{60}$ blowcounts of less than 10, and commonly less than 5. Post-liquefaction residual strengths were estimated using the correlation proposed by Seed and Harder (1990), and these indicated very low values, commonly only about 50 to 200 psf. With such low residual shear strengths, major levee displacements and/or failure would be expected if major portions of the levee embankment were triggered to liquefy.

Of somewhat lesser concern, but still potentially serious, was the occurrence of potentially liquefiable sandy and silty soils in the foundation zone (beneath the levee embankments). These soils tended to have variable SPT blowcounts, but generally somewhat higher than those in the loose embankment soils. The liquefiable foundation soils were also less hazardous due to levee and foundation geometries, as well as due to the irregular and discontinuous nature of some of these natural foundation deposits. Potential liquefaction of foundation soils was not a benign condition, however, and liquefaction of foundation soils was eventually judged to contribute approximately 25% to 30% of the overall liquefaction-related hazard (with liquefaction of levee embankment fills contributing the remainder.)

The sub-team worked together to assemble and review the available geotechnical data. Each of the individuals then prepared independent assessments of expected levee failure frequencies for various levels of shaking within each of the four Damage Potential Zones. These individual assessments, and their basis, were then shared and discussed to develop a single set of overall consensus estimates. These consensus estimates of potential number of levee failures were presented as a range for each level of shaking and for each of the four Damage Potential Zones. Each range was considered to represent about an 80-percent confidence level for the range of "expected" number of liquefaction-induced levee failures for a particular level of shaking.

ESTIMATES OF LEVEE FAILURES FOR NON-LIQUEFACTION EARTHQUAKE-INDUCED DISPLACEMENTS

Based on Newmark-type cyclic inertial deformation analyses for a range of levels of static (non-seismic) stability, the sub-team concluded that any levee reaches which might fail without major strength losses such as liquefaction would have to be only marginally stable during static conditions. The effect of seismic shaking would be to either trigger or induce deformations as a result of inertial effects. To estimate the number of failures associated with a non-liquefaction deformation mode of failure, the sub-team proceeded in the following steps:

1. The number of marginally stable levee sites in each Damage Potential Zone was first estimated based on the experience of the sub-team members in dealing with problem sites. Three levels of marginal stability were considered. The estimated numbers of potentially marginal sites in each zone are listed in Table B-2. Also presented in Table B-2 are the estimated ranges of yield acceleration, k_y, for each level of marginal stability (k_y is the level of acceleration at which yielding and onset of permanent deformations will occur).

2. Estimates of earthquake-induced deformations were calculated using the Newmark double-integration method for a selected number of accelerograms. Seven accelerograms were selected to provide a reasonable range of duration and frequencv content characteristics representative of the levels of seismic excitation being considered (M~5 to 7). These records from "stiff soil" or "rock" sites were then modified by means of site response analyses, using computer program SHAKE91 (Idriss et al., 1991), to develop motions representative of typical Delta levee embankment and foudation soil conditions. The base accelerograms were input as outcrop motions at a stiff soil base layer and then propagated through a deep Delta soil profile up to the surface of the levee. Near-surface motions (at the bases of potential deformation zones) were then scaled to different peak accelerations, and these were then double-integrated to obtain displacements for a range of yield accelerations. An allowance was made to account for spatial and temporal incoherence across a potential slide mass or deformation zone. Figure B-1 and Table B-3 present the results of these calculations. For the purposes of relating probabilistic base accelerations developed in Chapter 3 to a deformation mode of failure, the following was assumed:

   - The base acceleration would be amplified through soft Delta deposits by a factor of 1.6. Thus, a "stiff soil" acceleration of 0.1g would lead to a peak acceleration of 0.16g at the crown of the levee.

   - The average peak acceleration of a potential sliding mass would be approximately 40 percent of the levee crown acceleration. This is based on the work by Makdisi and Seed (1977) and assuming that the marginal sites have relatively deep potential sliding surfaces.

   - Thus, the average acceleration of potential sliding surface, k_{max}, is approximately 65 percent of the base acceleration of a stiff soil outcrop motion [$1.6 \times 0.4 \approx 0.65$].

TABLE B-2: ESTIMATED NUMBER OF MARGINALLY STABLE LEVEE SITES IN NON-LIQUEFIED REACHES WITHIN DAMAGE ASSESSMENT ZONES

Stability Category	Approximate Yield Acceleration k_y(g)	Estimated Number of Sites in each Damage Potential Zone				
		Zone I (20 miles)	Zone II (301 miles)	Zone III (116 miles)	Zone IV (223 miles)	Total (660 miles)
A	0.00 - 0.01	1 - 2	6 - 12	0.3 - 2	0.7 - 3	8 - 19
B	0.01 - 0.03	1 - 3	12 - 24	0.7 - 3	1.3 - 7	15 - 37
C	0.03 - 0.05	3 - 8	20 - 60	1.7 - 5	3.3 - 10	28 - 83

TABLE B-3: ESTIMATED EARTHQUAKE-INDUCED DISPLACEMENTS IN NON-LIQUEFIED REACHES WITHIN DAMAGE ASSESSMENT ZONES

Magnitude 6.0 Bedrock/Stiff Soil Peak Acceleration (g)	Average Peak Acceleration[1] k_{max}(g)	Earthquake-Induced Displacement for Stability Categories[2]		
		A (k_y=0.005g)	B (k_y=0.02g)	C (k_y=0.04g)
0.05	0.033	0.1 - 0.3 ft [0.2 ft.]	0.0 - 0.0 ft. [0.1 ft.]	0.0 - 0.0 ft. [0.1 ft.]
0.10	0.065	0.3 - 1.1 ft [0.6 ft.]	0.1 - 0.2 ft. [0.1 ft]	0.0 - 0.0 ft. [0.1 ft.]
0.15	0.10	0.7 - 2.3 ft [1.4 ft]	0.1 -0.7 ft. [0.3 ft.]	0.0 - 0.2 ft. [0.1 ft.]
0.20	0.13	1.1 - 3.6 ft [2.2 ft]	0.3 - 1.2 ft. [0.6 ft.]	0.1 - 0.4 ft. [0.15 ft.]
0.30	0.20	2.2 - 7.1 [4.2 ft]	0.9 - 2.8 ft. [1.5 ft.]	0.3 - 1.4 ft. [0.6 ft.]

Notes: 1. Average Peak Acceleration assumed to be equal to 65 percent of the base bedrock/stiff soil motion.
2. Range and best estimate of earthquake-induced displacements calculated using the Newmark double-integration method.

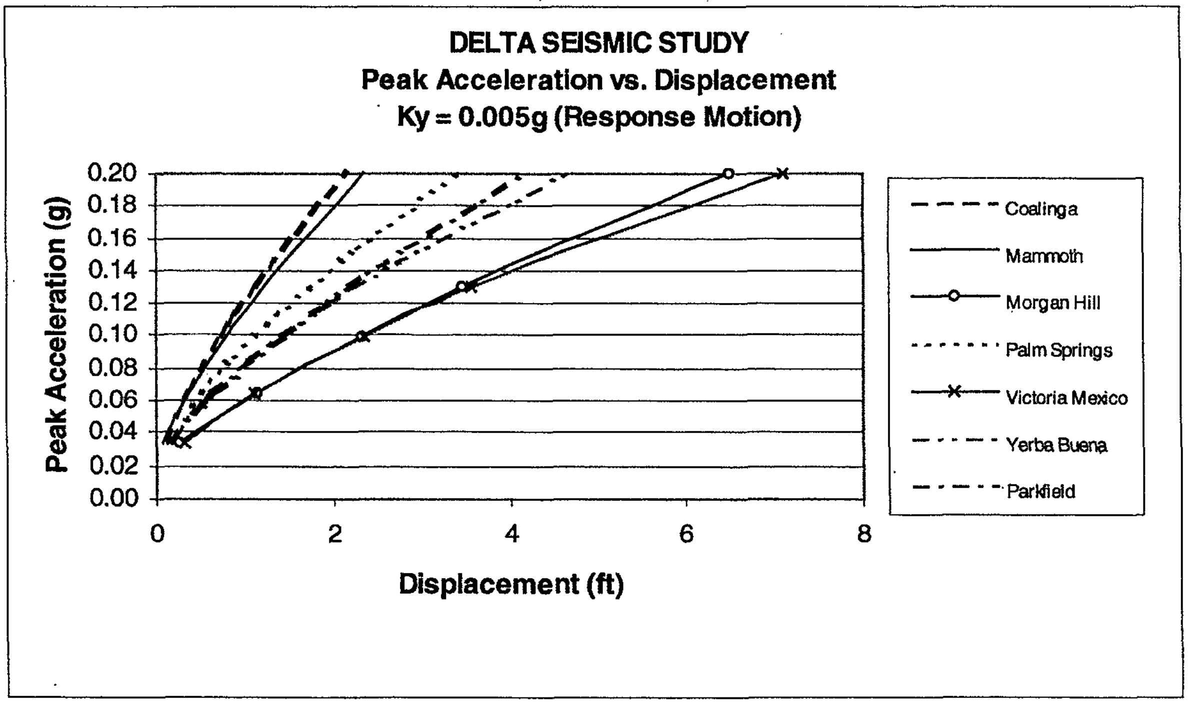

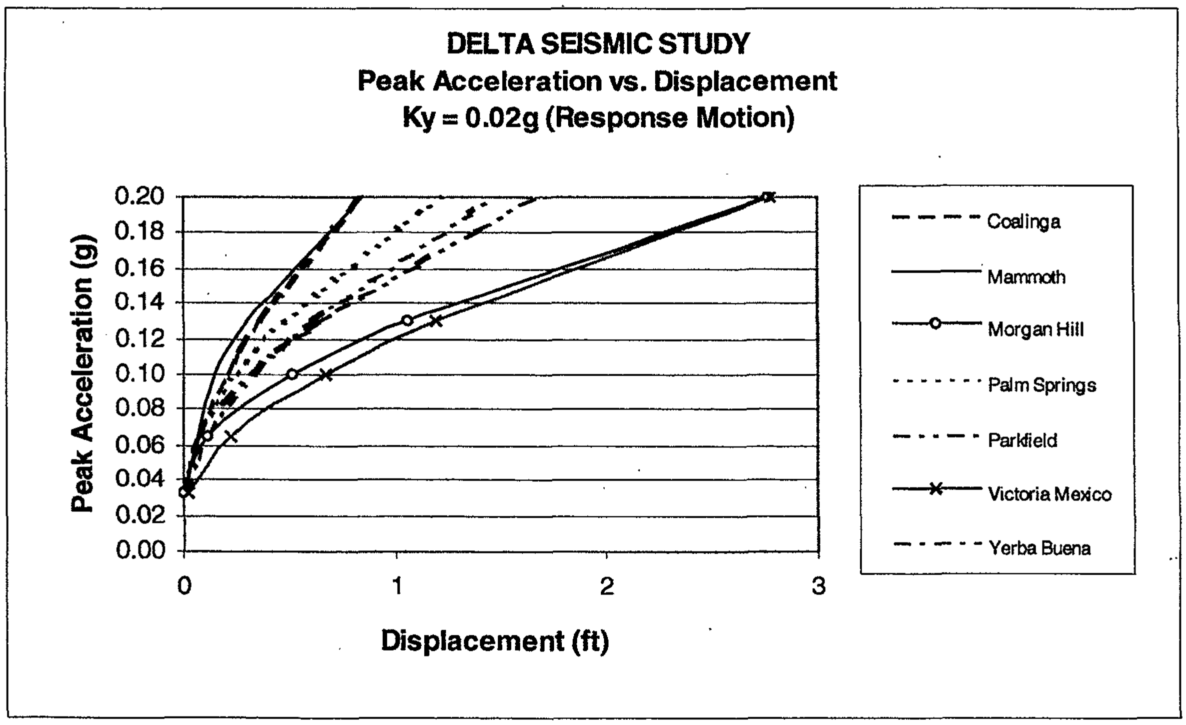

Figure B-1: Range of Calculated Deformations for Selected Accelerograms

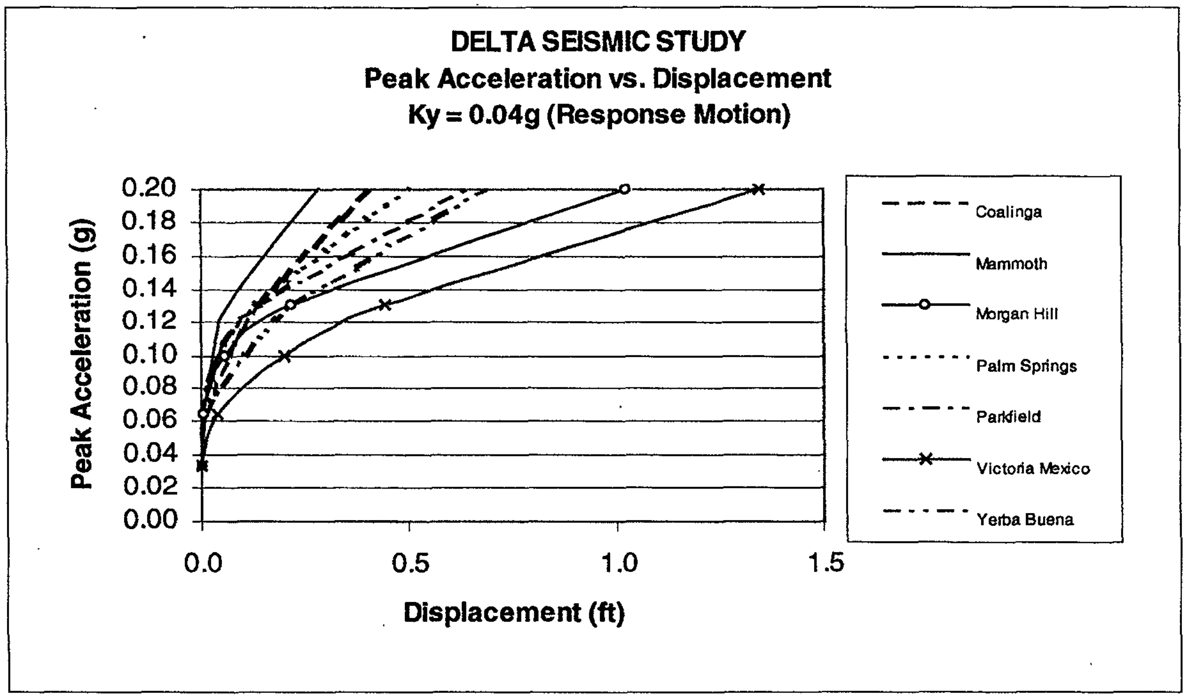

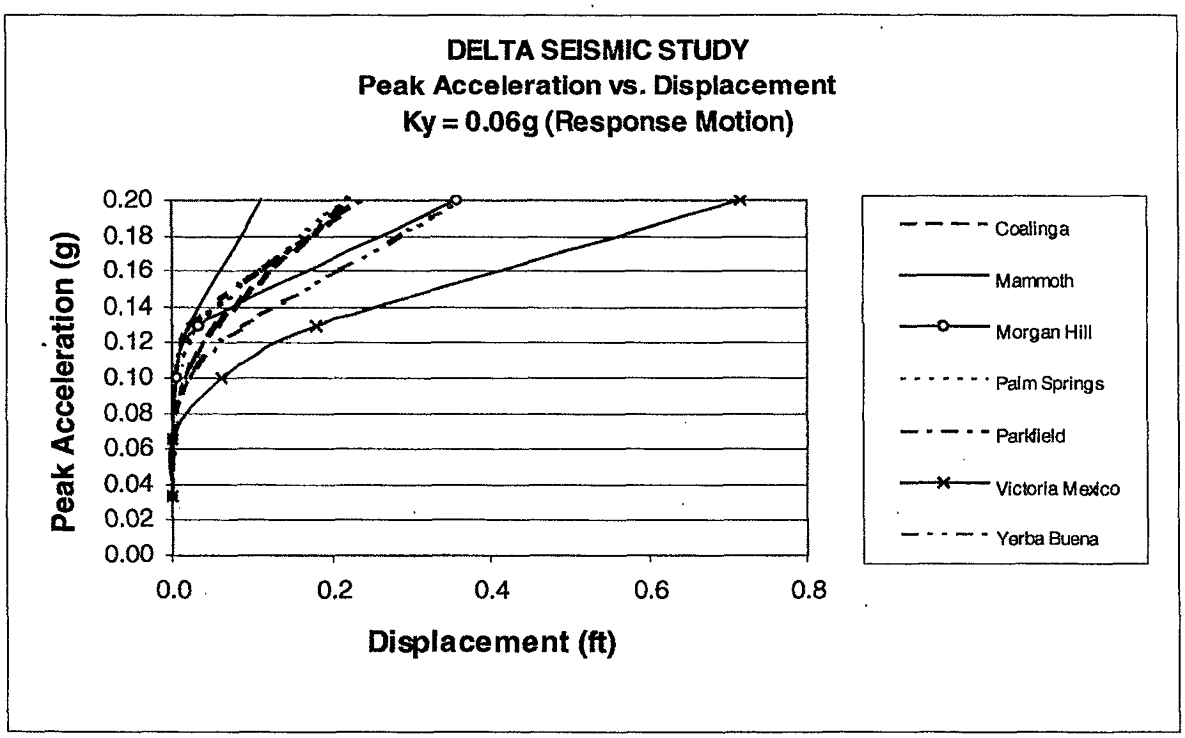

Figure B-2: Range of Calculated Deformations for Selected Accelerograms

For the purposes of these evaluations, the median values of calculated displacement from the seven accelerograms was selected for use. This was judged to be representative of the cyclic inertial deformations expected to result from earthquakes of $M_w \approx 6$. For larger and smaller magnitudes, the induced deformations would be greater or smaller due to the longer or shorter durations of shaking (larger or smaller numbers of cycles of loading). Accordingly, these deformation estimates were next scaled for magnitude (duration) effects using the scaling factor illustrated in Figure B-4. This was based on Burean, et al. (1988), and closely matches the similar works by Makdisi and Seed (1977).

3. The estimated levee deformations were then converted into probabilities of failure using an approximate relationship developed by the sub-team based on their experience with static levee distress in the Delta (see Figure B-2 and Table B-4). As discussed previously, the hazard curve in Figure B-2 jointly accounts for the following issues and variables;

    1. cracking associated with various deformation levels,
    2. potential exacerbation of seepage problems due to cracking and slumping,
    3. potential overtopping,
    4. potential inboard toe and/or face erosion and piping, and
    5. varying outboard water levels in rivers and sloughs due to both daily tidal fluctuations, and seasonal flow variations.

4. The failure probabilities were then summed for the different levels of marginal stability within a Damage Potential Zone, and then totaled as the number of failures for the non-liquefaction deformation mode of failure (see Table B-5).

ESTIMATED POTENTIAL NUMBER OF LEVEE FAILURES

The total number of potential levee failures for both liquefaction and non-liquefaction deformation modes of failure are presented in Table B-6 and Figure B-3. As may be noted in both places, the failure potential associated with liquefaction is far greater than that estimated for non-liquefaction failures. This is probably related to the relatively low magnitude and corresponding short duration of a typical Magnitude 6 earthquake. Accordingly, there are only a very small number of acceleration peaks which would exceed any particular yield acceleration.

ESTIMATED POTENTIAL LEVEE FRAGILITY

It should also be noted that the estimated numbers of failures shown in Table B-6 and Figure B-3 assume that the entire Delta is shaken to the same level of earthquake motion (e.g. 0.2g). This is unrealistic as no one earthquake event will ever do this. A better way of representing the potential for failure is to normalize the estimated number of failures by levee length for each Damage Potential Zone. A normalized levee fragility can then be determined in the form of estimated number of failures per 100 miles of levee (these values were obtained by taking the values in Table B-6 and then dividing by the levee length in each zone and then multiplying by 100). The estimated levee fragility values for both liquefaction and non-liquefaction modes of failure, for causative events of $M_w \approx 6.0$, are shown in TableB-7.

SEISMIC STABILITY OF LEVEES IN THE SACRAMENTO - SAN JOAQUIN DELTA

PROBABILITY OF FAILURE ASSOCIATED WITH EARTHQUAKE-INDUCED DISPLACEMENTS

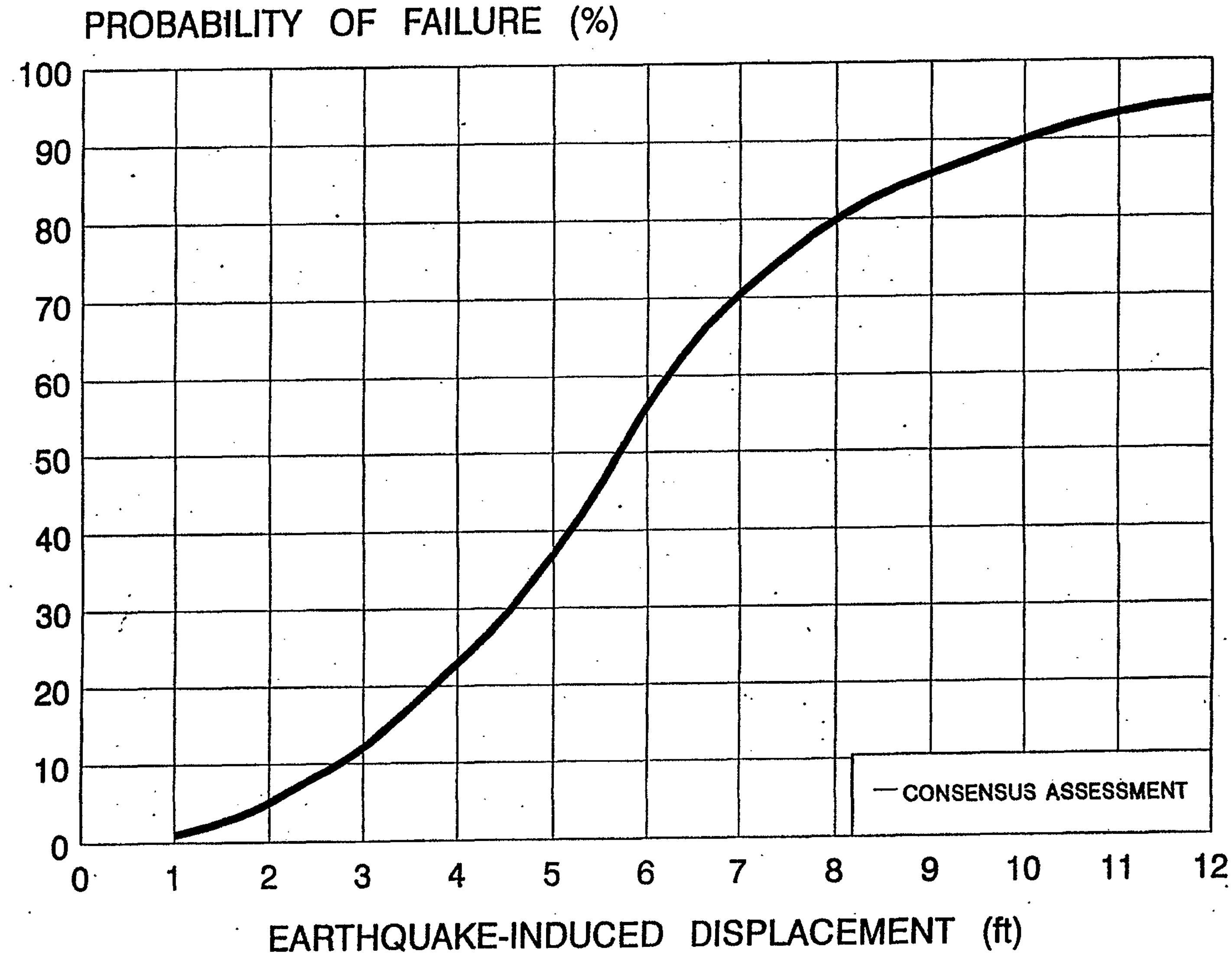

FIGURE B-2: PROBABILITY OF FAILURE ASSOCIATED WITH EARTHQUAKE-INDUCED DISPLACEMENTS

TABLE B-4: ESTIMATED PROBABILITIES OF LEVEE FAILURE ASSOCIATED WITH EARTHQUAKE-INDUCED DISPLACEMENTS IN NON-LIQUEFIED REACHES

Magnitude 6.0 Bedrock/Stiff Soil Peak Acceleration (g)	Average Peak Acceleration[1] k_{max}(g)	Estimated Probability of Levee Failure for Stability Categories[2]		
		A (k_y=0.005g)	B (k_y=0.02g)	C (k_y=0.04g)
0.05	0.033	**0.2%** [0.2 ft.]	**0.1%** [0.1 ft.]	**0.1%** [0.1 ft.]
0.10	0.065	**0.6%** [0.6 ft.]	**0.1%** [0.1 ft]	**0.1%** [0.1 ft.]
0.15	0.10	**2.6%** [1.4 ft]	**0.3%** [0.3 ft.]	**0.1%** [0.1 ft.]
0.20	0.13	**6.0%** [2.2 ft]	**0.6%** [0.6 ft.]	**0.2%** [0.15 ft.]
0.30	0.20	**25.0%** [4.2 ft]	**3.0%** [1.5 ft.]	**0.6%** [0.6 ft.]

Notes: 1. Average Peak Acceleration assumed to be equal to 65 percent of the base bedrock/stiff soil motion.
2. Estimated Probability of Levee Failure for non-liquefied levees based on estimated earthquake-induced deformations calculated using the Newmark method (see Table B-3).

TABLE B-5: ESTIMATED NUMBER OF LEVEE FAILURES ASSOCIATED WITH EARTHQUAKE-INDUCED DISPLACEMENTS IN NON-LIQUEFIED REACHES

Magnitude 6.0 Rock/Stiff Soil Peak Acc. (g)	Damage Potential Zone	Levee Length (miles)	Estimated Number of Levee Failures in Non-Liquefied Reaches		Estimated Failure Rate (Fragility) Failures per 100 miles
0.05	I	20	[1x0.002+1x0.001+3x0.001]-[2x0.002+3x0.001+8x0.001]=	**0.006 - 0.015**	**0.030 - 0.075**
	II	301	[6x0.002+12x0.001+20x0.001]-[12x0.002+24x0.001+60x0.001]=	**0.044 - 0.108**	**0.015 - 0.036**
	III	116	[0.3x0.002-0.7x0.001+1.7x0.001]-[2x0.002+3x0.001+5x0.001]=	**0.003 - 0.012**	**0.003 - 0.010**
	IV	223	[0.7x0.002+1.3x0.001+3.3x0.001]-[3x0.002+7x0.001+10x0.001]=	**0.006 - 0.023**	**0.003 - 0.010**
0.10	I	20	[1x0.006+1x0.001+3x0.001]-[2x0.006+3x0.001+8x0.001]=	**0.010 - 0.023**	**0.050 - 0.12**
	II	301	[6x0.006+12x0.001+20x0.001]-[12x0.006+24x0.001+60x0.001]=	**0.068 - 0.156**	**0.023 - 0.052**
	III	116	[0.3x0.006+0.7x0.001+1.7x0.001]-[2x0.006+3x0.001+5x0.001]=	**0.004 - 0.020**	**0.004 - 0.017**
	IV	223	[0.7x0.006+1.3x0.001+3.3x0.001]-[3x0.006+7x0.001+10x0.001]=	**0.009 - 0.035**	**0.004 - 0.016**
0.15	I	20	[1x0.026+1x0.003+3x0.001]-[2x0.006+3x0.001+8x0.001]=	**0.032 - 0.069**	**0.16 - 0.35**
	II	301	[6x0.006+12x0.001+20x0.001]-[12x0.026+24x0.003+60x0.001]=	**0.212 - 0.444**	**0.070 - 0.15**
	III	116	[0.3x0.026+0.7x0.003+1.7x0.001]-[2x0.026+3x0.003+5x0.001]=	**0.012 - 0.066**	**0.010 - 0.057**
	IV	223	[0.7x0.026+1.3x0.003+3.3x0.001]-[3x0.026+7x0.003+10x0.001]=	**0.025 - 0.109**	**0.011 - 0.049**
0.20	I	20	[1x0.060+1x0.006+3x0.002]-[2x0.060+3x0.006+8x0.002]=	**0.072 - 0.154**	**0.36 - 0.77**
	II	301	[6x0.060+12x0.006+20x0.002]-[12x0.060+24x0.006+60x0.002]=	**0.472 - 0.984**	**0.16 - 0.33**
	III	116	[0.3x0.060+0.7x0.006+1.7x0.002]-[2x0.060+3x0.006+5x0.002]=	**0.026 - 0.148**	**0.022 - 0.13**
	IV	223	[0.7x0.060+1.3x0.006+3.3x0.002]-[3x0.060+7x0.006+10x0.002]=	**0.056 - 0.242**	**0.025 - 0.11**
0.30	I	20	[1x0.250+1x0.030+3x0.006]-[2x0.250+3x0.030+8x0.006]=	**0.298 - 0.638**	**1.5 - 3.2**
	II	301	[6x0.250+12x0.030+20x0.006]-[12x0.250+24x0.030+60x0.006]=	**1.980 - 4.080**	**0.66 - 1.4**
	III	116	[0.3x0.250+0.7x0.030+1.7x0.006]-[2x0.250+3x0.030+5x0.006]=	**0.106 - 0.620**	**0.92 - 0.53**
	IV	223	[0.7x0.250+1.3x0.030+3.3x0.006]-[3x0.250+7x0.030+10x0.006]=	**0.234 - 1.020**	**0.11 - 0.46**

TABLE B-6: ESTIMATED NUMBER OF FAILURES FOR BOTH LIQUEFIED AND NON-LIQUEFIED REACHES

Magnitude 6.0 Rock/Stiff Soil Peak Acc. (g)	Damaged Potential Zone	Levee Length (miles)	Estimated Number of Levee Failures		
			Liquefied Reaches	Non-Liq. Reaches	Total
0.05	I	20	0 - 0.13	0.01 - 0.02	**0.01 - 0.15**
	II	301	0 - 0.25	0.04 - 0.11	**0.04 - 0.36**
	III	116	0 - 0.07	0 - 0.01	**0 - 0.04**
	IV	223		0.01 - 0.02	**0.01 - 0.09**
	Total	**660**	**0 - 0.48**	**0.06 - 0.16**	**0.06 - 0.64**
0.10	I	20	0 - 0.5	0.01 - 0.02	**0.01 - 0.52**
	II	301	0 - 1.0	0.07 - 0.16	**0.07 - 1.16**
	III	116	0 - 0.2	0 - 0.02	**0 - 0.22**
	IV	223	0 - 0.3	0.01 - 0.04	**0.01 - 0.34**
	Total	**660**	**0 - 2**	**0.09 - 0.24**	**0.09 - 2.24**
0.15	I	20	0.5 - 2	0.03 - 0.07	**0.53 - 2.07**
	II	301	2 - 5	0.21 - 0.44	**2.21 - 5.44**
	III	116	0.3 - 2.6	0.01 - 0.07	**0.31 - 1.47**
	IV	223		0.03 - 0.11	**0.73 - 2.71**
	Total	**660**	**3.5 - 11**	**0.28 - 0.69**	**3.78 - 11.69**
0.20	I	20	1 - 4	0.07 - 0.15	**1.07 - 4.15**
	II	301	5 - 15	0.47 - 0.98	**5.47 - 15.98**
	III	116	1 - 3	0.03 - 0.15	**1.03 - 3.15**
	IV	223	2 - 5	0.06 - 0.24	**2.06 - 5.24**
	Total	**660**	**9 - 27**	**0.63 - 1.52**	**9.63 - 28.52**
0.30	I	20	3 - 6	0.30 - 0.64	**3.30 - 6.64**
	II	301	15 - 30	1.98 - 4.08	**16.98 - 34.08**
	III	116	3 - 7	0.11 - 0.62	**3.11 - 7.62**
	IV	223	5 - 13	0.23 - 1.02	**5.23 - 14.02**
	Total	**660**	**26 - 56**	**2.62 - 6.36**	**28.62 - 62.36**

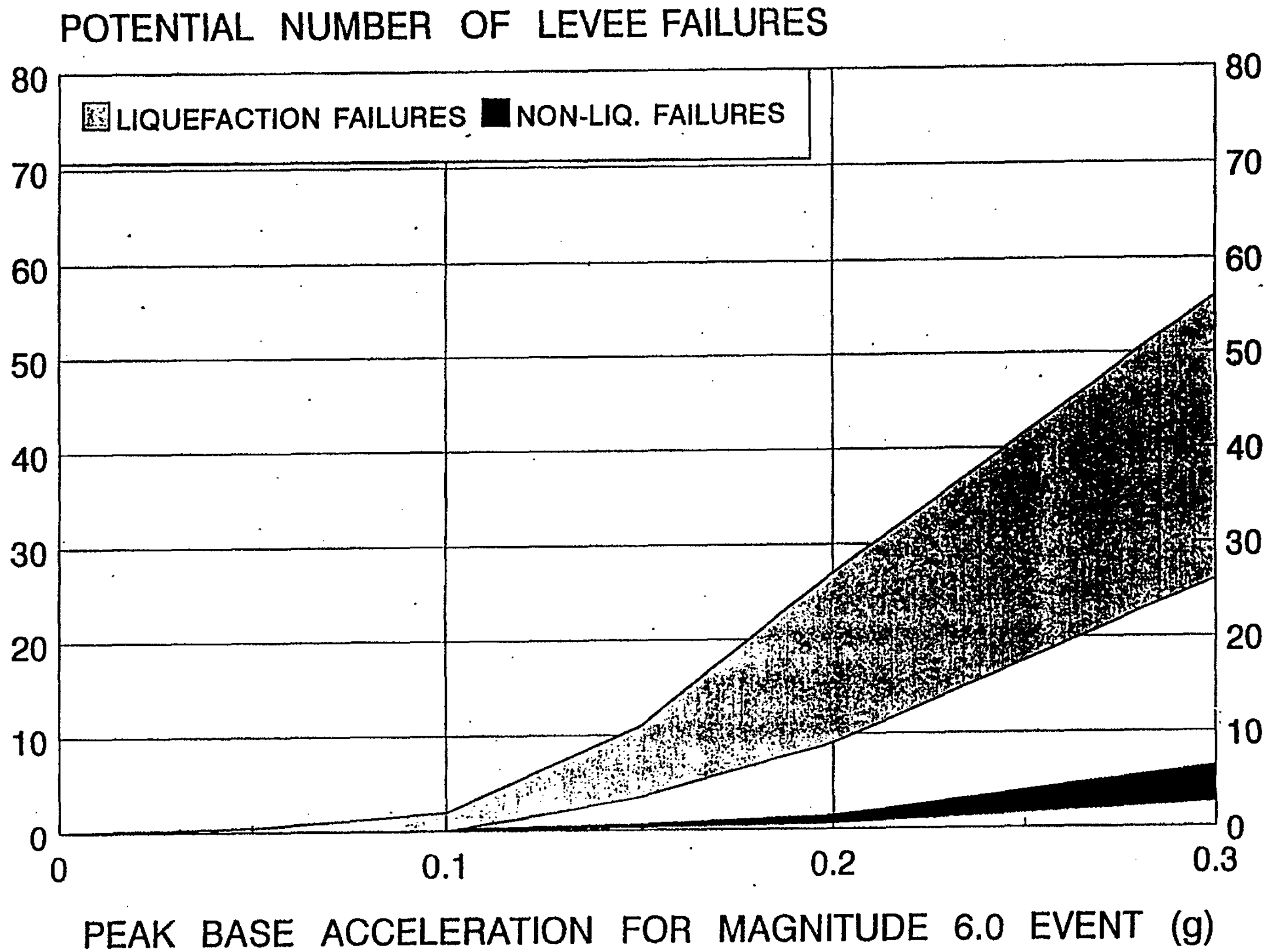

Note: Assessment assumes that the entire Delta area is shaken by the postulated earthquake shaking

FIGURE B-3: ESTIMATED NUMBER OF LEVEE FAILURES FOR DIFFERENT LEVELS OF EARTHQUAKE SHAKING

TABLE B-7: ESTIMATED FAILURE RATE (FRAGILITY) FOR BOTH LIQUEFIED AND NON-LIQUEFIED REACHES - FAILURES PER 100 MILES

Magnitude 6.0 Rock/Stiff Soil Peak Acc. (g)	Damaged Potential Zone	Levee Length (miles)	Estimated Fragility - Number of Levee Failures per 100 miles: Liquefied Reaches	Non-Liq. Reaches
0.05	I	20	0.005 - 0.50	0.030 - 0.075
	II	301	0.001 - 0.083	0.015 - 0.036
	III	116	0.001 - 0.033	0.003 - 0.010
	IV	223	0.001 - 0.033	0.003 - 0.010
0.01	I	20	0.20 - 2.5	0.050 - 0.12
	II	301	0.080 - 0.33	0.023 - 0.052
	III	116	0.050 - 0.15	0.004 - 0.017
	IV	223	0.050 - 0.15	0.004 - 0.016
0.15	I	20	2.5 - 10.	0.16 - 0.35
	II	301	0.66 - 1.7	0.070 - 0.15
	III	116	0.29 - 1.2	0.010 - 0.057
	IV	223	0.29 - 1.2	0.011 - 0.049
0.20	I	20	5. - 20.	0.36 - 0.77
	II	301	1.7 - 5.0	0.16 - 0.33
	III	116	0.88 - 2.3	0.022 - 0.13
	IV	223	0.88 - 2.3	0.025 - 0.11
0.30	I	20	15. - 0.	1.5 - 3.2
	II	301	5.0 - 10.	0.66 - 1.4
	III	116	2.4 - 5.9	0.092 - 0.53
	IV	223	2.4 - 5.9	0.11 - 0.46

Magnitude Correction Factors

The estimates for levee failures and fragility presented in the previous tables are for earthquake shaking associated with a magnitude 6.0 event. For the same level of shaking, larger earthquake magnitudes will induce more damage and levee failures than smaller events because larger magnitude earthquakes have longer durations and larger numbers of strong cycles of shaking. To adjust the fragilities for earthquake magnitudes other than Magnitude 6.0, the following corrections were used:

A. Liquefaction Mode of Failure:

A magnitude correction factor for the liquefaction mode of failure was developed using the Idriss (1997) magnitude scaling factors for triggering liquefaction. These corrections are slightly larger than those previously used by Seed et al. (1984).

B. Non-Liquefaction Deformation Mode of Failure:

A magnitude correction factor for the non-liquefaction deformation mode of failure was developed using the Earthquake Severity Index described by Bureau et al. (1988). This correction is much larger than the one for liquefaction, but is comparable with the deformation results obtained by Makdisi and Seed (1977).

For both failure modes (liquefaction, and non-liquefaction cyclic inertial deformation), the principal fragility estimates (Table B-7) were developed for events of $M_w \approx 6.0$, as that was central to the range of magnitudes principally contributing to the overall risk for the Delta. Figure B-4 shows the magnitude correction factors used for both modes of failure.

SEISMIC STABILITY OF DELTA LEVEES

MAGNITUDE CORRECTION FACTORS TO LEVEE FRAGILITY

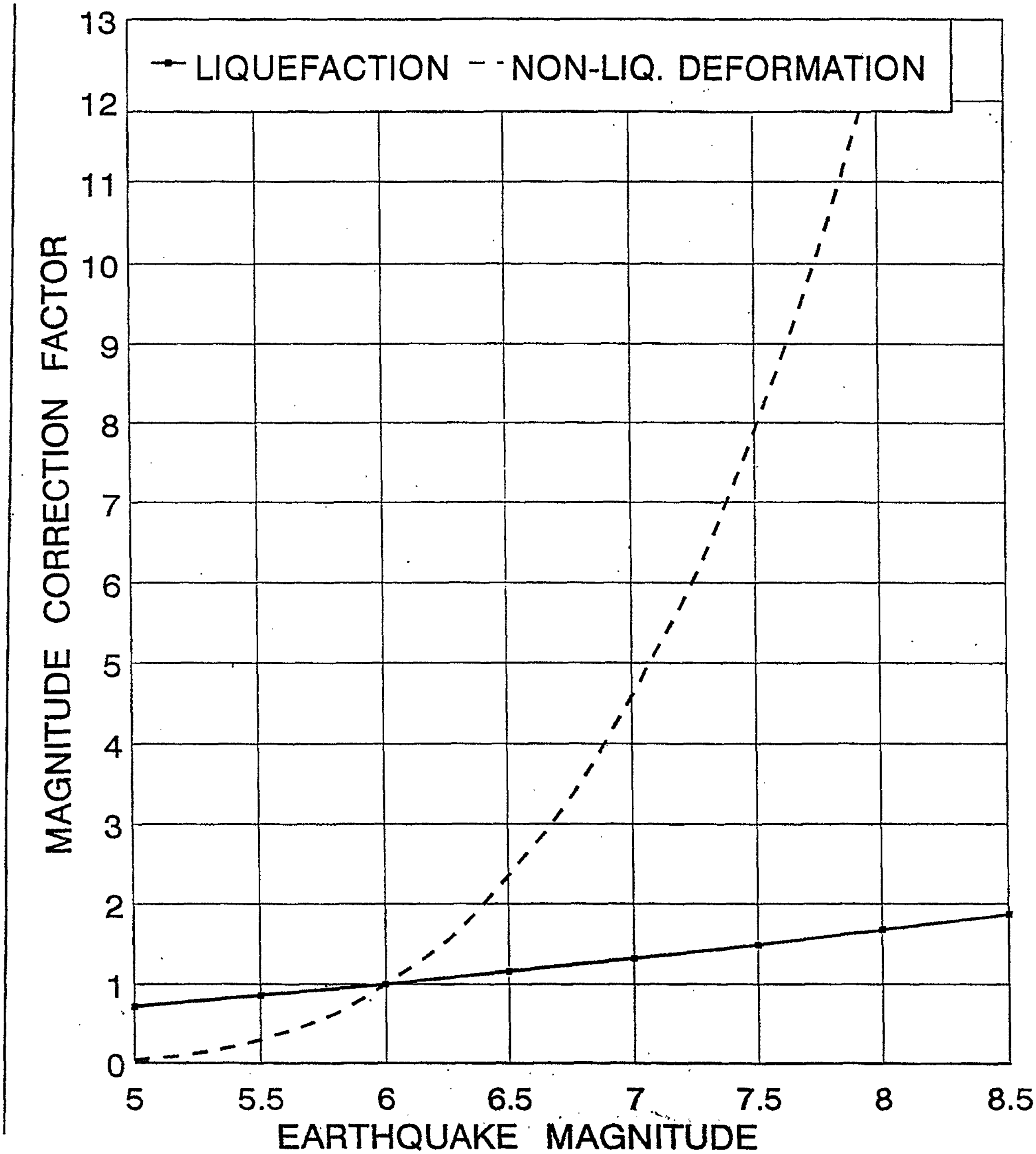

FIGURE B-4: MAGNITUDE CORRECTION FACTORS FOR LIQUEFACTION AND NON-LIQUEFACTION DEFORMATION MODES OF FAILURE

APPENDIX C
PROBABILISTIC LEVEE FAILURE METHODOLOGY

APPENDIX C
PROBABILISTIC LEVEE FAILURE METHODOLOGY

The mathematical models used in the calculation of the probability of levee failures are described in this Appendix. To apply the probabilistic approach, we need to first parameterize the point estimates of the fragilities.

C1. PARAMETRIC MODELS FOR LEVEE FRAGILITIES

The point estimates of the levee fragilities developed for this study were fit to simple equations to facilitate the probabilistic calculations. The simplified models for the median and coefficient of variation (cov) for both liquefaction and non-liquefaction induced failures are given below.

FRAGILITY CURVES FOR LIQUEFACTION INDUCED FAILURES

The median fragility liquefaction for In liquefaction induced failures is modeled by

$$frag_{Li}(pga,M)=0.8\exp(p_1+p_2[\ln(pga)+c_1+c_2M+c_3M^2+c_4M^3]+c_{5i})$$

The coefficients p_1, p_2, c_1, c_2, c_3, c_4, and c_5 were estimated from the central value of the range given in the point estimates. The 0.8 factor represents the interpretation of the sub-team that the median fragility is not at the center of the range given in the point estimates, but rather it is approximately at 40% of the range.

The coefficient of variation for all zones is modeled by

$$cov_L=(b_1+b_2pga)/1.3$$

with a constraint that it not be less then 0.3/1.3. The factor of 1.3 represents the interpretation of the fragility group that the range on the fragility given in the point estimates represents the 80% confidence interval..

The distribution of the fragility is modeled as an asymmetric distribution based on the judgement of the sub-team. This asymmetry is modeled using two different normal distributions above and below the median. The standard deviation (cov*median) is scaled by 1.2 for values above the median and by 0.8 for values below the median. This results in a distribution that is skewed to the right (skewed to higher numbers of failures).

The levee fragility group estimates of the ranges of numbers of failures for each zone is based on the total number of failures for each zone. That is, the standard deviation does not apply to a single levee, but rather to the total number of levees in each zone. This impacts the use of the standard deviation in the probabilistic evaluation. Specifically, the distribution is applied t the median number of breaks in each zone (summation of the median number of breaks for each levee in a zone). This distribution is truncated at 1.5 standard deviations above and below the median.

The coefficients for these models are listed in Table C-1.

FRAGILITY CURVES FOR NON-LIQUEFACTION INDUCED FAILURES

The median fragility for non-liquefaction induced failures is modeled by a bilinear model:

If

$$\ln(pga)+c_1+c_2M+c_3M^2+c_4M^3\leq-2.3,$$

then

$$frag_{Ni}(pga,M)=\exp\{p_1+p_2[\ln(pga)+c_1+c_2M+c_3M^2+c_4M^3]+c_{5i}\}$$

otherwise,

$$frag_{Ni}(pga,M)=\exp\{p_1+p_2[\ln(pga)+c_1+c_2M+c_3M^2+c_4M^3]+c_{5i}+p_3\ln(pga)\}$$

The coefficient of variation is modeled by

$$cov_{Ni}=b_{1i}/1.3$$

The factor of 1.3 represents the interpretation that the range on the fragility given in the point estimates represents the 80% confidence interval. A normal distribution is used for the number of failures. This distribution is truncated at 1.5 standard deviations above or below the median.

The coefficients for these models are listed in Table C-2. All of the coefficients are constant for all zones except for C_5 and b_1 which can vary by zone as shown in Table C-2.

C2. PROBABILISTIC METHODOLOGY

The levee failure probability is an extension of standard probabilistic seismic hazard analysis. The difference is that instead of calculating the probability of the ground motion exceeding a specified value at a location, we compute the probability of specified number of levee failures being exceeded in a single earthquake. That is, we consider the entire levee system simultaneously.

In the following probabilistic seismic hazard analysis, we consider all possible earthquake magnitudes, locations, and ground motion. For each possible earthquake, we then compute the probability of one or more levee failures occurring within the Delta. This process is repeated for two or more failures, three or more failures, and so on.

Let μ_{Lij} be the median number of failures due to liquefaction for the j^{th} levee in the i^{th} zone. Then

$$\mu_{Lij} = frag_{Li}(pga, M) * L_j$$

where $frag_{Li}$ is the median fragility, pga is the median peak acceleration at the center of the island, M is the magnitude of the earthquake, and L_j is the length of the j^{th} levee in miles. The median number of failures for the i^{th} zone is given by:

$$\mu_{Li} = \sum_{j=1}^{Ni} \mu_{Lij}$$

and the standard deviation of the number of failures due to the uncertainty in the ground motion is given by:

$$\sigma_{GLij} = \mu_{Lij} P2\sigma_{pga}(M)$$

based on propagation of errors. Assuming that the peak acceleration variability is uncorrectable between levees (which is reasonable for separation distance of greater than 500m), then the standard deviation of the total number of failures within the zone is given by:

$$\sigma_{GLi} = \sqrt{\sum_{j=1}^{Ni} \sigma_{GLij}^2}$$

Since the standard deviation due to uncertainty in the fragility is for the zone and not for individual levees, the fragility uncertainty is fully correlated for each levee within a zone. Therefore, the standard deviation of the total number of failures within a zone due to fragility variability is given by:

$$\sigma_{FLi} = \sum_{j=1}^{Ni} \text{cov}_L \, \mu_{Lij}$$

Similar equations are developed for the non-liquefaction induced failures.

We then use a Monte Carlo approach to sample the distributions for the number of failures in each zone and sum the number of failures from liquefaction and non-liquefaction failures for each zone. Finally, we sum up the number of failures for all the zones to get the total number of failures in the levee system. The frequency of failures in the Monte Carlo sampling defines the conditional probability of the number of failures for a given earthquake magnitude and location.

Let(P(fail>N_F I M, A, W, Hx, Hy) be this conditional probability of the number of failures exceeding N for the given magnitude (M), rupture area (A), rupture width (W), energy center along strike (Hx), and energy center along dip (Hy).

Then the rate of failures is given by:

$$\nu(Fail > N) = \sum_{k=1}^{NF} N_k \int_M \int_A \int_W \int_x \int_y f_m(M) f_A(M) F_W(M) f_x(x) f_y(y) P(fail > N_F | M, A, W, x, y) dM dA dW dx d$$

where f_m, f_A, f_W, f_x, f_y are the probability density functions for magnitude, rupture area, rupture width, and energy center. The N_k is the rate of earthquake above the minimum magnitude (here taken as 5.0) for the k^{th} source and NF is the number of faults.

In this equation, the conditional probability of failure is multiplied by the probability of the specified earthquake occurring (given that an earthquake has happened) and then multiplied by the rate of earthquake for the given seismic source. This rate of failure is then summed over all the seismic sources to give the total rate of various numbers of levees failing in a single earthquake. A Poisson assumption for the earthquake occurrence is used to convert the rate of failures into a probability of failures. The result is a hazard curve for the number of levee failures in a single earthquake.

Table C-1.
Fragility Model Coefficients for Liquefaction Induced Failures

Coefficient	All Zones	I	II	III	IV
p1	7.33				
p2	3.02				
c1	-3.47				
c2	0.97				
c3	-0.0838				
c4	0.0031				
c5		0.0	-1.55	-2.23	-2.23
b1	0.94				
b2	-2.05				

Table C-2.
Fragility Model Coefficients for Liquefaction Induced Failures

Coefficient	All Zones	I	II	III	IV
p1	-1.32				
p2	0.54				
p3	2.49				
c1	-75.7				
c2	28.6				
c3	-3.61				
c4	0.156				
c5		0.0	-0.115	-0.810	-2.08
b1		0.38	0.38	0.60	0.60

Printed by
Department of Water Resources
Reprographics